Summer 8-2008

Identification of Two Distinct Glutaminyl Cyclase Isoforms in *Drosophila melanogaster*

Amanda Thigpen Parker
University of Southern Mississippi

The University of Southern Mississippi

IDENTIFICATION OF TWO DISTINCT GLUTAMINYL CYCLASE ISOFORMS IN *DROSOPHILA MELANOGASTER*

by

Amanda Thigpen Parker

A Dissertation
Submitted to the Graduate Studies Office
of The University of Southern Mississippi
in Partial Fulfillment of the Requirements
for the Degree of Doctor of Philosophy

Approved:

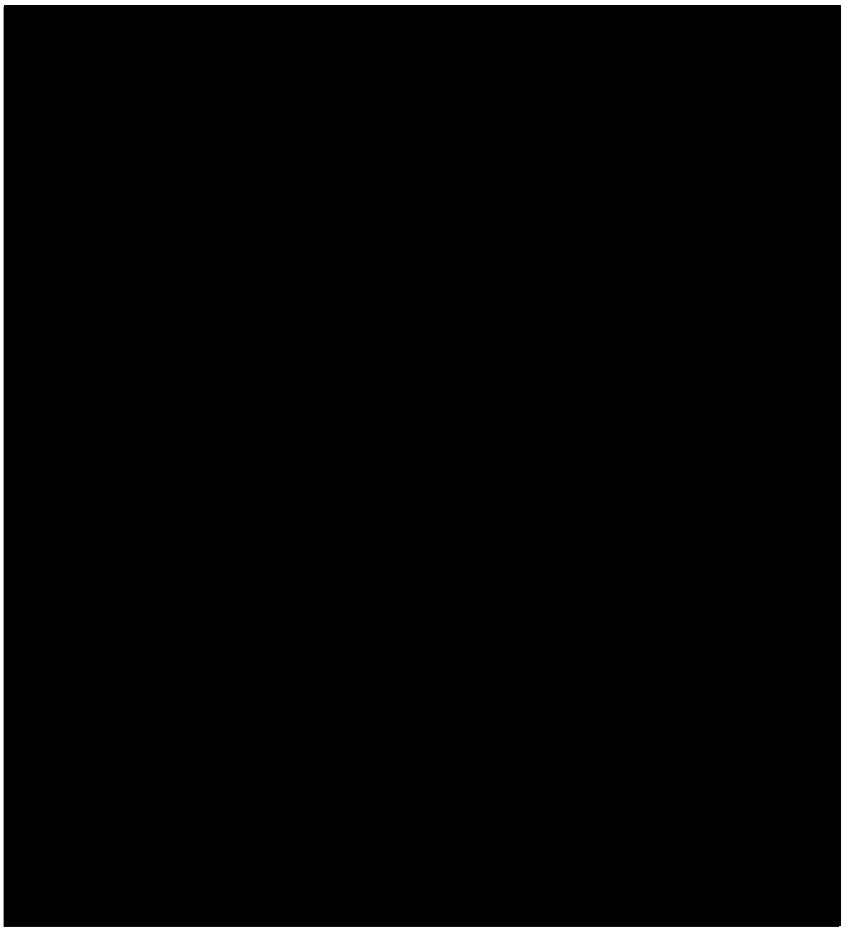

August 2008

The University of Southern Mississippi

IDENTIFICATION OF TWO DISTINCT GLUTAMINYL CYCLASE ISOFORMS IN *DROSOPHILA MELANOGASTER*

by

Amanda Thigpen Parker

Abstract of a Dissertation
Submitted to the Graduate Studies Office
of The University of Southern Mississippi
in Partial Fulfillment of the Requirements
for the Degree of Doctor of Philosophy

August 2008

ABSTRACT

IDENTIFICATION OF TWO DISTINCT GLUTAMINYL CYCLASE ISOFORMS IN *DROSOPHILA MELANOGASTER*

by Amanda Thigpen Parker

August 2008

Sequence analyses revealed two putative glutaminyl cyclase genes in *Drosophila melanogaster* with greater than 60% amino acid sequence identity to previously identified glutaminyl cyclase in humans. Expression, purification, and characterization of both putative proteins revealed two enzymatically active glutaminyl cyclase enzymes. Comparison of the *Drosophila melanogaster* glutaminyl cyclase enzymes to the published human glutaminyl cyclase revealed the enzymes were very similar. The Km values obtained were identical to those of human glutaminyl cyclase for three different substrates tested. However, the *Drosophila* glutaminyl cyclases demonstrated lower turnover numbers. Both *Drosophila* glutaminyl cyclase isoforms were inhibited by imidazole, imidazole derivatives, and metal chelators. The predicted tertiary structure of the *Drosophila* glutaminyl cyclase isoforms revealed a conservation of the overall tertiary structure and active site amino acids when compared to human glutaminyl cyclase.

Localization studies demonstrated differential location of the two isoforms within the *Drosophila melanogaster* embryo. One isoform was expressed at much higher levels and found within the developing nerve cord suggesting this isoform of the *Drosophila* glutaminyl cyclase is important in neuronal development. These glutaminyl cyclase isoforms join peptidyl-glycine α-amidating monooxygenase and prohormone convertase

2 as the known bioactive peptide processing enzymes in *Drosophila* and provide the first evidence of two distinct glutaminyl cyclase isoforms located within one organism.

Evolutionary studies revealed further links between bacterial aminopeptidases and the mammalian and insect glutaminyl cyclases. Previous work demonstrated a common fold and active site between human glutaminyl cyclase and bacterial aminopeptidase. Slight aminopeptidase activity was observed in the human glutaminyl cyclase and both glutaminyl cyclase isoforms. It was also determined the glutaminyl cyclases were able to bind leucine derivatives which are common aminopeptidase substrates. This observation led to the identification of a new class of competitive inhibitors for glutaminyl cyclases.

ACKNOWLEDGMENTS

The encouragement, guidance, and support of many people have made the completion of my dissertation work possible. First, my advisor, Dr. Robert Bateman, saw my potential as an undergraduate. With his help I was able to "see the light" and become a true "chemistry lab rat". His faith in me helped me to become the researcher I am today. I also would like to give a special thanks to my committee members, Dr. Evans, Dr. Heinhorst, Dr. Huang, and Dr. Guo. Their patience and guidance throughout my change in projects is greatly appreciated. My gratitude also goes to my fellow graduate students that were always there for me when I needed help, advice, or simply someone to talk with.

My deepest thanks and respect goes to Dr. Sandra Leal. This very special lady became a second advisor to me in my last year when things were getting really tough. She shared so much knowledge and support with me I could never thank her enough. I now owe all my *Drosophila* techniques to her.

My gratitude also goes to all the supporting organizations. Financial support was received from the University of Southern Mississippi, the Department of Chemistry and Biochemistry, ASBMB travel awards, and NSF-GAANN grant.

As I prepare to leave the University I called home for more than 10 years my deepest love and appreciation goes out to my family. They have supported me throughout my college career. As the first graduate with a higher level college degree in my family their pride in me gives me so much strength to strive to achieve all my goals.

TABLE OF CONTENTS

LIST OF TABLES

Table

LIST OF ILLUSTRATIONS

Figure

LIST OF ABBREVIATIONS

Aβ	β-amyloid peptide
AAP	*Aeromonas* aminopeptidase
AKH	adipokinetic hormone
Ala	alanine
AMC	4-methylcourmarinelamide
AMP	ampicillin
AP	aminopeptidase
Asp	aspartic acid
ATP	adenosine triphosphate
bp	base pairs
cAMP	cyclic adenosine monophosphate
Ca	calcium
CD	cicular dichroism
CDI	carbonyl di-imidazole
cDNA	complementary deoxyribonucleic acid
CMK	chloromethyl ketone
Co	cobalt
CP	carboxypeptidase
CPE	carboxypeptidase E
Cys	cysteine
dNTP	deoxynucleotide triphosphate
dQC	*Drosophila* QC
dQC_{pET}	*Drosophila* QC bacterial expression vector/expressed protein
dQC-LK	*Drosophila* QC-like isoform
$dQC\text{-}LK_{TOPO}$	*Drosophila* QC-like bacterial expression vector/expressed protein
$dQC\text{-}LK_{IMPACT}$	*Drosophila* QC-like bacterial expression vector/expressed protein
DTT	dithiothreitol
FBS	fetal bovine serum
Gln	glutamine
Glu	glutamic acid
Gly	glycine
GnRH	gonadotropin-releasing hormone
GST	glutathione-S-transferase
His	histidine
HPLC	high performance liquid chromatography
hQC	human glutaminyl cyclase
hQC-GST	human glutaminyl cyclase glutathione-S-transferase construct
HRP	horse radish peroxidase
IPTG	isopropyl thiogalactoside
Kb	kilobase pairs
kD	kiloDaltons
Leu	leucine
MALDI-TOF	Matrix Assisted Laser Desorption Ionization - Time of Flight
MBP	maltose binding protein

Mn	manganese
mRNA	messenger ribonucleic acid
βNA	β-naphthylamine
NADH	nicotinamide adenine dicnucleotide
NTP	nucleotide triphosphate
NADPH	nicotinamide adenine dinucleotide phosphate
His	histidine
PAL	peptidyl α-amidating lyase
PAM	peptidyl glycine α-amidating monooxygenase
PBS	phosphate buffer saline
PC	prohormone convertase
PCR	polymerase chain reaction
PGAP	pyroglutamate aminopeptidase
pGlu	pyroglutamic acid
PHM	α-hydroxylating monooxygenase
pNA	para-nitroanilide
poly-His	poly-histidine
Pro	proline
PTSF	serine protease inhibitor
QC	glutaminyl cyclase
rER	rough endoplasmic recticulum
SDM	Schneider's *Drosophila* Media
SDS-PAGE	sodium dodecyl sulfate polyacrylamide gel electrophoresis
Ser	serine
SFM	serum free media
TRH	thyrotropin-releasing hormone
Trp	tryptophan
Zn	zinc

CHAPTER I

LITERATURE REVIEW

Introduction

Hormones, the chemical messengers of the endocrine system, are used for signaling and regulation in most living organisms. They are responsible for initiating and regulating many reactions throughout the body, such as hunger and feeding, growth, sexuality, and development. Hormones are produced within specialized cells termed endocrine glands and secreted directly into the bloodstream for travel to target cells.

There are four major types of hormones. The steroid family hormones are produced and travel through plasma membranes by diffusion due to their hydrophobic nature. Examples include corticoids secreted from the adrenal gland and steroids secreted from the testes, ovaries, and adrenal glands. Their mechanism of action involves a receptor-hormone complex that controls transcription and mRNA stability. Amino acid and fatty acid derivatives are two other classes of hormones that are less common. Amino acid derivatives include catecholamines and fatty acid derivatives include prostaglandins and thromboxanes. They are relatively fast acting and rapidly degraded.

The final class of hormones is polypeptide hormones. These hormones though typically composed of a few amino acids can range up to hundreds of amino acids in size. Regardless of final mature protein size, all polypeptide hormones are secreted as large precursors which are subsequently modified. Examples of commonly known peptide hormones include insulin and glucagon, which are produced in the pancreas and exert an effect throughout the body by controlling glucose metabolism, and leptin, which is produced in fat cells, is responsible for regulating body weight, metabolism, and

reproductive function. Another group of polypeptide hormones, the gonadotropins, are produced in the pituitary and function to regulate sexual processes.

Peptide hormones require a more complex mechanism of action than other hormone types. The peptide must interact with a receptor to activate a second messenger and protein kinase activity. Most commonly a peptide hormone binds the receptor protein, activating a G-protein. The active G-protein activates adenylyl cyclase leading to the release of cAMP. The cAMP then initiates a cascade of reactions leading to activation and inactivation of specific enzymes. This activity demonstrates that a relatively small amount of hormone can exert a large cascade effect on the target cell. (Lindberg 1996; Bear 2001)

Post-translational Processing

Secretory Pathway

Many proteins, including various peptide hormones, are produced as inactive precursors that require the activity of post-translational processing enzymes to achieve maturity. Post-translational modifications of peptides are believed to occur within the secretory pathway. In the secretory pathway, shown in figure 1, proteins are synthesized and modified throughout various types of cell machinery involving the activity of many different enzymes. Proteins are produced in an immature form, typically as large precursor polypeptides, at the ribosomes and cotranslationally inserted into the lumen of the rough endoplasmic reticulum. Once synthesized, the immature proteins are transported to the Golgi apparatus for proper sorting. Proteins secreted by the regulated secretory pathway are enclosed into secretory granules for extracellular release of

concentrated mature peptide under the regulation of external stimulation and control. Other proteins, under the control of the constitutive secretory pathway, are continually produced and secreted from the specific cell types regardless of presence or absence of environmental factors.

During the initial delivery of the newly synthesized polypeptide into the lumen of the rER, proteins are folded into proper tertiary structure, disulfide bonds are formed to aid in maintaining the proper tertiary structure, and N-linked glycosylation occurs if the proper conserved sequences are present and accessible. Further post-translational maturation occurs during transit from the rER through the Golgi apparatus including modification of N-linked sugars, O-linked glycosylation, tyrosine sulfation, N-acetylation, and serine phosphorylation. Final modifications such as exoproteolysis, endoproteolysis, amidation, and pyroglutamate (pGlu) formation occur in the transport of partially mature polypeptides to the secretory granules. (Lindberg 1996; Beinfeld 1998; Canaff 1999)

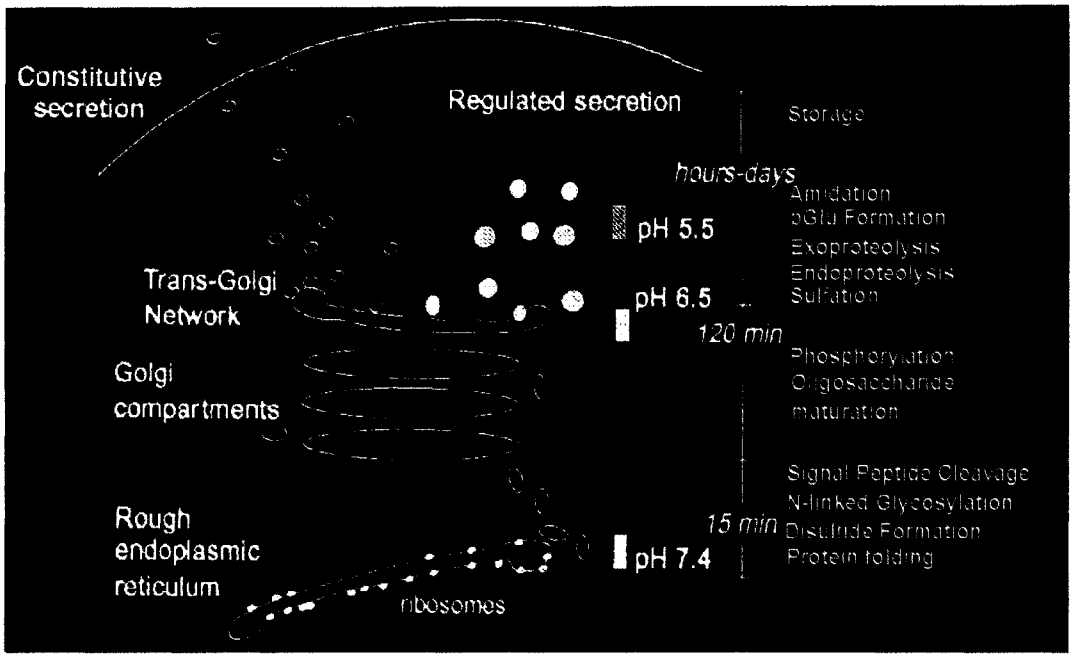

Figure 1: **Secretory pathway.** Diagram demonstrating the biosynthetic secretory pathway in which peptide hormones are synthesized, modified, and transported into vesicles for further proteolytic processing. (Lindberg 1996)

Secretory Pathway Enzymes

Prohormone Convertase

Four major enzymes are responsible for some of the important peptide hormone modifications that occur within the secretory pathway. Proteolytic maturation by exoproteolysis and endoproteolysis is catalyzed by two major families of enzymes. Prohormone convertases (PCs) are responsible for endoproteolytic cleavage of large precusor sequences. There are multiple forms of PCs with varying expression levels in different cells types. Prohormone convertase 2 (PC2) appears to be the most catalytically efficient and most widely distributed PC in neural and endocrine tissues and cell lines. Therefore, PC2 is believed to be a major prohormone convertase required for peptide

hormone and neuropeptide maturation. (Beinfeld 1998) PC2 is calcium activated and prefers an acidic pH for optimal activity both of which are properties of the secretory granule environment. (Lindberg 1996) PC2, which is produced as an immature pro-polypeptide, is coexpressed with a neuroendocrine secretory protein termed 7B2. In the late stages of the rER following folding of the proPC2, 7B2 binds the proPC2 facilitating the transport of proPC2 complex into the secretory pathway. Once in the secretory granules 7B2 is released and proPC2 is converted to active PC2 due to the low pH, high calcium environment. (Canaff 1999; Zhou 1999)

PC2 deficiencies have been linked to various disease states. One study linked the lack of PC2 or the chaperone 7B2 has been linked to optic atrophy, insulin-dependent diabetes mellitus, vasopressin-sensitive diabetes, and neurosensory hearing loss. In this study, authors observed subjects could not properly process vasopressin and insulin resulting in major defects of various neurological processes. (Gabreels 1998) Deficiencies in PC1 genes have been linked to monogenic obesity due to improper enzyme function. (Arner 2000) A possible link between PCs and specific tumor types was suggested due to a high frequency of PCs in tumors. (Kimura 2000) Other studies have provided possible links between Alzheimer's and prion diseases. PC2 was shown to be essential for complete processing of amyloid polypeptide. (Wang 2001) Similar studies provided similar results for amyloid peptide but also established the requirement of PC for processing of prion disease peptides. (Checler 2002)

Carboxypeptidase

Further proteolytic reactions are catalyzed by another group termed carboxypeptidases (CPs). These enzymes are responsible for removing terminal dibasic residues. Similar to PCs, there are multiple carboxypeptidase enzymes. The most important CP in peptide hormone maturation is carboxypeptidase E, CPE, which removes C-terminal basic amino acids. Carboxypeptidase E is found in secretory granules, activated by Zn^{2+}, and has an acidic pH optimum. (Canaff 1999)

Mice homozygous for $Ser^{202}Pro$ mutation of the CPE allele demonstrated marked hyperproinsulinemia and developed late onset obesity. Research demonstrated the homozygous mutants lacked CPE enzyme activity along with decreased levels of processed insulin, neurotensin, and melanin-concentration hormone. These results demonstrate that abnormal maturation of neuropeptides and peptide hormones affect overall body regulation, specifically the peptide hormones involved in hunger and feeding. (Rovere 1996) Similar studies demonstrated a link between mutations of CPE to late onset obesity in double mutant mice. (Berman 2001)

Peptidyl glycine α-amidating monooxygenase

Terminal modifications include amidation and pyroglutamate formation. Peptidylglycine α-amidating monooxygenase (PAM) removes C-terminal glycine residues to produce a C-terminal amide, the most common terminal modification. Amidation occurs on over 50% of all neuropeptides. Amidation is a two-step reaction catalyzed by the enzymes α-hydroxylating monooxygenase (PHM) and peptidyl α-amidating lyase (PAL). These two enzymes together form the catalytic unit known as

PAM. (Lindberg 1996) In the reaction first PHM catalyzes hydroxylation of the glycine in a reaction that requires copper, ascorbate, which serves as a nitrogen donor, and molecular oxygen, which serves as an oxidizing agent. Second, PAL, a zinc dependent enzyme, converts the intermediate into the amidated peptide resulting in the release of glyoxylate. (Steveson 2003)

Similar to other processing enzymes, deficiencies in PAM have been linked to various disease states. An increase in amidation activity in human plasma was observed in patients with hypothyroidism and thyroid carcinoma demonstrating a link between proper PAM activity and thyroid health. (Wand 1985) Examination of the relationship between amidation and amyloid peptide neurotoxicity revealed amidation of amyloid peptide reduced the activity due to a decrease in amyloid peptide aggregation but did not alter the neurotoxicity. (Forloni 1997) Microarray studies demonstrated an upregulation of PAM expression in metastic breast cancer. (Hao 2004)

Glutaminyl Cyclase

The final enzyme glutaminyl cyclase (QC) removes N-terminal Gln residues to produce a pyroglutamic acid residue. The formation of this residue is believed to serve a protective function on the N-terminus. Figure 2 demonstrates the action of these enzymes on the maturation of thyrotropin releasing hormone, a peptide hormone requiring the secretory pathway for maturity. (Pohl 1991)

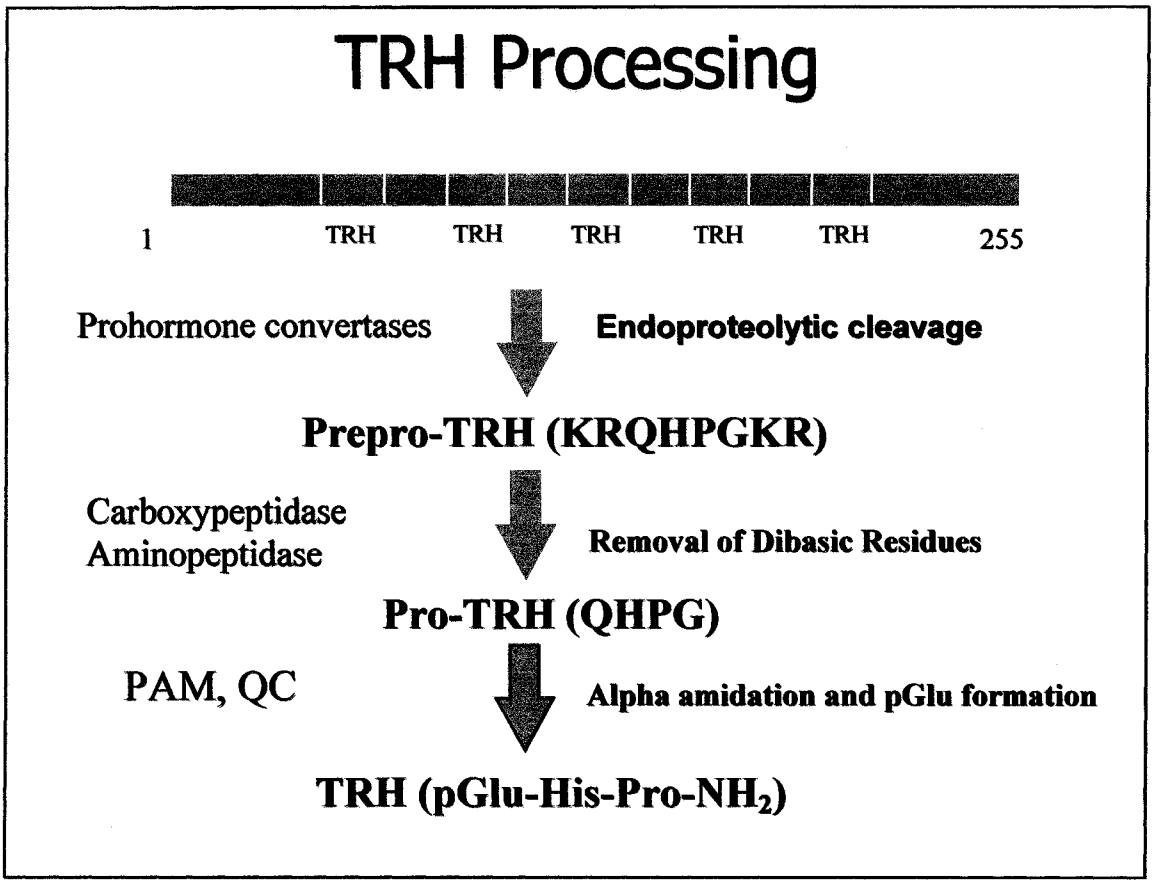

Figure 2: **Thyrotropin-releasing hormone maturation.** Post-translational maturation of thyrotropin-releasing hormone (TRH) from rat brain requires endoproteolytic cleavage of a large precursor by prohormone convertase followed by exoproteolytic cleavage by carboxypeptidases and aminopeptidases. Final maturation requires both PAM and QC for terminal modification. Complete processing results in 5 mature, functional copies of TRH.

Pyroglutamic Acid and Common pGlu Peptides

The common N-terminal secretory pathway modification produces pyroglutamic acid (pGlu), also known as 5-oxo-L-proline or pyrrolidone carboxylic acid. This modified amino acid can be found on the N-terminus of many neuropeptides and peptide

hormones in many species of plants, insects, and mammals. The pGlu modification is formed due to the activity of the enzyme glutaminyl cyclase during protein biosynthesis or as an intermediate in amino aid metabolic and transport pathways. Non-enzymatic cyclization of glutamine has been observed though the level is much slower. The presence of the N-terminal pGlu residue has been shown to be important in receptor binding and/or protection from proteolytic digestion. The table below demonstrates the peptide sequence of many peptides from different species that contain the N-terminal pyroglutamic acid residue.

Table 1: **Common pGlu Peptides.**

Peptide Name	Species	Peptide Sequence
Thyrotropin-releasing hormone	Human	pGlu-His-Pro-NH_2
Gonadotropin-releasing hormone	Human	pGlu-His-Trp-Ser-Tyr-Gly-Leu-Arg-Pro-Gly-NH_2
Gastrin I	Human	pGlu-Gly-Pro-Trp-Leu-$(Glu)_5$-Ala-Tyr-Gly-Trp-Met-Asp-Phe-NH_2
Fertilization promoting peptide	Human	pGlu-Glu-Pro-NH_2
Morphogenetic neuropeptides	Human	pGlu-Pro-Pro-Gly-Gly-Ser-Lys-Val-Ile-Leu-Phe
Neuropeptide	Human	pGlu-Pro-Pro-Gly
Stem cell inhibitory peptide	Human	pGlu-Glu-Asp-Cys-Lys
Growth-hormone releasing factor	Human	pGlu-Gln-Gly-Glu-Ser-Asn-Gln-Glu-Arg-Gly-Ala-Arg-Ala-Arg-Ala-Arg-Leu-NH_2
Growth-inhibiting pentapeptide	Mouse	pGlu-Glu-Asp-Ser-Gly-OH
Caerulin-like peptide	Amphibian	pGlu-Asp-Tyr-(HSO_3)-Lys-Gly-Trp-Met-Asp-Phe-NH_2
Adipokinetic hormone	Insect	pGlu-Lys-Thr-Phe-Ser-Pro-Asp-Trp-NH_2
Leucosulfakinin-II	Insect	pGlu-Ser-Asp-Asp-Tyr-(SO_3H)-Gly-His-Met-Arg-Phe-NH_2
Corazonin	Insect	pGlu-Thr-Phe-Gln-Tyr-Ser-Arg-Gly-Trp-Thr-Asn-NH_2
Chitinase	Plant	pGlu-Cys-Glu-Thr-Thr-Ile-Tyr-Cys-Cys-Ser-Gln-His...

Evidence of QC involvement in various disease states

Evidence of the involvement of QC, one of the important post-translational processing enzymes, has been observed in many different disease states including Alzheimer's disease, cancer, fat, and bone mineral density. Initial studies with β-amyloid

peptide (Aβ), the peptide commonly found in senile plaques, revealed the dominant form of the peptide contained a modified glutamate residue at the amino-terminal third position. The modified Aβ peptide was believed to be more likely to be deposited into senile plaques than the unmodified peptide due to its increase in hydrophobicity. (Saido 1995) Further studies confirmed the pyroglutamate modification of the glutamate residue in over 50% of Aβ accumulated in senile plaques. This study also revealed the amino-terminal modification greatly influenced toxicity, interaction with cell membranes, and degradation in Aβ peptides. (Russo 2002) These observations led to the investigation of the role of QC in senile plaque formation. Human QC expressed in both yeast and bacterial expression systems and papaya QC were tested with an Aβ peptide containing a glutamate residue. Experimental evidence demonstrated the glutamate was converted to pyroglutamate at a pH of 6.0 in the presence of both enzymes. This provided the first evidence for the conversion of glutamate instead of glutamine. (Schilling 2004) To further investigate the possible involvement of QC in the formation of pGlu-modified Aβ peptides researchers tested the effect of QC inhibitors *in vivo*. Using mammalian cells expressing the unmodified Aβ peptide, QC activity was investigated using a HPLC method. Once the conversion of the Aβ peptides was confirmed, various QC inhibitors were added. These inhibitors decreased the amount of Aβ peptide conversion. (Cynis 2006)

Various studies have revealed a possible link between cancer and QC. An early study revealed that pGlu modifications were essential for chemotaxis and protection from degradation in human monocyte chemotactic protein (MCP-2). (Coillie 1998) This study suggested a possible role of pGlu modifications and QC in cancer progression.

Microarray studies revealed that a ten-fold increase in QC expression occurs in melanocytes when compared to normal cells suggesting a possible role of QC in these cell types. (Curto 2002) Gene expression profiling of breast cancer cells, β-catenin expressing cancer cells, and thyroid cancer cells also revealed a similar upregulation of QC expression. (Lee 2003; Chamorro 2005; Jarzab 2005)

A link between QC and fat regulatory genes was established by a genome-wide analysis of *C. elegans* fat regulatory genes. This study used RNAi to disrupt the expression of 16,757 genes necessary for normal fat storage. Disruption of QC expression resulted in a decrease in the amount of fat stored in high fat mutants suggesting QC is involved in the storage of fat in *C. elegans*. (Ashrafi 2003)

Bone mineral density (BMD) is a key signature of osteoporosis. Studies of adult women with low radial BMD have demonstrated variations in the QC gene of the pituitary play a potential pathogenic role in osteoporosis. Using regression analyses, several SNPs of the QC gene were suggested to determine, in combination with other factors, the radial BMD. Overall it is suggested that QC may contribute to the susceptibility of osteoporosis. (Ezura 2004)

Glutaminyl cyclase

Discovery and Early Research

Glutaminyl cyclase (QC) (E.C. 2.3.2.5) is responsible for post-translational cyclization of amino terminal glutaminyl residues forming pyroglutamic acid. The first evidence of an enzyme responsible for such a conversion occurred in 1938 when Damodaran et al. observed ammonia formation due to proteolysis of wheat gluten in the

presence of crude papain. (Damodaran 1938) This discovery was followed in 1963 with the publication of enzymatic cyclization of glutamine and glutaminyl peptides. (Messer 1963) In 1965 glutaminyl cyclase was first identified and purified from dried papaya latex demonstrating QC activity in plants. (Messer 1965) This was followed by observation of QC activity in different mammalian tissues (Busby Jr. 1987; Bockers 1995) and bacteria (Chen 1989; Beck 1994). Though the amino acid sequence of plant and bacterial QCs varies substantially from mammalian QCs, the amino acid sequence of QCs is highly conserved from yeasts to humans. Figure 3 demonstrates an amino acid alignment for QC from various species demonstrating the conservation of the sequences.

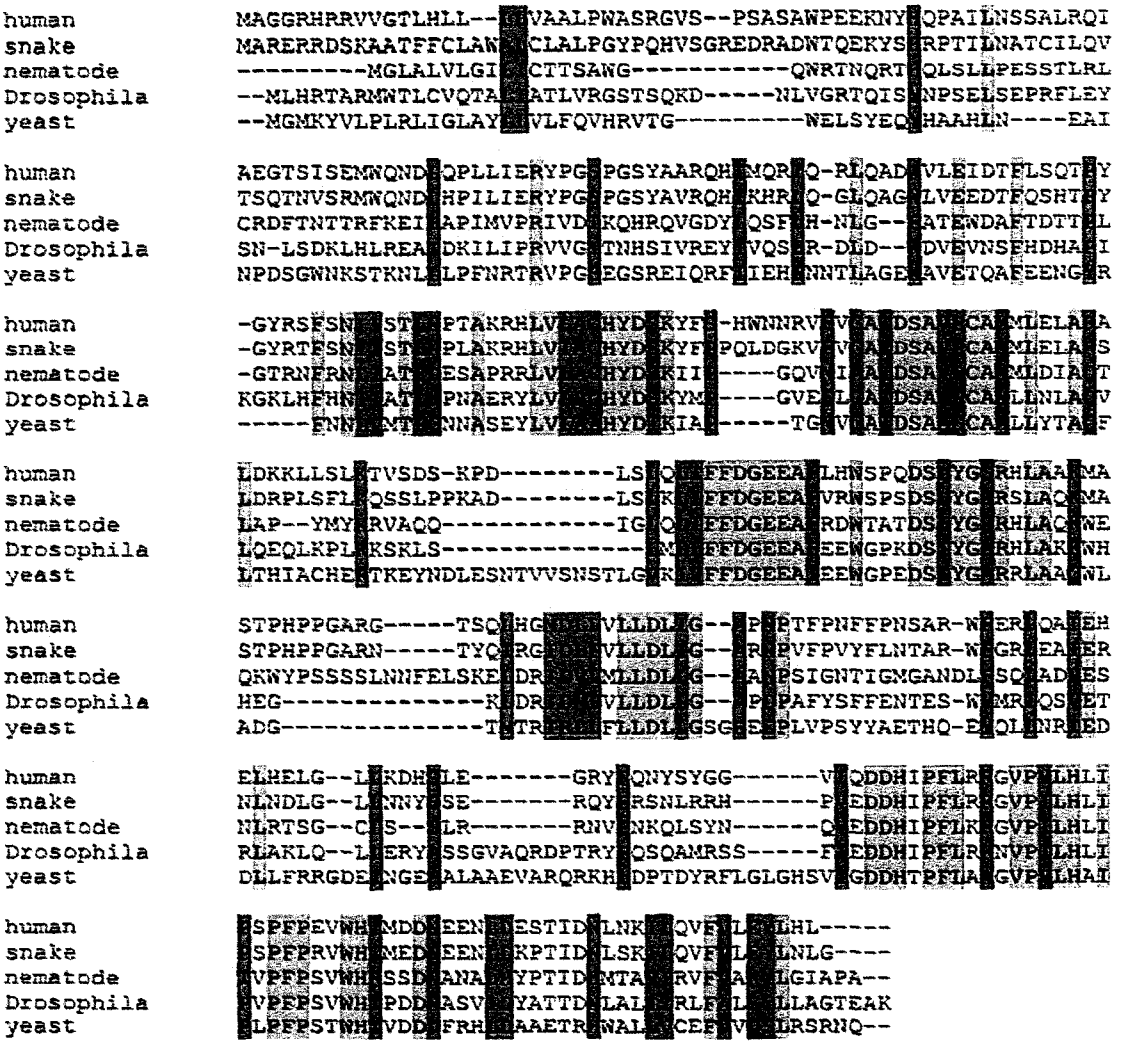

Figure 3: **Protein sequence alignment QC from various sources.** The sequence of QC from yeasts to humans is highly conserved and differs significantly from plant and bacterial QCs. The light shaded areas represent areas of sequence identity among all species. The darker shaded areas represent areas of high sequence homology representing substitutions in only one sequence. The alignment was produced using Clustal W.

Plant Glutaminyl Cyclase

Plant QCs appear to serve a different function than animal QCs due to the lack of nervous system and/or peptide hormones in plants. While attempting to determine the physiological function of plant QCs, Armani et al. first demonstrated the rate of spontaneous N-terminal glutamine cyclization was too slow to account for the observed *in vivo* cyclization. Furthermore, the presence of the pGlu peptides in seed storage proteins suggested a role for QC in plant protein storage and secretion. Other proposed functions include specificity of binding and protection from proteolysis. (Amrani 1997)

Research involving plant glutaminyl cyclase began with the purification of papaya QC. Papaya QC, a basic protein with pI near 9.0, was purified by cation exchange chromatography. Gel filtration chromatography was used to determine the size of papaya QC at approximately 25 kDa. Papaya QC is stable in the pH range from 4 to 11 with its optimum activity around 8.4 – 9.4, depending on substrate. (Messer 1965) Substrate specificity studies and kinetic analyses of purified papaya QC (Gololobov 1994; Gololobov 1996) revealed similar parameters to the purified mammalian QCs. (Busby Jr. 1987; Fischer 1987) The enzymatic mechanism of papaya QC was proposed to involve a simple intramolecular cyclization of the glutamine residue to a pyroglutamic acid residue from studies on pH and temperature dependency, proton inventory, and molecular modeling rather than the alternative double-displacement mechanism. (Gololobov 1994)

Further studies of plant QCs resulted in the purification of papaya QC to near homogeneity allowing further characterization and stability studies. Research revealed the protein lacked disulfide bridges and covalently linked phosphate groups. The extreme stability of the protein was further demonstrated by the resistance to proteolysis

by papaya cysteine proteinases, trypsin, and chymotrypsin. Spectral studies demonstrated papaya QC was composed of greater than 50% β-sheets and less than 5% α-helices, quite different from the predicted structure of mammalian QCs at the time. (Oberg 1998; Zerhouni 1998) These results were verified by the elucidation of the papaya QC crystal structure. (Azarkan 2005; Wintjens 2006) Further plant QCs were identified in *Arabidopsis thaliana*, *Glycine max*, *Solanum lycopersicum*, *Lotus japonicus*, and *Zea mays* based on similarities in DNA sequence.

In 2006 the crystal structure of *C. papaya*, shown in figure 4, was resolved providing the first crystal structure for the plant, bacteria, and parasite QC archetype. The structure was shown to contain a five-bladed beta-propeller coordinating one zinc ion, with two additional alpha-helices and one beta hairpin. The zinc was determined to maintain a role in the structural integrity of the enzyme along with other structural features observed such as large hydrophobic pockets. The enzyme active site was deduced by structure with Tris inhibitor bound and sequence alignment. Highly conserved residues such as W83, W110, W169, Q24, E69, N155, K225, F22 and F67 have a suggestive role in catalysis. (Wintjens 2006) The crystal structure of the plant QC demonstrated major differences when compared to the predicted structure of human QC provided by Booth et al. (Booth 2004)

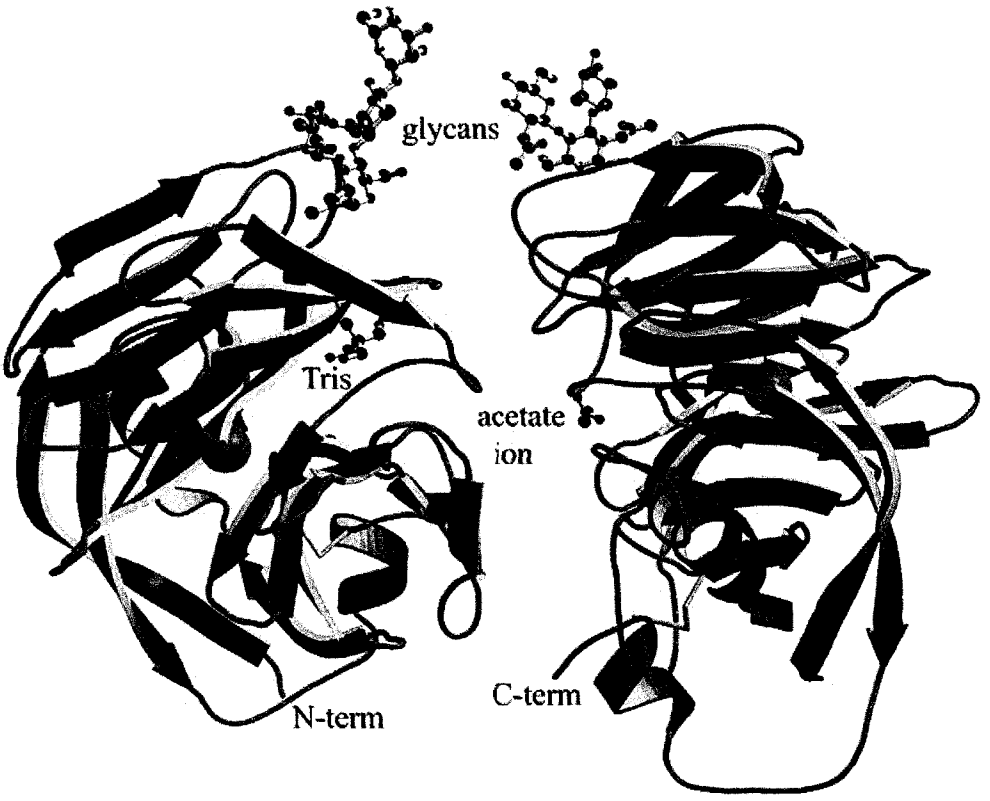

Figure 4: **Crystal Structure of *C. papaya* QC.** Crystal structure of *C. papaya* QC dimer bound to inhibitor Tris and acetate ion. The active site region is located near the inhibitor binding site.

Bacterial Glutaminyl Cyclase

The cyclization of glutamine to pyroglutamic acid with ammonia release was observed in 1989 in *Streptococcus bovis*. (Chen 1989) Though the enzyme has not been isolated from this species, protein sequence homology searches reveal sequences in many different bacteria, including *Streptococcus* and *Caulobacter*, with high amino acid sequence homology to plant QC. However, as seen with plants, the bacterial QCs do not have a high sequence identity with mammalian QCs. This suggests the bacterial QCs and plant QCs may have evolved from a common ancestor. The protein sequence alignment

of selected plant and bacterial QCs is shown below with the human QC protein sequence. The alignment demonstrates a 61% identity among *C. papaya* and *A. thaliana* protein sequences. The *C. crescentus* and *S. pyogenes* QC sequences contain a 43% and 30% sequence identity with the *C. papaya* sequence. The plant and bacterial sequences all have less than 10% sequence identity with the human QC. Figure 5 represents the amino acid sequence alignment for the plant and bacterial QCs.

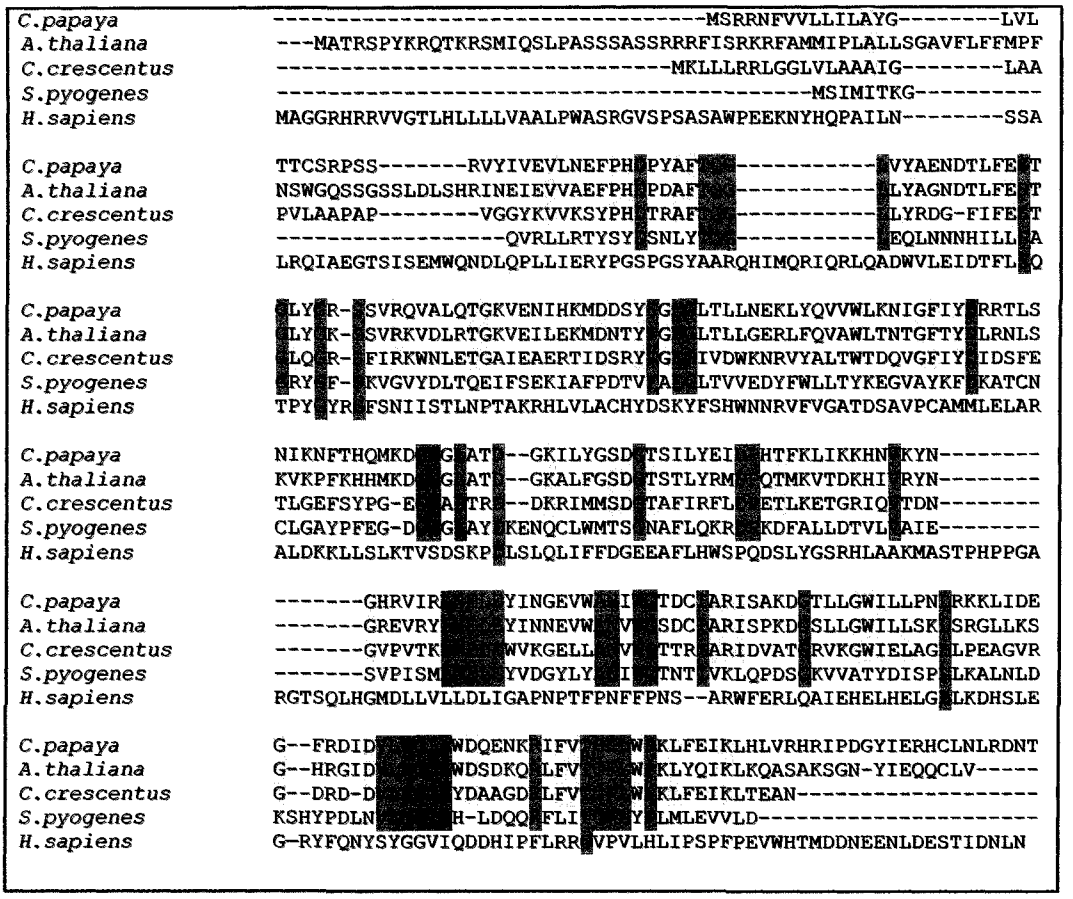

Figure 5: **Protein sequence alignment of plant and bacterial QC.** Dark shaded areas represent areas of sequence identity among all plant and bacterial species. Light shaded areas represent areas of conserved substitutions within the plant and bacterial proteins. Sequences include *C. papaya* (AAC27745), *A. thaliana* (NP_567727.1), *C. crescentus* (AAK24617), *S. pyogenes* (AAK33505). *H. sapiens* QC protein sequence is included for comparison. The alignment was produced using the Clustal W program.

Mammalian Glutaminyl Cyclase

A mammalian QC capable of converting N-terminal glutamine residues to pyroglutamic acid residues was independently discovered in 1987 in bovine pituitary and rat hypothalamus by Fischer et al. (Fischer 1987) and pig pituitary, rat brain, and human B-lymphocytes by Busby et al. (Busby 1987). Fisher et al. demonstrated the QC activity by monitoring conversion of Gln-GnRH to pGlu-GnRH by reverse-phase HPLC. The QC from bovine pituitary had a molecular weight of 43,000 – 55,000 Daltons verified by gel filtration and a pH optimum of 8.0. Kinetic studies revealed the QC followed Michaelis-Menten kinetics with a Km value of 63 uM and Vmax of 690 pmol/ug/hour. These results were confirmed by substrate specificity studies. These studies also demonstrate the QC was not able to act on internal glutamine residues suggesting QC activity occurred in the later stages of processing. Subcellular distribution studies revealed the QC was fractioned along with secretory granules. Vesicle lysis without detergent resulted in release of QC indicating QC was not an integral membrane protein. Inhibition studies revealed addition of ATP, glucose-6-phosphate dehydrogenase, glucose, $NADP^+$, or EDTA had minimal effect on enzyme catalysis. (Fischer 1987)

Busby et al. further confirmed the N-terminal cyclization reaction occurred very slowly under physiological conditions using the conversion of Gln-His-Pro-NH_2 to pGlu-His-Pro-NH_2 for analysis. Addition of a QC enzyme from pig pituitary, rat brain, and B-lymphocytes catalyzed this reaction. Porcine pituitary QC was shown to be a glycoprotein with molecular weight 55,000 Daltons measured by gel filtration and a pH optimum of 7.2 – 7.5. Affinity studies also identified important sulfhydryls within the enzyme. Enzyme activity was rapidly lost below pH 5.0 and above pH 8.0. Further

purification by DEAE chromatography using step gradients resulted in two activity peaks with Km and Vmax values of 0.2 mM and 0.038 umol/mg/min for peak 1 and 0.6 mM and 0.023 umol/mg/min for peak 2, respectively. DEAE purification of QC from human B-lymphocytes resulted in one peak of activity with specific activity of 0.015 nmol/hr/ug. Inhibition studies revealed inhibition by 1,10-orthophenanthroline and stimulation by EDTA for the human QC. In preliminary studies, QC from bovine adrenal medulla was contained in the soluble chromaffin vesicle fraction further suggesting the inclusion of QC in secretory pathway processing. (Busby 1987)

Preliminary work relied on radioimmunoassay and HPLC analyses to study QC activity. In 1988, a radioimmunoassay was presented by Koger et al. (Koger 1989). Independently Consalvo et al. developed an improved HPLC assay. In this assay both model peptide substrate containing N-terminal glutamine residues and product containing N-terminal pyroglutamate residues were monitored by HPLC with fluorometric detection. (Consalvo 1988) Shortly following a coupled spectrophotometric assay for QC was published by Bateman in 1989. This assay utilized the liberation of ammonia upon N-terminal glutamine cyclization of a substrate. A second reaction, involving α-ketoglutarate, glutamate dehydrogenase, and NADH, using the ammonia, produced glutamate and NAD^+. The NADH oxidation followed at 340 nm allowed the QC activity to be quantified. (Bateman 1989)

In 1991, Pohl et al. purified QC to homogeneity from bovine anterior pituitary. Purification included extraction from bovine anterior pituitary secretroy granules followed by various FPLC techniques and IEF-PAGE under non-denaturing conditions and SDS-PAGE. The resulting protein was used as a probe to isolate a 2088 bp cDNA

clone from an anterior pituitary cDNA library. Transfection of COS-7 monkey cells with the predicted QC cDNA construct resulted in expression of a 361 amino acid protein with QC activity. Nucleotide sequencing revealed the first 27/28 amino acids contained features of an endoplasmic recticulum signal sequence. Using Northern blot analyses various bovine brain regions were probed with QC mRNA demonstrating the highest expression levels found in anterior pituitary and striatum. QC mRNA was also expressed in lower levels in neurointermediate pituitary, cerebral cortex, hypothalamus, anterior and posterior thalamus, cerebellum, hippocampus, and retina. QC mRNA was observed to a small extent in brain stem, heart atrium, heart ventricle, kidney, thymus, and skeletal muscle. No expression was observed in spleen, lung, or liver. These expression patterns are similar to those of PAM. This observation along with the signal sequence prediction and substrate specificity studies further indicate QC is involved in secretory pathway post-translational enzyme processing. (Pohl 1991)

In 1994, Song et al. expressed human pituitary QC by isolating a human pituitary cDNA clone from a human pituitary cDNA library. The human QC sequence was predicted by screening the human library with primers designed against the bovine QC sequence. The cDNA coded for a 361 amino acid protein of molecular mass 40,876 Daltons. Expression of two QC constructs, one containing a maltose binding protein (MBP) domain and another containing a poly-hisitidine tag, in bacteria resulted in purification of active enzyme by affinity chromatography. Expression was confirmed by western blot using polyclonal peptide antibodies raised against the bovine QC sequence. The MBP-hQC was 83,000 Daltons and the poly-His-hQC was 40,000 Daltons had specific activities of 10 nmol/min/mg and 1500 nmol/min/mg, respectively. Substrate

specificity studies revealed the poly-His-hQC had no detectable reactivity with substrate containing an N-terminal glutamate residue or large aromatic groups in the second position. Kinetic studies of various substrates revealed a k_{cat}/K_m of 85.5 $min^{-1}mM^{-1}$ for Gln-Gln-Gln, 79.5 $min^{-1}mM^{-1}$ for Gln-Gln, 58.6 $min^{-1}mM^{-1}$ for Gln-Ala, 11.7 $min^{-1}mM^{-1}$ for Gln-Gly, and 4.61 $min^{-1}mM^{-1}$ for Gln-NH_2. (Song 1994)

Further examination of expression levels of QC in bovine and porcine pituitary and hypothalamus was completed using immunocytochemistry and *in situ* hybridization. QC was found more abundant in pituitary than hypothalamus. These studies revealed a specific pattern of QC expression in certain cell types suggesting the QC N-terminal conversion is less widespread than the PAM C-terminal conversion. The high expression levels of QC did not coincide with the highest levels of known pyroglutamate peptides. (Bockers 1995)

Sequence analyses of mammalian QCs by Temple et al. revealed the conservation of two cysteine residues among all sequences. Using a poly-His-hQC heterologous protein, the two cysteine residues were mutated demonstrating a slight decrease in enzyme activity. These results suggest the two thiols are not essential for catalytic activity. (Temple 1998)

Bovine QC tissue distribution was examined by immunoreactivity and enzyme activity in 1999 by Sykes et al. QC was observed to be abundant in the brain and pituitary by both methods. Antibody specificity was observed in bovine hippocampus, hypothalamus, kidney, striatum, and anterior pituitary. The specific activity of bovine QC ranged from 60 nmol/min/mg to 3 nmol/min/mg in order of decreasing activity from

thymus, hippocampus, hypothalamus, kidney, striatum, adrenal, spleen, anterior pituitary, and thyroid. (Sykes 1999)

In 2002, three continuous spectrophotometric assays were developed to monitor QC acitivity. In these assays, one chromogenic substrate, glutamine-p-nitroanilide (Gln-pNA), and two fluorogenic substrates, glutaminyl-2-naphthylamide (Gln-BNA) and glutaminyl-4-methylcoumarinelamide (Gln-AMC) were used to follow QC activity. All assays required the addition of a secondary enzyme, pyroglutamate aminopeptidase, to release the chromogenic or fluorogenic component monitored. (Schilling 2002)

Expression studies in bacteria and yeasts were followed by the expression of human QC in insect cells. Booth et al. completed the expression of human QC in *Drosophila* S2 cell culture under the control of an inducible promoter and fused to a BiP secretion signal. Purification of human QC was completed with dye affinity chromatography directly from cell culture. The fully active enzyme was 37,000 Daltons and confirmed by peptide mass mapping and Western blotting. The enzyme was confirmed to contain a disulfide bond and contained one glycosylated asparagine residue, N49, verified by enzymatic deglycosylation and amino acid mutation. (Booth 2003)

Snake venom glutaminyl cyclase was identified in 2006. The presence of QC in venom glands was predicted due to the presence of various pyroglutamate containing peptides in snake venom. This study resulted in cDNA isolation and enzyme expression in bacterial expression system. Expressed protein was verified by sequencing and aligned with known QCs demonstrating the evidence of QC in peripheral tissues. (Pawlak 2006)

Enzymatic Reaction and Inhibition Studies

Initial insights into the QC mechanism were provided by Temple et al. Due to the problem of protein expression in inclusion bodies with previous bacterial expression of human QC, another hQC construct using the glutathione-S-transferase (GST) fusion protein was developed. Affinity purification using the sepahrose-4B glutathione column resulted in purification of hQC-GST with specific activity of 1000 nmol/min/mg. The expressed protein was sensitive to DEPC and acetyl-imidazole suggesting the involvement of histidines or tyrosines and a possible acid/base catalysis mechanism. (Temple 1998)

Further evaluation of the QC mechanism revealed essential histidine residues in human pituitary QC. Treatment with DEPC inactivated recombinant human QC with the modification of three essential histidine residues. However, sequence analyses revealed four conserved histidines among mammalian QCs. Mutational studies of all four histidine residues to glutamine residues resulted in two inactive enzymes (H140→Q140 and H330→Q) and two enzymes with increased Km values (H307→Q and H319→Q). These results suggested the H140 and H330 played a role in catalysis and H307 and H319 played a role in substrate binding. (Bateman 2001)

Further studies revealed evidence for a disulfide bond important to catalytic activity. Schilling et al. expressed human QC in the secretory pathway of yeasts. Following purification, recombinant QC was analyzed by MALDI-TOF to verify correct proteolytic processing resulting in a 38,795 Daltons protein containing N-glycosylation at both predicted sites and CD spectroscopy to verify correct secondary structure. The enzyme had similar kinetic values to human QC expressed in bacteria. Enzyme activity

was almost completely eliminated by addition of DTT suggesting the presence of an important disulfide bond. Fluoresence spectra suggest the loss of enzyme activity is due to change in protein conformational change. (Schilling 2002)

In 2003, inhibition studies identified human QC as a metalloenzyme. Heterocyclic chelators such as 1,10-phenanthroline and dipicolinic acid were shown to inhibit QC in a time-dependent manner while EDTA effect was negligible. The presence of Zn^{+2} resulted in reactivation of inactivated enzyme while Co^{+2} and Mn^{+2} had little effect on enzyme activity. These results demonstrate the importance of the Zn^{+2} in enzyme catalysis. Competitive inhibition was demonstrated with imidazole and imidazole derivatives. (Schilling 2003) Furthermore, these results provide some insight into the mutation studies by Bateman et al. suggesting the mutated His140 and His330 are necessary for metal binding. (Bateman 2001)

Schilling et al. suggest a mechanism in which the metal ion interacts with the nitrogen to provide the correct positioning of the nitrogen to the γ-carbonyl carbon. An alternative suggestion is that the metal polarizes the γ-amide group of the substrate while stabilizing the oxanion formed by nucleophilic attack of the α-nitrogen on the γ-carbonyl carbon. The QC reaction proposed by Schilling is shown in figure 6.

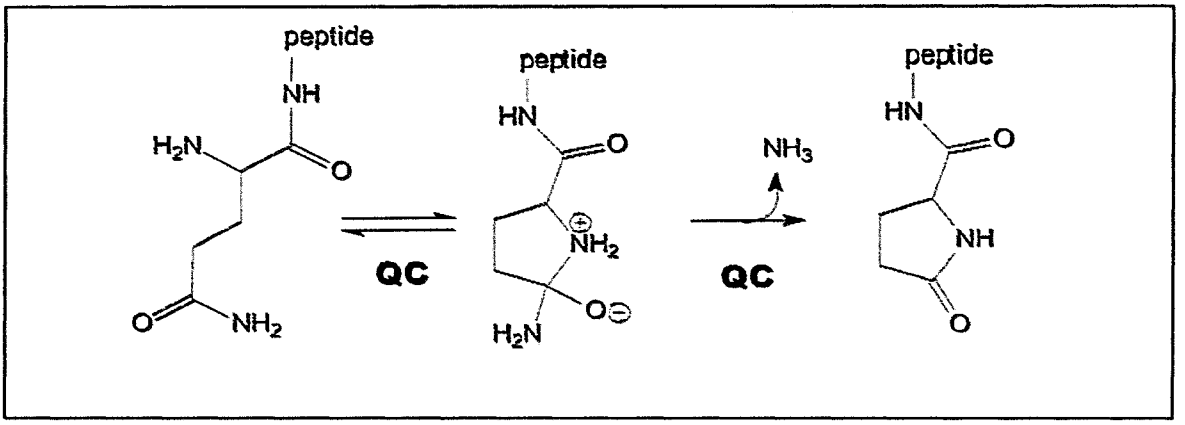

Figure 6: **Glutaminyl Cyclase Reaction.** The enzymatic reaction of glutaminyl cyclase including the predicted intermediate. (Schilling 2003)

Substrate specificity studies were completed by Schilling et al. in 2003 for both plant and mammalian QCs. Experiments demonstrated nearly all dipeptides and tripeptides tested were more reactive with the papaya QC. Higher turnover numbers were observed for substrates containing large hydrophobic residues C-terminal to the N-terminal glutamine. Both plant and mammalian QCs had similar specificity constants for oligopeptides. Mammalian QC activity was highly dependent on substrate size and pH compared to papaya QC, whereas a similar dependence on ionic strength was observed between enzymes from the two species. (Schilling 2003)

Isolation of murine QC presented further information absent of specific catalytic properties and inhibitors for mammalian QCs. Murine QC (mQC) was identified in an insulinoma cell line by enzymatic activity. RT-PCR was used to amplify the gene from the cell line and expression in yeast resulted in purification of the mQC. Murine QC is a glycoprotein of approximately 36,000 Daltons. Specificity studies demonstrated the specificity constants of mQC were somewhat lower than hQC. Similar to hQC, the mQC

demonstrated a low specificity for dipeptides and slightly higher specificity for longer peptides. Competitive inhibition was observed in the presence of imidazole derivatives, with slightly stronger inhibition observed for 1-substituted imidazole derivatives. Metal chelators 1,10-phenathroline and dipicolinic acid also inhibited mQC, but EDTA did not. Murine QC was also competitively inhibited by cystamine and several cystamine derivatives containing both an amino and thiol group. Inhibition by thiols has been observed in several aminopeptidase species. Such inhibition had not been observed for other mammalian QCs. Isolation of mQC also verified the presence of one zinc ion per catalytic unit of mammalian QC. (Schilling 2005)

Human QC Crystal Structure

Crystal structure isolation of human QC followed the expression of human QC isolated from bone marrow in a bacterial system. A bacterial construct containing human QC and a fused with a poly-histidine tag and FactorXa was developed allowing high level expression and purification of enzyme near homogeneity. The enzyme was verified by both enzymatic and structural examination. (Huang 2005)

Human QC crystal structures were presented in free-form, bound to substrate, and bound to three different imidazole inhibitors providing more definitive evidence of enzyme mechanism. Human QC structure revealed an α/β scaffold similar to that of zinc aminopeptidases. (Huang 2005) These results validated those of Booth et al. (Booth 2004) Two different binding modes were also identified due to different orientations of the Trp207 indole ring. (Huang 2005)

The authors identified specific residues important in binding and/or substrate stabilization and catalytic residues. The enzyme active site contains a single zinc ion coordinated by one water molecule and three conserved residues, Asp159, His330, and Glu202. The zinc bound water molecule is replaced during inhibitor binding. The authors propose a catalytic mechanism in which the conserved Glu201 transfers a proton from the α-amino group of the substrate to the leaving amide group. The zinc ion then stabilizes the substrate while a conserved Asp248 stabilizes the leaving amide group. (Huang 2005) A kinemage developed from the crystal structure is shown in figure 7.

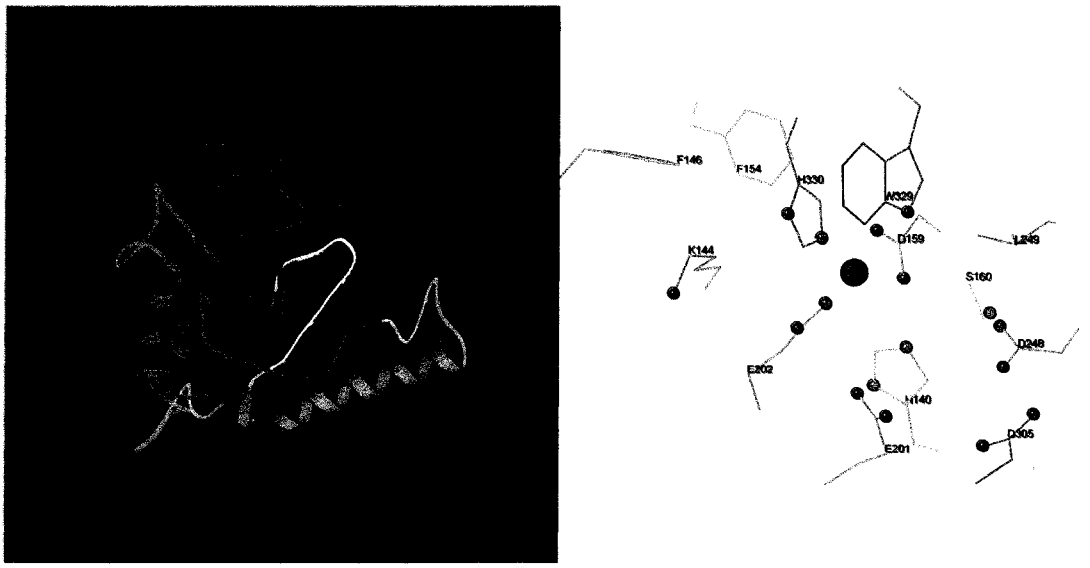

Figure 7: **Crystal Structure of human QC.** The image on the left represents the overall 3-D structure of human QC (PDB ID 2AFO). The image on the right represents the active site residues of the structure in teal with amino acid type and number and the zinc ion in purple.

Relationship to Bacterial Aminopeptidase

Human QC and a bacterial zinc aminopeptidase have been shown to share a common fold and active site though less than 16% sequence conservation is observed. (Booth 2004) This relationship could hold some clues about the evolution of the enzymes. The following study utilized a predicted 3-D structure of human QC expressed in *Drosophila* S2 cells. (Booth 2003) Overlay of the human QC 3-D structure with the bacterial aminopeptidase from *Aeromonas proteolytica* revealed a similar fold consisting of a central 8-stranded β-sheet surrounded by six α-helices on one side and three on the other with the active site located at the C-terminal end of the central two strands of the β-sheet. No similar overlay was identified between the plant QCs and bacterial zinc aminopeptidases. (Booth 2004) The human QC and bacterial aminopeptidase overlay is shown in figure 8.

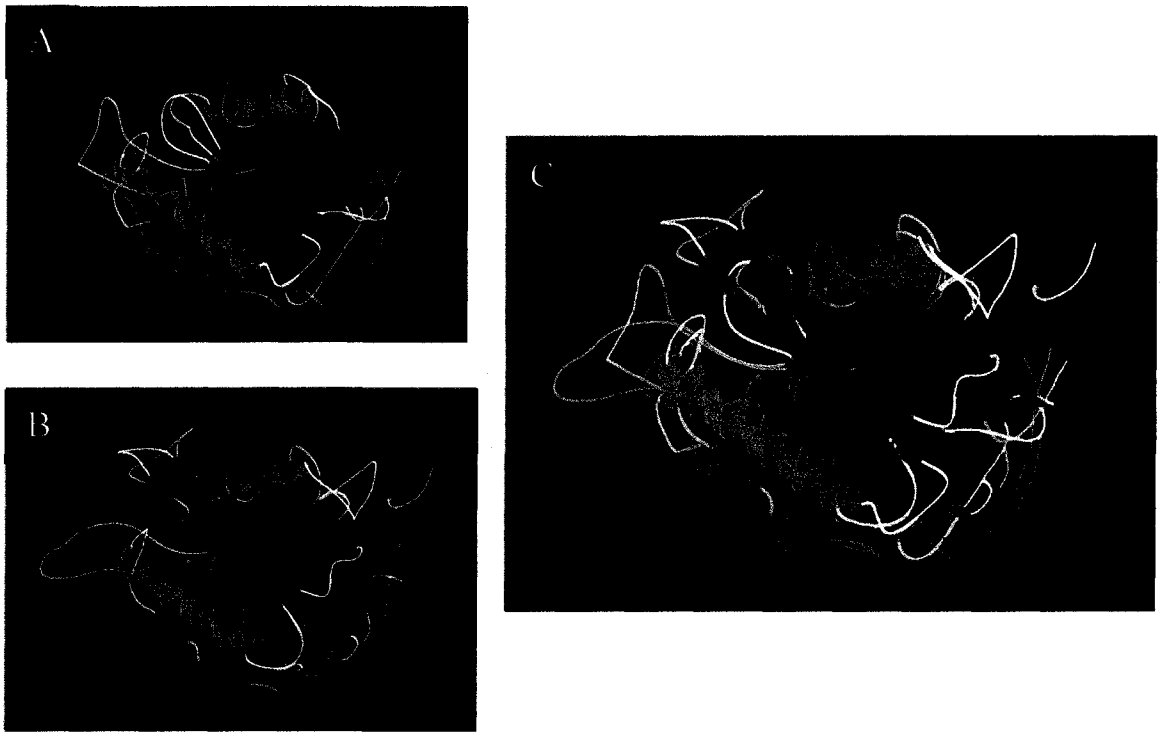

Figure 8: **Structure of human QC and zinc bacterial aminopeptidase.** (A) The predicted 3-D structure of human QC. (B) The predicted 3-D structure of zinc bacterial aminopeptidase. (C) Overlay of human QC and zinc bacterial aminopeptidase.

The amino acids within the hQC active site were also conserved within the predicted 3-D structure compared to the active site of the bacterial zinc aminopeptidase. Several of the conserved residues bind two zinc metals in the aminopeptidase, though only one metal has been identified in hQC. (Booth 2004)

Both human QC and bacterial aminopeptidase are both inhibited by metal chelators such as 1,10-phenanthroline, dipicolinic acid. This further suggests a relationship between enzymatic activity which is most likely due to the importance of Zn^{+2} for catalysis of both enzymes. (Schilling 2003)

Multiple Isoforms

Database analyses have revealed multiple isoforms of QC in many different species including humans, mice, cows, *Drosophila*, etc. The isoforms appear on different chromosomes in all species suggesting the presence of an isoform does not represent a gene duplication event. Amino acid sequence alignments reveal the conservation of all catalytic residues and most important binding residues identified by human QC crystal structure and mutagenesis studies. This suggests a conservation of enzyme activity and catalysis. Shown in figure 9 are example amino acid alignments of the human QC isoforms and *Drosophila* QC isoforms.

```
Human QC     MRSGGRGRPRLRLGERGLMEPLLPPKRRLLPRVRLLPLLLALAVGSAFYTIWSGWHR
Human QC-LK -MAGGR------------------HRRVVGTLHLLLLVAALPWAS------RGVSP

Human QC     RTEELPLGRELRVPLIGSLPEARLRRVVGQLDPQRLWSTYLRPLLVVRTPGSPGNLQ
Human QC-LK SASAWPEEKNYHQPAI--LNSSALRQIAEGTSISEMWQNDLQPLLIERYPGSPGSYA

Human QC     VRKFLEATLRSLTAGWHVELDPFTASTPLGPVDFGNVVATLDPRAARHLTLACHYDS
Human QC-LK ARQHIMQRIQRLQADWVLEIDTFLSQTPYGYRSFSNIISTLNPTAKRHLVLACHYDS

Human QC     KLFPPGS-TPFVGATDSAVPCALLLELAQALD---LELSRAKKQAAPVTLQLLFLDG
Human QC-LK KYFSHWNNRVFVGATDSAVPCAMMLELARALDKKLLSLKTVSDSKPDLSLQLIFFDG

Human QC     EEALKEWGPKDSLYGSRHLAQLMESIPHSP---GPTRIQAIELFMLLDLLGAPNPTF
Human QC-LK EEAFLHWSPQDSLYGSRHLAAKMASTPHPPGARGTSQLHGMDLLVLLDLIGAPNPTF

Human QC     YSHFPRTVRWFHRLRSIEKRLHRLNLLQSHPQEVMYFQPGEPFGSVEDDHIPFLRRG
Human QC-LK PNFFPNSARWFERLQAIEHELHELGLLKDHSLEGRYFQNYSYGGVIQDDHIPFLRRG

Human QC     VPVLHLISTPFPAVWHTPADTEVNLHPPTVHNLCRILAVFLAEYLGL
Human QC-LK VPVLHLIPSPFPEVWHTMDDNEENLDESTIDNLNKILQVFVLEYLHL
```

```
dQC      MRLLLRNYSLMEAVKRLLPRPRKKIYNLGACFELVDIPKISYNPSELSEPRFLEYSNLSD
dQCLK    --MAIGSVVFAAAGLLLLLLP--------PSHQQATAGNIG---SQWRD----------D

dQC      KLHLREAIDKILIPRVVGTTNHSIVREYIVQSLRDLDWDVEVNSFHDHAPIKGKLHFHNI
dQCLK    EVHFNRTLDSILVPRVVGSRGHQQVREYLVQSLNGLGFQTEVDEFKQRVPVFGELTFANV

dQC      IATLNPNAERYLVLSCHYDSKYMPG-VEFLGATDSAVPCAMLLNLAQVLQEQLKPLKK--
dQCLK    VGTINPQAQNFLALACHYDSKYFPNDPGFVGATDSAVPCAILLNTAKTLGAYLQKEFRNR

dQC      SKLSLMLLFFDGEEAFEEWGPKDSIYGARHLAKKWHHEG----------KLDRIDMLVLL
dQCLK    SDVGLMLIFFDGEEAFKEWTDADSVYGSKHLAAKLASKRSGSQAQLAPRNIDRIEVLVLL

dQC      DLLGAPDPAFYSFFENTESWYMRIQSVETRLAKLQLLERYASSGVAQRDPTRYFQSQAMR
dQCLK    DLIGARNPKFSSFYENTDGLHSSLVQIEKSLRTAGQLE----------GNNNMFLSRVS-

dQC      SSFIEDDHIPFLRRNVPILHLIPVPFPSVWHTPDDNASVIDYATTDNLALIIRLFALEYL
dQCLK    GGLVDDDHRPFLDENVPVLHLVATPFPDVWHTPRDNAANLHWPSIRNFNRVFRNFVYQYL

dQC      LAGTEAK-------
dQCLK    KRHTSPVNLRFYRT
```

Figure 9: **Alignments of QC-Isoforms.** Top alignment demonstrates the amino acid sequence alignment of human QC with isoforms. The bottom amino acid sequence alignment demonstrates the two *Drosophila* QC isoforms. Conserved amino acids are highlighted in grey.

QC Knock-out Data and QC Microarray Data

Human microarray data

Localization and relative expression levels of several gene products have been analyzed through the use of microarray and *in situ* hybridization studies. Microarray studies characterizing the human QC gene have been primarily involved in studying QC levels in various disease states compared to normal tissue. Therefore, relative expression levels for different cell types in humans are not available.

Drosophila microarray data

Microarray studies have demonstrated the relative expression levels of one isoform of *Drosophila* QC's (CG32412) mRNA in adult *Drosophila melanogaster*. Table 2 demonstrates the tissue studies, relative mRNA levels detected, and enrichment for the microarray study of gene CG32412. (Chintapalli 2007). Values greater than 100 were considered abundant and values greater than 1000 were considered remarkable. This study demonstrated the most significant expression levels of mRNA in the crop, ovaries, hindgut, head, male accessory glands, adult carcass, larval fat body, and testis in descending order. The enrichment value demonstrates the intensity of the signal in the tissue examined compared to the whole fly. No experiments were completed for the other *Drosophila* QC isoform (CG5679).

Table 2: **Microarray data for gene CG32412.**

Tissue Studied	mRNA Signal	Enrichment
Crop	927 ± 10	2.30
Ovary	896 ± 24	2.20
Hindgut	289 ± 4	0.70
Head	282 ± 13	0.70
Male accessory glands	271 ± 18	0.70
Adult carcass	196 ± 13	0.50
Larval fat body	140 ± 19	0.30
Testis	139 ± 5	0.30
Thoracicoabdominal ganglion	61 ± 2	0.20
Brain	57 ± 2	0.10
Midgut	50 ± 3	0.10
Larval tubule	18 ± 3	0.00
Tubule	14 ± 2	0.00
Whole fly	405 ± 28	

In situ hybridization studies of various genes throughout the genome provided by the Berkeley Drosophila Genome Project (BDGP) demonstrated the highest level of mRNA production in early embryonic stages. *In situ* images also revealed a high level of maternal QC-like mRNA in early stages which could lead to the large values obtained in early development. Later stages of development revealed QC-like mRNA present in the embryonic hypopharynx. Figure 10 demonstrates the relative amounts of QC-like mRNA observed throughout the *Drosophila* life cycle.

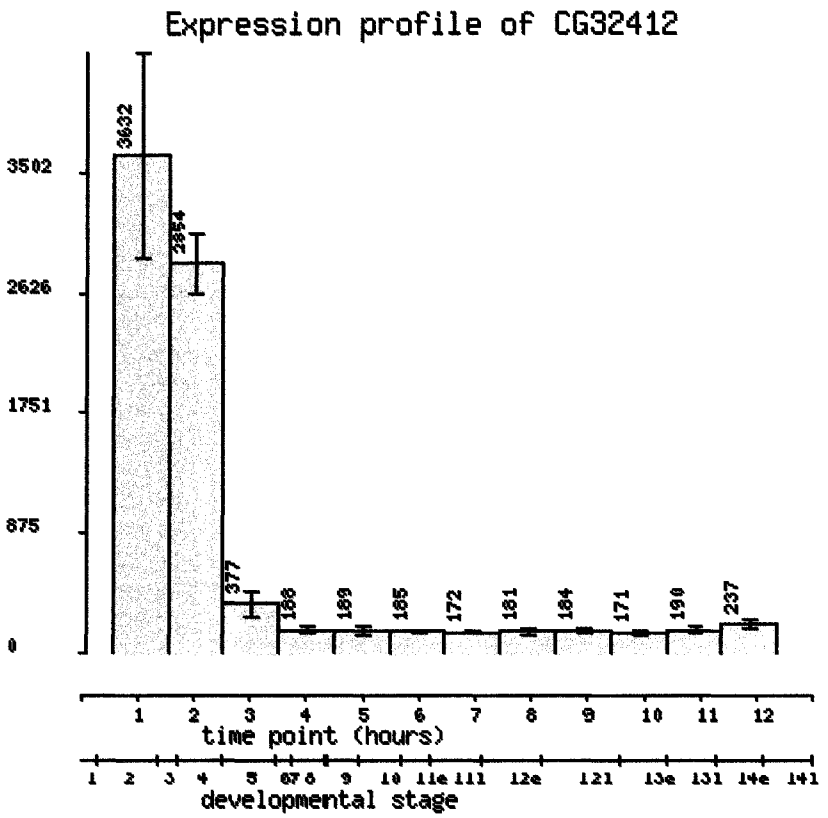

Figure 10: **Expression profile of CG32412.** *In situ* hybridization expression profile obtained from the BDGP database demonstrating the high level of QC-like mRNA in early *Drosophila melanogaster* development.

Drosophila melanogaster RNAi mutants of the CG32412 gene products were developed by the Vienna *Drosophila* RNAi Stock Center. Inability to produce this particular *Drosophila* QC isoforms resulted in a lethal mutation. Embryos were not viable. No RNAi lines have been developed for the other *Drosophila* QC isoform.

Drosophila melanogaster Model System

The *Drosophila melanogaster* model system is a popular system for biochemical and biological research due to its small size, ease of culture, and short generation time. It is one of the few systems whose entire genome is known and various mutant lines are available from the Bloomington Stock Center. Other important information can be obtained from FlyBase, a database of University of Indiana, which provides a collection of genetics and molecular biology information and tools.

The life cycle of *D. melanogaster* involves complete metamorphism with the life cycle including an egg, larval form, pupa, and flying adult. The larval stage has three instars. The complete metamorphosis is temperature dependent with an average life cycle of 12-15 days.

Flies have four pairs of chromosomes termed 2L;2R, 3L;3R, 4, and either XX or XY. The L refers to the left arm and the R refers to the right arm. Though recombination is almost completely absent it is more common in females. This recombination is controlled in the laboratory by the use of a balancer chromosome, a chromosome whose normal sequence is scrambled as the result of artificially induced breaks and rejoining, they are incapable of pairing with their normal homolog during prophase. These balancers are used in combination with typical phenotypic markers which affect eye color, eye shape, wing shape, wing vein morphology, bristle color, bristle shape, and cuticle pigmentation.

Drosophila melanogaster cell lines have been used to express heterologous gene products. Most commonly used cell lines are the Schneider S2 and S3 cell lines. These cell lines were derived from primary cultures of late stage *D. melanogaster* embryos.

Cells are maintained in an immortalized non-tumorgenic growth. Cells are capable of growth in Schneider's media with or without heat-inactivated fetal bovine serum (FBS). (Schneider 1972) The S2 cell line has been proven useful for transient or stable transfection. Once produced, the cell line is capable of maintaining ability to produce large amounts of heterologous protein. The use of *D. melanogaster* cell culture demonstrates another important use of the *D. melanogaster* model system.

Peptide Processing Enzymes Homologs

Various secretory pathway modifications such as N-terminal pGlu and C-terminal amide have been observed in many different *Drosophila* peptides. The study of *Drosophila* peptide processing enzymes has resulted in the expression and purification of various pathway enzymes from *Drosophila melanogaster* demonstrating *in vitro* the specific predicted enzymatic activity.

Prohormone convertase 2 homolog

The *Drosophila* homolog of the mammalian PC2 enzyme was first identified in 1999, termed *amontillado* (*amon*). Initially one major difference was observed between the mammalian enzyme and the *Drosophila* enzyme. *Drosophila* PC2 expression is highly regulated during development. Typically expression occurs within the final stages of embryogenesis mainly within sensory structures according to *in situ* hybridization studies. Mutant larvae did not show any gross anatomical differences however a reduction in specific egg hatching behavior was observed. Expression of PC2 restored this behavior unless active site residues were mutated. These initial results suggested the

major role of PC2 in *Drosophila* involved proper neuronal signaling during the egg hatching stage. (Siekhaus 1999)

Following the identification of a *Drosophila* PC2, the cDNA encoding *Drosophila* 7B2, was identified in *Drosophila*. The dPC2 and d7B2 were subcloned into HEK-293 cells without successful expression of proteolytic active enzyme. This was followed by the coexpression in *Drosophila* S2 cells. The expressed dPC2 was active suggesting the proper maturation of dPC2 requires *Drosophila* specific enzymatic processing. (Hwang 2000)

Mutation studies further identified the function of dPC2. dPC2 mutants displayed partial embryonic lethality, commonly die during the first to second instar, and are defective in larval growth. These results indicated the dPC2 is required for embryogensis and larval development and more specifically responsible for regulation of hatching, larval growth, and larval ecdysis. (Rayburn 2003)

Carboxypeptidase homolog

Scanning of the *Drosophila melanogaster* cDNA library using probes generated against the vertebrate carboxypeptidase E identified homologs to human CPE, CPN, and CPM. Northern blot analyses revealed a potential CPE gene in embryos. Results suggested a single protein is responsible for carboxypeptidase activity in *Drosophila*. (Bernasconi 1994)

Subsequently the silver (svr) gene was identified as the gene responsible for the translation of previously identified carboxypeptidase proteins. Silver gene mutations are lethal. Weak alleles resulted in several phenotypic abnormalities. (Setirle 1995)

Peptidyl glycine α-amidating monooxygenase homolog

Both the monooxygenase (PHM) and lyase (PAL) proteins associated with mammalian bifunctional PAM protein were observed in *Drosophila* head extracts. However, the bifunctional PAM protein was not detected. An active PHM-like protein was identified by both Northern and Western blot analyses and expressed independently suggesting the presence of different PHM and PAL genes. Disruption of the PHM gene resulted in lethality. (Kolhekar 1997)

Further study of the *Drosophila* amidation enzymes resulted in the validation of previous research identifying the presence of one monofunctional PHM gene, but also presented the discovery of two monofunctional PAL genes, PAL1 and PAL2. dPAL1 has a predicted transmembrane domain and is secreted poorly. dPAL2 is predicted to be secreted and soluble. Upon expression, dPAL2 was secreted and co-localized with hormone. Coexpression was observed in various neuroendocrine neurons but the dPAL1 was more broadly expressed. (Han 2004)

Glutaminyl cyclase homolog

An enzyme capable of QC activity with greater than 60% sequence homology was expressed, purified, and characterized from *D. melanogaster* independently by Parker et. al. (subject of this dissertation) and Schilling et. al. Both groups demonstrated a similar mode of activity and inhibition in the dQC when compared to human QC. Both groups also identified the presence of a dQC isoform within the *Drosophila* genome capable of QC activity. (Parker 2008; Schilling 2007)

Peptidomics of Adipokinetic Hormone Processing

Peptidomics techonology has aimed to identify the expressed peptides within in a cell including all post-translational modifcations. Adipokinetic hormone (AKH), the first peptide hormone to be sequenced from insects, has been studied extensively. AKHs regulate the release of lipid (diacylglycerol) and carbohydrate (trehalose) energy substrates during flight. Cell ablation studies of AKH producing cells resulted in loss of trehalose release and altered insect function. (Guillaume 2005) These peptide hormones are synthesized and stored for secretion by neurosecretory cells of the corpus cardiacum. Once released the AKH stimulates fat body target cells through adenylate cyclase activation and subsequent cAMP production. cAMP activates the breakdown of glycogen through conversion of glycogen phosphorylase to its active form. AKHs are also known to enhance production of inositol triphosphates through phospholipase c activation which mediate Ca^{2+} release from intracellular stores. Depletion of internal calcium storage results in an influx of extracellular calcium which activates triacylglyceral lipase to release diacylglycerols. Initially, the trehalose in the insect blood is responsible for providing energy during flight with additional trehalose provided from glycogen storage. Similtaneously, AKH is stimulating the release of diacylglycerols into the blood. (Van der Horst 2001)

The AKH gene (FlyBase ID FBgn0004552; CG1171) is located on chromosome 3L and sequence location 64A7. One gene produces one transcript and one polypeptide. AKH peptides are synthesized at the rER, transported to the golgi complex, and packaged into secretory granules for transport. The maturation of AKH requires the activity of various post-translational processing enzymes within the secretory granules as observed

by *in situ* hybridization studies. AKH is produced as a large 79 amino acid precursor cleaved to produce a 9 amino acid precursor which is subsequently modified to contain an N-terminal pGlu residue and C-terminal amide. Figure 11 summarizes the maturation of AKH.

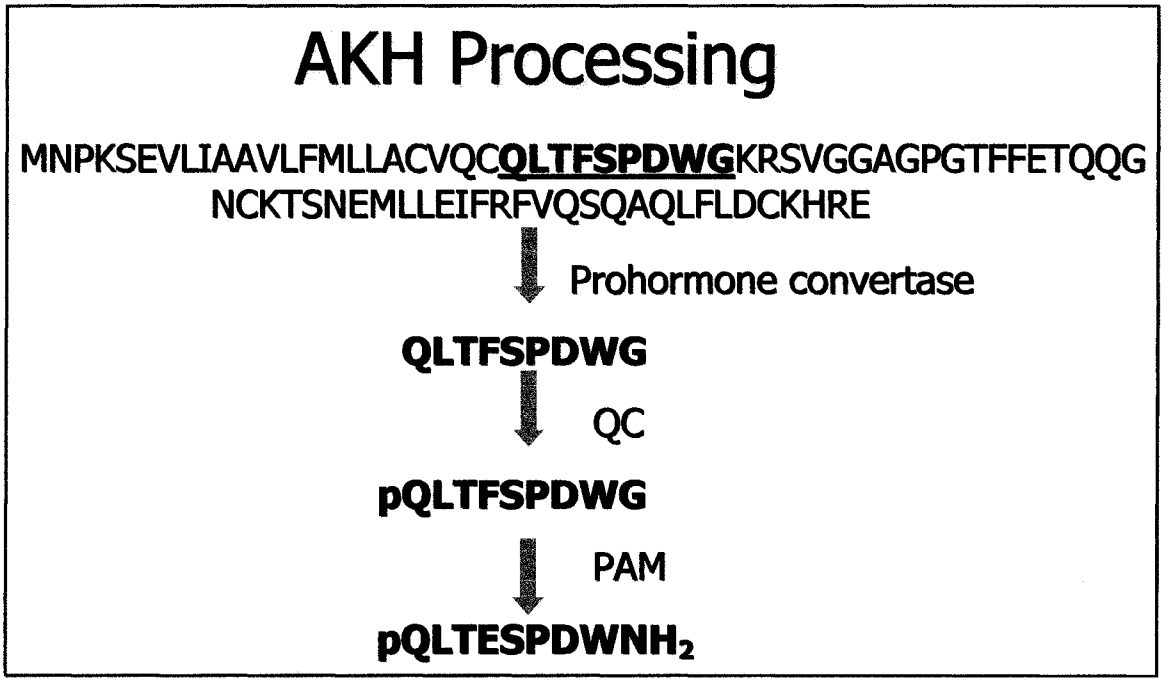

Figure 11: **Maturation of *Drosophila* AKH peptide hormone.**

Drosophila AKH and mammalian GnRH Relationship

The *Drosophila* AKH and mammalian gonadotropin-relesing hormone, GnRH, appear to require the same processing for proper enzymatic maturation. A structural and evolutionary link has been established between the *Drosophila* AKH receptor and rat GnRH receptor. This provides some evidence for the relationship between the two systems because the hormone receptors were shown to contain high sequence identity among the transmembrane region of the receptors which is normally only observed in

highly related species. Also, the two receptors were shown to contain common intron sequences suggesting an evolutionary relationship. (Staubli 2002)

Specific Aims and Hypotheses

Due to the similarity of *Drosophila* and mammalian peptide hormone processing and the presence of other peptide processing enzymes homologs in the *Drosophila* genome, we sought to identify a glutaminyl cyclase enzyme in *Drosophila*. Identification of this enzyme would complete the peptide hormone processing scheme in insects and provide the first evidence of such enzyme activity in *Drosophila*. A complete characterization of the *Drosophila* QC could also possibly lead to the use of insect QC as a possible target for insect pest control.

During initial database searches, multiple putative QC sequences were identified in *Drosophila*. Two *Drosophila* QCs were identified due to a high amino acid sequence identity to human QC. Both *Drosophila* QCs were expressed, purified, and characterized for comparison to the published data for human QC. Following expression and characterization studies of both *Drosophila* QC isoforms in our laboratory, another research group, Schilling and co-workers, published the expression and catalytic properties of both the *Drosophila* QC isoforms. All published kinetic properties and inhibitor studies were in agreement with our research. Therefore, we attempted to study the location of dQC and dQC-LK transcription and translation products to determine the biological function of two QC isoforms. This would allow determination of expression levels of both *Drosophila* QC isoforms separately and provide a possible explanation of the specific biological role of the two QC isoforms independently.

The evolution of QC was also examined. It is clear that QC possesses a zinc aminopeptidase structural fold, suggesting a possible common evolutionary origin.

Therefore, we attempt to identify promiscuous enzyme activity among the aminopeptidase and QC enzyme families. Other than the structural link between human QC and bacterial aminopeptidase, the mammalian post-translational processing system has been linked to the insect post-translational processing system. Sequence analyses have identified similarities with between mammalian hormone receptors and *Drosophila* hormone receptors suggesting this link in the peptide hormone processing systems. Therefore, my research aims to compare the enzymatic activity of the bacterial aminopeptidase and the insect and mammalian QCs. QC and aminopeptidase enzymatic analyses, along with the use of various phylogenetic tools, will allow a better understanding of the QC evolution and its relationship to bacterial aminopeptidases.

CHAPTER II

EXPERIMENTAL PROCEDURES

Routine Equipment

Analytical Balance	Citizen CY204 and CT604
Autoclaves	Amsco 3031-S and Amsco Steris Lab 250
Cooler	Master-Bilt Products
Freezer	Kenmore
Horizontal Gel Apparatus	Kodak BioMax QS710
Incubator	Fisher Isotemp Incubator Model 630D
Incubator/Shaker	New Brunswick Scientific Innova 4000
Laminar flow hood	NuAire
Microcentrifuge	Eppendorf 5415 C
Microwave	General Electric
pH Meter	Corning 240
pipettes	Rainin Corporation P-1000, P-200, P-100, and P20
Power Supply	Fisher FB105
Refrigerator	Kenmore
Spectrophotometer	Hitachi U2000
Microtiter plate reader	BioTek EL800
Fluorometer	Hitachi F2000
Thermocycler	Ericomp Power Block System
Vertical gel apparatus	Novex X Cell
Western transfer apparatus	Bio-Rad Trans-Blot
MALDI-TOF	Bruker Microflex series

Solutions

Luria-Bertani (LB) media

10 g/L	Tryptone peptone
5 g/L	Yeast Extract
10 g/L	NaCl
15 g/L	Agar

SOC media

20 g/L	Tryptone peptone
5 g/L	Yeast Extract
10 mM	NaCl
2.5 mM	KCl
10 mM	$MgCl_2$
10 mM	$MgSO_4$
20 mM	Glucose

Phosphate Buffered Saline (PBS), pH 7.4

140 mM	NaCl
2.7 mM	KCl
10 mM	Na_2HPO_4
1.8 mM	KH_2PO_4

TBE buffer

89 mM	Tris base
2 mM	EDTA
89 mM	Boric acid

TE buffer

10 mM	Tris
1 mM	EDTA

Western Blot Transfer Buffer

0.75 g/L	Glycine
19.38 g/L	Tris Base
20 mg/L	SDS
200 mL	Methanol

Western Blot Solution

10 mM	Tris base
0.9 %	NaCl
0.1 %	Tween

Hybridization Solution

50 %	Formamide (deionized)
5X	SSC
100 ug/mL	DNA (boiled salmon sperm)
50 ug/mL	heparin
0.1 %	Tween-20

20X SSC (100 mL), pH 7.0

17.5 g	NaCl
8.8 g	sodium citrate

PTX (500 mL)

50 mL	10X PBS
500 uL	Triton X-100

PBT (500 mL)

500 mL	1X PBS
5 g	Bovine serum albumin
500 uL	Triton X-100

General Methods

Glutaminyl cyclase spectrophotometric enzyme assay

Glutaminyl cyclase activity was tested using a previously published spectrophotometric assay. (Bateman 1989) This assay employs the ability of glutamate dehydrogenase to detect the ammonia released from the QC reaction. Typical QC reaction substrates used are Gln-NH_2 and Gln-tBE. The reaction of glutamate dehydrogenase with ammonia is coupled to the oxidation of NADH to NAD^+ resulting in a loss of absorbance at 340 nm. Routine experiments required a cocktail composed of 20 mM α-ketoglutarate, 1.7 mM NADH, 8.5 mM Gln-NH_2, and 24 U glutamate dehydrogenase in a total volume of 6.5 mL 50 mM MOPS at pH 7.5. Enzyme assays were completed in duplicate. First 50 uL of the properly diluted QC source were added to all test tubes. Additions of 100 uL of the cocktail mixture were added to one set of test tubes. These reactions were allowed to incubate at 37°C for 65 minutes in a water bath. After 60 minutes, 100 uL cocktail was added to the other set of test tubes, which were then allowed to incubate at 37°C for 5 minutes in a water bath. The reactions were stopped simultaneously by addition of 500 uL cold water. The absorbance of each tube was measured at 340 nm using a Hitachi U-2000 spectrophotometer. Differences between the two time points represented the change in absorbance over 60 minutes. Typically, 0.01 absorbance units represented the production of 1 nanomole of product. The assay was used with varying substrate and/or inhibitor concentrations for kinetic analysis. Detailed protocols follow.

Glutaminyl cyclase fluorometric enzyme assay

Alternatively, QC activity was analyzed using a fluorometric enzyme assay previously described by Schilling et. al. (Schilling 2002). This assay employs the release of a fluorometric compound upon cyclization of an N-terminal Gln by QC activity followed by removal of the pGlu residue by a pyroglutamate aminopeptidase (PGAP). Two substrates were used for these assays, Gln-AMC and Gln-βNA at a concentration of 0.05 mM. Pyroglutamate aminopeptidase was obtained from a collaborator and 2.5 uL was used in each assay. Initially, the substrate and PGAP were combined in a 20 mM Tris buffer at pH 7.5 to a total volume of 625 uL. Addition of 25 uL properly diluted QC source was used to initiate the reaction. Excitation/emission wavelengths for Gln-AMC were 380/465 nm and 320/410 in the case of Gln-βNA, respectively. Assays were allowed to proceed for 5 minutes. All fluorometric analyses were completed using a Hitachi F-2000 spectrophotometer.

Aminopeptidase spectrophotometric assay

Aminopeptidase (AP) activity was tested using a colorometric assay. 0.1 mM leucine para-nitroanilide (leu-pNA) was used as a substrate. In the presence of active AP, the N-terminal leucine is cleaved resulting in the release of pNA, a yellow colored compound. Routine assays required the addition of substrate and 100 uM Zn to 50 mM MOPS pH 7.5 to a final volume of 500 uL. Addition of 5 uL AP source was added to initiate reaction. Typical assays were allowed to proceed overnight. Release of pNA was measured spectrophotometrically at 412 nM using a Hitachi U-2000.

Polymerase chain reaction (PCR)

Polymerase chain reactions (PCR) were completed using a standard protocol. In reactions forward and reverse primers were designed with a minimum of 18 complementary nucleotides, a G-C content of 40% - 60%, and within 0.5°C difference in melting temperature. Typical reactions contained 200 ng of each primer, 0.3 uM each dNTP, 1X reaction buffer containing varying concentrations of $MgCl_2$, and either 1 U Taq polymerase or 2 U PfX polymerase (Invitrogen). Reactions were completed with one melting cycle at 95°C for 5 minutes followed by 25 to 30 cycles at 95°C for 1 minute, melting temperature for 1 minute, and 72°C for 2 minutes. A final extension cycle of 72°C for 10 minutes was used.

Polyacrylamide gel electrophoresis and Western blotting

Sodium dodecyl-sulfate polyacrylamide gel electrophoresis (SDS-PAGE) was used routinely throughout experiments. Typically 10% or 15% pre-cast Tricine gels (Invitrogen) were used for protein separation in Tricine buffer (Invitrogen). Following SDS-PAGE proteins were transferred to a nitrocellulose membrane (Invitrogen) at 250 mAmps for 1 hour at 4°C using Western blot transfer solution. Membrane blotting included a 1 hour wash in 5% non-fat milk, 1 hour wash in varying dilutions of primary antibody, three 10 minute washes in western blot solution, 1 hour wash in 1/10,000 dilution of secondary antibody, three 10 minute washes in western blot solution, and developing with minimal volume NBT/BCIP (Sigma) until precipitate formed.

Mass spectroscopy

Routine MALDI-TOF utilized the Bruker Daltonics Microflex. Typical samples were prepared by in-gel trypsin digestion. Protein samples were separated by SDS-PAGE and visualized with Simply Blue SafeStain (Invitrogen). Protein bands for analysis were removed with a razor blade and placed in clean microcentrifuge tubes. Two 45 minute washes of 100 mM NH_4HCO_3 in 50% acetonitrile at 37°C removed all stain from the gel slices. Next gel slices were dehydrated for 5 minutes at room temperature in 100 uL 100% acetonitrile. A 10 to 15 minute lyophilization followed to remove all acetonitrile. Next gel slices were allowed to incubate in 20 uL trypsin gold (20 ug) at room temperature for 1 hour. Gel slices were covered with 40 mM NH_4HCO_3 and allowed to incubate overnight at 37°C. The following morning, protein fragments were extracted from the gel slice with one 10 minute wash with 150 uL water and two 60 minute washes in 50% acetonitrile, 5% TFA at room temperature. The extractions were then pooled and dried in a speed vacuum at room temperature for 4 hours. To clean the samples, the pellet was resuspended in 10 uL 0.1% TFA. Protein sample was loaded onto C18 ziptips previously equilibrated with 10 uL 50% acetonitrile followed by 0.1% TFA. Matrix was washed with 0.1% TFA and eluted with 50% acetonitrile, 0.1% TFA. For non-digested protein analysis only the C18 protocol was required to remove salt from sample. Protein samples were mixed 1:1 with a 10 mg/mL matrix solution. α-cyano-4-hydroxycinnamic acid (Sigma) and sinapinic acid (Sigma) were commonly used matrices which were prepared fresh by dissolving in 50% acetonitrile, 0.1% TFA.

Peptide Hormone Expression in *Drosophila* Schneider 2 (S2) Cells

General maintenance of Drosophila S2 cells

Drosophila S2 cells (Invitrogen R690-07) were maintained in adherent culture in Schneider's *Drosophila* medium (SDM) (Invitrogen) supplemented with 10% heat-inactivated fetal bovine serum (Hyclone). Cells were initiated from liquid nitrogen stock by quickly thawing at 37°C and transferring contents to complete SDM after an initial washing step. Cells are initially transferred to a T-25 cm^2 flask. Cells were allowed to incubate at 28°C with loosened caps for aeration. After a concentration of greater than 2 X 10^6 viable cells per mL, the culture was sub-cultured at a seeding density of 5 X 10^5 viable cells per mL for subsequence growth in a T-75 cm^2 flask. Cell viability was determined using trypan blue exclusion methods and a hemacytometer chamber with manual counting. To maintain the cell line, frozen stocks were generated at a concentration of greater than 1 X 10^7 viable cells per mL in SDM with 10% DMSO.

S2 cells were adapted to grow under serum-free conditions in suspension culture in an attempt to eliminate contaminating proteins in media. Cells were subjected to increasing amounts of Serum Free Medium (SFM) (Invitrogen 10797) until cells were capable of maintaining normal growth rates under serum free conditions. Cells were maintained in 100% SFM in suspension culture at 28°C at 125 rpm in shaker flasks. Typical cell cultures were maintained at greater than 1 X 10^7 viable cells per mL with a seeding density of 1 X 10^5 viable cells per mL for subculturing. Similar initiating and freezing techniques were used in serum free cell culture.

Cloning and expression of Drosophila Adipokinetic Hormone (AKH)

Drosophila adipokinetic hormone (AKH) was obtained by PCR amplification from the *Drosophila* S2 cell genome using the following primer set: 5'-GCTGAATCGAAGTGGACCAG-3' and 5'-GTGTGCGTGCTAGACATCGT-3'. PCR reaction required an annealing Tm of 60°C and used 2 U Pfx proofreading polymerase. Immediately following PCR amplification, 1 U Taq polymerase was added to facilitate the addition of adenine overhangs for subsequent TOPO reactions. PCR product was gel purified and subsequently ligated into the pMT/V5-His-TOPO vector (Invitrogen) by combining the purified PCR product, vector, and concentrated salt solution followed by incubation at room temperature for 5 minutes. Constructs were transformed into One Shot TOP10 chemically competent *E. coli* and plated overnight on LB agar containing 25 ug/mL AMP. Resulting colonies were analyzed by restriction digest and sequencing.

Drosophila S2 cells were transfected with AKH construct using calcium phosphate transfection. Initially cultured cells were prepared for transfection by seeding 3 X 10^6 cells in a 35 mm plate in 3 mL complete media resulting in a final cell concentration of 1 X 10^6 cells per mL. These cells were allowed to grow to a final cell density of 3 X 10^6 cells per mL. Once the proper cell concentration was reached, solution A was prepared to contain 240 mM $CaCl_2$ and 19 ug recombinant DNA in a final volume of 300 uL. Solution B was prepare to contain 300 uL 50 mM HEPES, 1.5 mM Na_2HPO_4, 280 mM NaCl, pH 7.1. Solution A was slowly added to solution B dropwise with constant mixing. The resulting solution was allowed to incubate at room temperature for 40 minutes allowing a precipitate to form. Finally, the solution was added dropwise to the cells and allowed to incubate 24 hours at 28°C. The following day the calcium

phosphate solution was removed from the cells and cells were allowed to incubate in complete media. In 1 to 2 days copper sulfate was added in a final concentration of 500 uM and allowed to incubate for 4 days. To the production of a stable cell line, the AKH construct was co-transfected with 1 ug pCoHygro vector (Invitrogen) providing the cells with hygromycin resistance. Incubation in complete media for 3 to 4 weeks following transfection was required prior to induction with copper sulfate.

Cloning and expression of human Gonadotropin-releasing Hormone

A synthetic DNA construct for the human gonadotropin-releasing hormone (GnRH) was developed to contain the coding sequence for the final translation product of human GnRH and a *Drosophila* secretion signal by overlap extension PCR. Overlap extension PCR requires the combination of two primers which contain a minimum of 18 nucleotide complementary regions allowing the production double-stranded DNA. The two primers used in the PCR reaction were 5'-TTATCCAGGGCGCAGTCCATAGGACCAGTGCTGCCCGAGCGAGAGGCCAACAAAGGCCAC-3' and 5'-AATATGAAGTTATGCATATTACTGGCCGTCGTGGCCTTTGTTGGCCTCTCGCTCGGG-3'. Touchdown PCR was utilized using annealing temperatures from 74°C to 60°C. Resulting PCR product was cloned into pMT/V5-His-TOPO vector. All subsequent reactions followed the same protocol as the *Drosophila* AKH construct analysis and expression in *Drosophila* S2 cells.

Heterologous Protein Expression in Bacterial Expression Systems

Cloning, expression, and purification of Drosophila glutaminyl cyclase

The putative *Drosophila* glutaminyl cyclase (QC) was identified by BLAST searching using the human QC protein sequence. Two putative sequences with greater than 60% sequence identity were identified. The gene with the highest sequence identity was chosen for expression studies. A cDNA vector from Berkeley *Drosophila* Genome Project (RE61650) was obtained containing gene CG5976.

PCR amplification of the putative QC gene from the cDNA vector used primers 5'-CACCCTGGTGGATATTCCTAAGATATCCTACA-3' and 5'-CTACTTGGCCTCGGTTCC-3'. PCR reactions required an annealing temperature of 55°C and utilized 2.5 U Pfx proofreading polymerase. PCR product was inserted into the pET160/GW/D-TOPO vector (Invitrogen) under TOPO cloning standard conditions. PCR product was combined with pET160/GW/D-TOPO vector and concentrated salt solution for a 5 minute incubation at room temperature. Resulting reaction was transformed into One Shot chemically competent TOP10 *E. coli* cells and plated on LB agar containing 25 ug/mL AMP. Transformants were analyzed by restriction digest and sequencing. Correct *Drosophila* QC (dQC) colonies were purified using Qiagen mini-prep spin columns and maintained for further reactions.

Expression of the *Drosophila* QC required the transformation of One Shot chemically competent BL21 cells (Invitrogen). A 10 mL overnight LB culture containing 25 ug/mL AMP was inoculated with BL21 cells containing the dQC vector, and was used to inoculate 2-250 mL LB cultures containing 25 ug/mL AMP. The large cultures were allowed to grow to mid-log phase at 37°C and then induced with 0.1 mM IPTG for 3

hours at room temperature. Cells were collected by centrifugation at 3,000 x g for 10 minutes at 4°C. The resulting pellet was either frozen at -80°C overnight or immediately used for purification.

Purification utilized the expressed poly-His tag. Pelleted cells were resuspended in 30 mL 20 mM Tris pH 7.5, 1 mM PTSF. Sonication of the cells on ice in three 30 second bursts on ice resulted in cell lysis. Cell lysate was then clarified by centrifugation at 10,000 x g for 10 minutes at 4°C to pellet all insoluble material. The supernatant was loaded onto 3 mL Ni-NTA resin (Invitrogen) in batch and allowed to bind with gentle agitation at 4°C for 1 hour. Following binding the flow through was removed and the resin was washed in batch. The resin was allowed to settle by centrifugation at 100 x g in a swinging bucket centrifuge for 3 minutes. Removal of the flow through was followed by addition of 30 mL 20 mM Tris pH 7.5, 500 mM NaCl, 20 mM imidazole. Resin was centrifuged, supernatant removed, and the wash step repeated two subsequent times. Two wash steps with 30 mL 20 mM Tris pH 7.5, 500 mM NaCl, 50 mM imidazole and one wash step with 30 mL 20 mM Tris pH 7.5, 50 mM imidazole followed. Finally, the resin was placed in a disposable column and allowed to settle. The *Drosophila* QC (dQC) was eluted in 1 mL fractions with 20 mM Tris pH 7.5, 250 mM imidazole. Fractions were visualized on the gel and stained with the lumio reagent to determine the location of eluted dQC. The dQC was dialyzed against 50 mM MOPS pH 7.5 for subsequent enzyme assays.

Kinetic analyses of Drosophila glutaminyl cyclase

Activity of dQC was verified using both the spectrophotometric and fluorometric assays described above. Initially, QC activity was verified by using the basic spectrophotometric assay at various time points and using various substrates.

To evaluate the kinetics of the expressed dQC assays utilizing substrates ranging from 2 mM to 14 mM for Gln-NH_2 and Gln-tBE were used in the spectrophotmetric assay. Protocol described above was slightly altered to eliminate error in calculations. Assay cocktail was prepared in ½ amount of buffer and only 50 uL was used in each assay tube. The substrates were prepared to add a total of 50 uL to each assay tube providing the correct final substrate concentration. Kinetic constants were determined by plotting the resulting velocities and substrates on Michaelis-Menton plots using Kaliedograph.

Fluorometric kinetics were determined similarly with substrate concentrations ranging from 20 uM to 200 uM for Gln-βNA.

Cloning, expression, and purification of Drosophila glutaminyl cyclase-like protein

To evaluate the function of the other potential *Drosophila* QC identified by original BLAST searches, another cDNA vector was obtained from Berkeley *Drosophila* Genome Project (GH11174) containing gene CG32412.

The same protocol was used to clone the dQC-LK gene into the pET160/GW/D-TOPO vector. Primers used were 5'-CACCATCGGTTCCGTAGTTTTTG-3' and 5'-CTATGTTCGGTAAAAACGCA-3'. Initial expression results for the dQC-LK_{TOPO} revealed the majority of heterologous protein was located in the insoluble fraction.

Attempts at expressing for longer periods of time at lower IPTG concentrations and inducing at lower temperatures resulted in slightly better results but attempts were unsuccessful at forcing an adequate fraction of the protein into the soluble fraction. Therefore, an alternative expression system was chosen.

Expression of the dQC-LK protein was successfully completed using the IMPACT system (NEB). *Drosophila* QC-LK was amplified from the cDNA clone using primers 5'-TACTATACATATGATCGGTTCCGTAGTTTTTG-3' and 5'-TACTATAGCAGGAAGAGCCTGTTCGGTAAAAACGCAA-3'. Primers were designed with NdeI and SapI restriction sites for subsequent enzymatic reactions. PCR reaction required a single annealing temperature of 50°C and 2.5 U Pfx proofreading polymerase. The resulting 1100 bp band was purified from the PCR reaction using the GeneClean Turbo kit from QBiogene. One micrgram of the PCR product and 1 ug vector pTXB1 were digested for 1 hour at 37°C with NdeI and SapI. Using the ratio of 0.89 ng insert to 1 ng vector, the digested fragments were ligated overnight at 16°C. Ligation reaction was transformed into OneShot TOP10 chemically competent cells (Invitrogen) and plated on LB containing 25 ug/mL AMP. Resulting colonies were screened for dQC-LK insert using restriction digestion and sequencing.

The verified dQC-LK_{IMPACT} clones were transformed into OneShot chemically competent BL21 cells (Invitrogen) for expression. Ten mL overnight LB cultures containing 25 ug/mL AMP were inoculated with the vector. Two 250 mL LB cultures containing 25 ug/mL AMP were inoculated with the overnight culture and allowed to grow to mid-log phase at 37°C. Temperature was lowered to 25°C and the cells were induced by addition of 0.4 mM IPTG for 3 hours. Cells were collected by centrifugation

at 3,000 x g for 10 minutes at 4°C. Cells were either frozen at -80°C or used immediately for purification.

Purification of the dQC-LK_{IMPACT} clones required a chitin column (NEB). Cell pellet was resuspended in 100 mL 20 mM Tris pH 7.8, 500 mM NaCl, 1 mM PTSF. Cells were sonicated on ice in three 30 second bursts. Cell lysate was centrifuged at 15,000 x g for 10 minutes to pellet cell debris. Supernatant was applied to 10 mL chitin column prewashed with 10 bed volumes 20 mM Tris pH 7.8, 500 mM NaCl. Column was then washed with 20 bed volumes 20 mM Tris pH 7.8, 1 M NaCl. Three bed volumes of 20 mM Tris pH 7.8, 50 mM DTT was added to the resin. The column was then stopped and allowed to incubate overnight at 4°C. The following morning, the column was eluted with 20 mM Tris pH 7.8, 500 mM NaCl. SDS-PAGE and coomassie staining were used to evaluate the purification of dQC-LK protein. The heterologous protein was dialyzed overnight against 50 mM MOPS pH 7.5 for subsequent enzymatic assays.

Testing aminopeptidase activity

The aminopeptidase activity of hQC (expression system designed by Temple), dQC and dQC-LK was analyzed using the p-nitroanilide aminopeptidase assay described above using 0.1 mM leu-pNA, 0.1 mM ala-pNA, and 0.1 mM gly-pNA as substrates. The assays were completed for different time points, at different pHs ranging from 6.5 to 8.5, and zinc and cobalt concentrations ranging from 0 to 0.1 mM. Assays were run using the microtiter plate reader with buffer and substrate as well as buffer and enzyme

blanks as negative controls. Leucine aminopeptidase (Sigma) was used as a positive control in all assays.

Testing effect of leucine derivatives on QC activity

Effect of leucine and various leucine derivatives were tested as inhibitors of hQC and dQC. Inhibitors tested include leucine, leucine-NH_2, leu-gly, leu-ala, leu-leu, and leucine chloromethyl ketone (leu CMK). Inhibition testing utilized the flurometric assay under standard conditions as describes previously with the addition of inhibitor tested. Ki determination utilized the spectrophotometric assay with final concentrations of leucine peptides ranging from 0.25 mM to 5 mM. Effect of leu CMK was evaluated using the spectrophotometric assay. These assays utilized timed preincubation of the QC tested with various concentration of leu CMK along with a QC and buffer control. Following the predetermined preincubation time, the cocktail was added and the typical assay described above was completed.

Analyses of Native *Drosophila* Glutaminyl Cyclase

Antibody screening of crude Drosophila melanogaster extracts

Wild type adult *Drosophila melanogaster* were obtained to evaluate the presence of a signal using human QC antibodies. Three different antibodies were used for all cytochemistry studies. One antibody obtained from Novus Biologicals was developed against a truncated portion of the hQC-GST construct previously expressed. Two other antibodies were developed previously in the lab against a highly conserved portion of the

amino acid sequence of QC. Table 3 summarizes the antibodies used throughout experiments including antibody epitope, company, and antibody source.

Table 3: **QC Antibodies.**

Antibody Name	Antibody type	Epitope	Company	Antibody source
Polyclonal	Commercial polyclonal	Truncated hQC-GST construct protein	Novus Biologicals	Mouse
5247	Anti-peptide	CHYDSKYFPHWDDRV		Rabbit
5248	Anti-peptide	CHYDSKYFPHWDDRV		Rabbit

Drosophila crude extracts were developed by flash freezing adult *Drosophila melanogaster* in liquid nitrogen for three 10 second freezes. Frozen flies were manually grinded to a fine powder. The powder was suspended in 100 mM Tris pH 7.5, 150 mM NaCl, 0.2 mM EDTA, 0.3 M sucrose, 1 mM PTSF and homogenized. The homogenate was centrifuged at 3000 rpm for 5 minutes to pellet cell debris and nuclear pellet. The supernatant was transferred to a fresh tube and centrifuged at 15,000 rpm for 30 minutes to separate the cytosolic and membrane fractions. Both fractions were separated using SDS-PAGE and transferred to nitrocellulose membrane for blotting.

Peptide antibody affinity purification

Previously prepared peptide antibodies 5247 and 5248 were purified using affinity chromatography. Affinity resin was prepared by coupling hQC-GST and the protein containing the peptide used for antibody production to a carbonyldiimidazole-activated resin. CDI-activated resins contain a reactive carbonyl diimidazole which covalently

attach to proteins via the amine group. For the coupling reaction, 5 mg hQC-GST in 50 mM borate pH 9.5 was placed on 1 mL prepared resin and allowed to bind overnight with gentle agitation in the cold room. After coupling 50 mM Tris pH 9.5 was added to block remaining reactive groups. After equilibration with PBS, the antibody serum was applied to resin and allowed to couple for 1 hour with gentle agitation in the cold room. The resin was washed with 5 bed volumes PBS and eluted in 0.5 mL fractions with 50 mM glycine pH 2. pH was immediately neutralized with Tris base. Purified antibody were used at a dilution of 1/500.

Production of Drosophila melanogaster QC mutants

Drosophila melanogaster QC mutants were obtained from Bloomington *Drosophila* Stock Center at Indiana University. Mutants were deficient in Chromosome III region 64 and balanced with TM6B-Tb^1, a mutation marker which produces a tubby phenotype. Tubby phenotype was used to verify the presence of mutation. Flies were expanded for 15 days until a larger density was reached. At the 15 day point, virgin females (genotype: def/TM6B-Tb^1) were phenotypically selected and crossed with male (genotype: TM3-Sb-LacZ/TM6B-$Tb^{1)}$. The genotype TM3-Sb-LacZ is a commonly used mutation marker for the third chromosome. Resulting stubble phenotype was used to verify the presence of properly crossed flies (genotype: def/TM3-Sb-LacZ) within the progeny. Table 4 summaries all genetic crosses completed to produce the mutant fly line. This table represents important genotype and phenotypes associated with QC deficiency cell lines used during double mutant selection. Only genotype maintained after cross is listed.

Table 4: **Important Fly Line Genotype/Phenotype**

Fly Type	Genotype	Phenotype	Deficiency present
Virgin females	def/ TM6B-Tb[1]	Tubby – larvae are short, fat	+
Crossing males	TM3-Sb-LacZ/TM6B-Tb[1]	Stubble – shorter hairs	-
Progeny flies	def/TM3-Sb-LacZ	Stubble – shorter hairs	+

Collection and preparation of Drosophila embryos

Oregon R (or) strains of *Drosophila* were used as wild-type in all experiments. *Drosophila* adults were maintained in cages on grape juice plates for 4 hours. Plates were collected at 4 hours and aged to either 0-4 hours, 4-8 hours, 8-12 hours, 12-16 hours, 16-20 hours, and 16-24 hours before collection. Once the appropriate time had passed, the embryos were collected following standard protocols. Collection included removal of the chorion, outer membrane, with a 50% bleach wash for 3 minutes followed by a 2 minute wash of 2 mL formaldehyde and 2 mL heptane. Lower formaldehyde layer was removed and 6-10 mL methanol was added. The test tubes containing embryos were shaken vigorously for 2 minutes. Embryos, now on bottom of tube due to loss of membranes and fatty components, were placed in a 1.5 mL eppendorf tube and washed 5X with 1 mL methanol. Embryos were stored for up to 1 month in 1 mL methanol.

Immunocytochemistry of Drosophila embryos

Roughly 30 – 50 uL prepared embryos were utilized per reaction tube. The storage methanol was removed and the embryos were washed with 1 mL PTX for 10 minutes while shaking. The PTX was removed and the wash was repeated for 20 minutes while shaking. Next the embryos were washed with 1 mL of PBT one time for 10

minutes and 6 times for 5 minutes while shaking. Next, 300 uL of the primary antibody was added the embryos and the embryos were incubated at room temperature on their side for 2 hours. To remove primary antibody, the embryos were washed 3 times with 1 mL of PBT for 10 minutes, and then 300 uL of the secondary antibody was added. Embryos were incubated again at room temperature for 2 hours on their side. Next, embryos were washed 6 times for 10 minutes each with 1 mL PBT. During the washes, the Avidin-Horseradish peroxidase solution was prepared at a 1:100 dilution of each in PBT and allowed to incubate in the dark for 30 minutes. Three hundred microliters of the solution was added to each reaction tube and allowed to incubate at room temperature for 30 minutes wrapped in foil. Embryos are washed twice with 1 mL of PBT for 5 minutes per wash followed by two 10 minute washes using 1 mL of PTX. The peroxidase reaction is then developed by adding 270 uL of peroxidase substrate and 30 uL of DAB to the embryos. The staining is monitored through a dissection microscope. Embryos are placed in PTX and washed. For double staining, the procedure is repeated using new antibodies against the LacZ protein used as a marker in mutants.

RNA in situ methods

Using the QC (RE61650) and QC-LK (gh11174) cDNA vectors used for protein expression, RNA *in situ* probes were developed. The probes were designed to contain a T7 promoter site for subsequent reactions. Both antisense and sense strands were amplified to provide both experimental conditions and control conditions. Table 5 provides the sequences of the sense and antisense primers used to develop probes in the

study. Initial PCR reaction used the following primers in with typical PCR conditions and annealing temperatures of 55°C for dQC and 57°C for dQC-LK.

Table 5: ***In situ*** **Hybridization Primers.**

Forward dQC antisense: ATGCGTCTGCTACTCAGAAATTATTC Reverse dQC antisense: TAATACGACTCACTATAGGGAGACTACTTGGCCTCGGTTCC Forward dQC sense: TAATACGACTCACTATAGGGAGAATGCGTCTGCTACTCAGAAATTATTC Reverse dQC sense: CTACTTGGCCTCGGTTCC Forward dQC-LK antisense: ATGGCGATCGGTTCCGTAC Reverse dQC-LK antisense: TAATACGACTCACTATAGGGAGACGACAATTCACTGGTGACGTG Forward dQC-LK sense: TAATACGACTCACTATAGGGAGAATGGCGATCGGTTCCGTAC Reverse dQC-LK sense: CGCAAATCCACTGGTGACGTG

Once DNA was amplified to contain the T7 promoter site, it was cleaned using a GENECLEAN turbo purification kit. To complete the transcription reaction the MEGAscript T7 transcription kit (Ambion) was used. Briefly, the DNA product was combined with NTP mixture, 10X reaction buffer containing T7 RNA polymerase, and 3.5 mM DIG-UTP (Roche) and incubated at 37°C for 3 hours. TURBO DNase (Ambion) was added to reaction and allowed to incubate at 37°C for an additional 15 minutes. Product was recovered using MEGAclear Kit (Ambion). RNA was quantified for following studies.

Fixed embryos were placed in an eppendorf tube and rinsed with PTX 3 times. Next, embryos were rocked for 10 minutes at room temperature in 50:50 hybridization solution:PTX followed by a 2 minute rinse in hybridization solution. Embryos are then pre-hybridized for 1 – 2 hours in 1 mL hybridization solution at 55°C. During pre-hybridization the probes are prepared by adding approximately 500 ug probe for 100 uL hybridization solution, heating to 80°C for 3 – 5 minutes, and then placing on ice. Once

the pre-hybridization solution is removed the probe is added to the embryos and allowed to sit at 55°C for 2 – 4 days. Next the hybridization solution plus probe is discarded and the embryos are washed 4 times for 15 minutes, 2 times for 30 minutes, and allowed to stand overnight at 55°C in hybridization solution. The embryos are then washed for 20 minutes rocking at room temperature in hybridization solution: PTX in the dilution 3:1, 1:1, and 1:3. The embryos are then washed 5 times in PTX for about 10 minutes each. Pre-adsorbed anti-DIG antibodies are diluted 1:2000 over embryos and allowed to incubate overnight at 4°C. Finally, the anti-DIG antibody solution is removed, the embryos are washed 4 times for 20 minutes in PTX at room temperature, and then exposed to NBT/BCIP for approximately 10 - 40 minutes in the dark. Embryos are viewed under microscope for analysis.

Analyses of Native Mammalian Glutaminyl Cyclase

Antibody screening of mouse tissues

Mouse customized tissue blot containing 7 days old adrenal, 0 days old brain, 7 days old brain, 7 days old cerebellum, 7 days old cerebrum, 7 days old thymus, 7 days old skin, 7 days old eye, and whole fetus was obtained from ProSci, Inc. Tissue blot was developed using both a 1/2000 dilution of polyclonal antibody, 1/10000 dilution of anti-mouse secondary antibody, and developed with NBT/BCIP. Tissue blots were stripped using a standard protocol. The blot was incubated in a sealed plastic container at 50°C for 30 minutes in a solution of 100 mM 2-mercapoethanol, 2% SDS, 62.5 mM Tris-HCl, pH 6.7. The blot was rinsed with WBS and reprobed as usual. The tissue blot was

developed again using a 1/500 dilution of purified peptide antibody 5247, 1/10000 dilution of anti-rabbit secondary antibody, and developed with NBT/BCIP.

Computer Predictions and Phylogenetic Analyses

Property Predictions of *Drosophila* QCs

Various prediction programs were used to determine properties of the expressed proteins. Amino acid sequences were obtained from the NCBI databank. The following programs located in the ExPASy Proteomics Tools were used to predict the properties of both *Drosophila* QC isoforms by inserting the amino acid sequences into the program. TargetP was used to predict the subcellular localizations of all proteins. All predictions utilized the protein sequences with predicted signal sequences removed once the signals were predicted using TargetP. Physical properties were predicted using ProtParam program. Glycosylation site predictions utilized the program NetNGlyc.

Development of Phylogenetic Trees

Development of Phylogenetic trees utilized the program PhyloDraw. Sequences were obtained from the NCBI website by completing BLAST searches with the human QC as the source sequence. All sequences were then aligned based on either sequence similarity or tertiary structure similarity. Aligned sequences were imported into the PhyloDraw program and used to develop trees based on either sequence conservation or tertiary structure conservation.

CHAPTER III

RESULTS

Peptide Hormone Expression in *Drosophila* Schneider 2 (S2) Cells

Cloning and Expression of Drosophila Adipokinetic Hormone (AKH)

Amplification of the *Drosophila* AKH from *Drosophila* S2 cells resulted in a 400 bp band utilized for subsequent cloning. Analysis of positive clones was initially confirmed by restriction digestion using EcoRI and NotI providing a 3.7 kb and a 300 bp band and followed by sequencing.

The pMT/V5-His-TOPO containing the AKH gene was transiently transfected into *Drosophila* S2 cells using the standard calcium phosphate transfection protocol. A parallel transfection with pMT/V5-His-TOPO (no insert) was used as a negative control. Samples collected were analyzed by SDS-PAGE. It was initially determined the relatively small amount of protein product possibly produced would not be sufficient to observe over all contaminating proteins in the serum media. Therefore, stable transfections were completed to produce larger cultures. SDS-PAGE gels still demonstrated a large amount of contaminating proteins possibly masking the production of the AKH. Figure 12 is an example of a gel observing the banding pattern of the contaminating proteins.

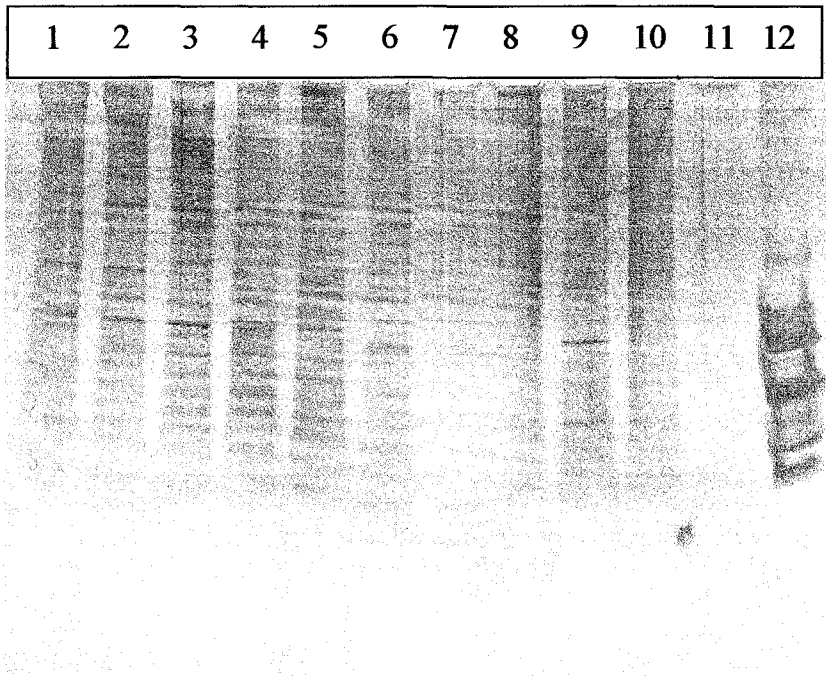

Figure 12: **AKH Serum Media Expression Results.** Lane 12 contains a polypeptide standard. Lane 11-7 contains a control lane of blank vector pMT/V5-His-TOPO induced with copper sulfate in 1 day increments. Lane 6 contains the zero time point expression vector induced with copper sulfate. Lanes 5-1 represent 1 day increments in expression time course. Small bands were observed in lanes 5-1 suggesting expression of the AKH but the serum media contained too much contamination.

Cells were adapted to grow under serum free conditions due to the high levels of protein contamination in media samples. Though the protein amounts were decreased in the media, protein production from non-transfected cells in controls produced multiple bands when visualized by SDS-PAGE. Therefore, it was concluded the protein could not be produced without the presence of contaminating proteins in transiently transfected cell lines. Figure 13 demonstrates the banding pattern observed during AKH production in serum-free media.

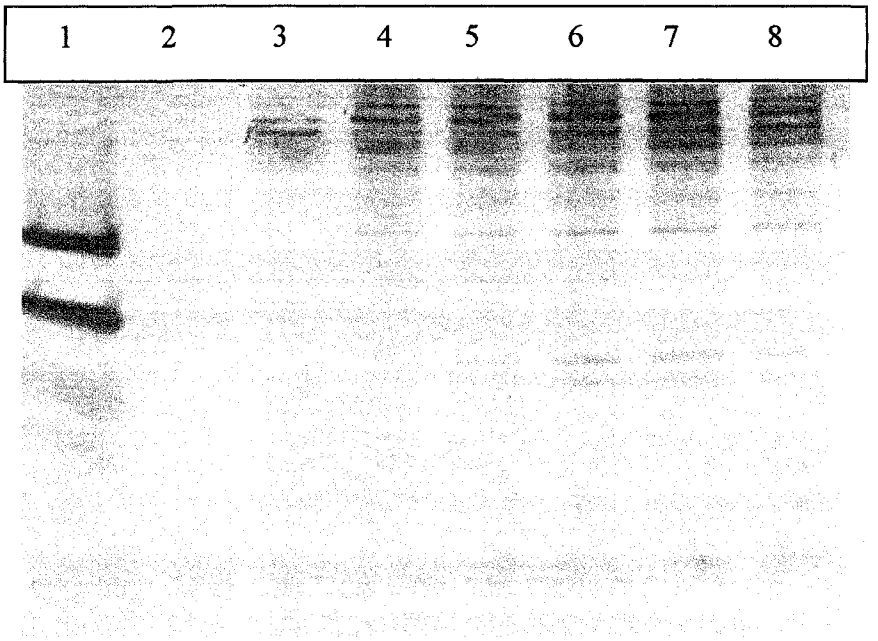

Figure 13: **AKH Serum-free Media Expression Results.** Lane 1 contains a polypeptide standard. Lane 2 contains a control lane of blank vector pMT/V5-His-TOPO induced with copper sulfate for 1 day. Lane 3 contains the zero time point expression vector induced with copper sulfate. Lanes 4-8 represent 1 day increments in expression time course. Large bands present in lanes 4-8 are too large to represent AKH. The same bands are observed in control expression for longer time points.

Inductions of stable cell lines, both serum and serum-free cultures, resulted in cell death. Upon addition of various $CuSO_4$ concentrations, cells were no longer viable when viewed using tryphan blue staining. Cell death resulted in production of no protein product.

Cloning and expression of Human Gonadotropin-releasing Hormone (GnRH)

Human GnRH was designed synthetically containing the mature GnRH sequence and a self-cleaving BiP secretion signal. Positive clones were identified using restriction digestion by *AvaI* resulting in 700 bp, 1100 bp, and 1800 bp bands.

Similar protocols were followed for expression in S2 cells. SDS-PAGE analyses of the transfected cell media resulted in similar banding patterns observed in the AKH transfection experiments. Induction of peptide hormone production in stable cell lines resulted in cell death.

Expression of *Drosophila* Glutaminyl Cyclase (dQC)

Drosophila QC coding region amplification from the cDNA vector RE61650 resulted in DNA fragments of approximately 1100 bp, which were subcloned in the bacterial expression vector, pET160/GW/D-TOPO. The pET160/GW/D-TOPO vector contained an inducible promoter, *lac* operon, an N-terminal polyhisitidine (poly-His) tag for purification, and an N-terminal Lumio® tag enabling in-gel fluorescent protein detection. Figure 14 diplays a diagram of the expression vector.

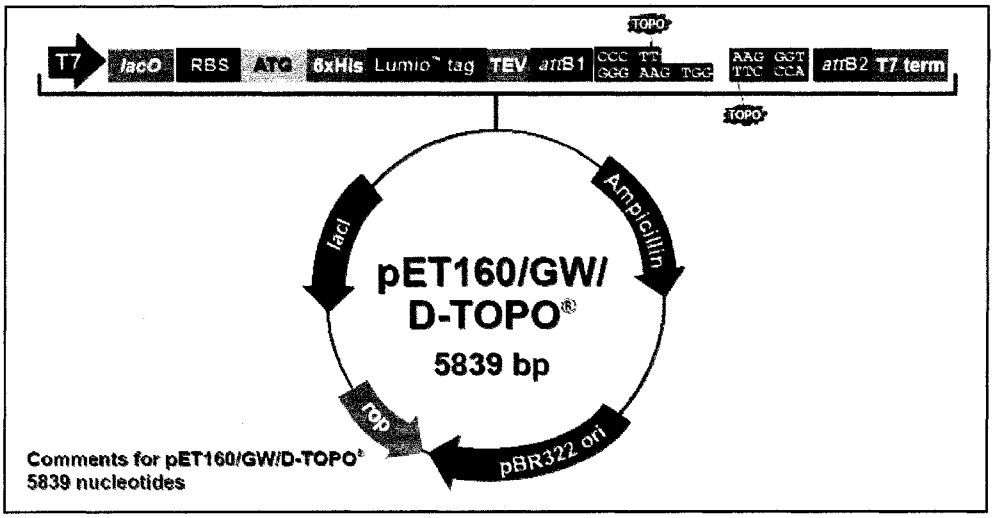

Figure 14: **pET160/GW/D-TOPO expression vector.** This figure represents the vector map of the pET160/GW/D-TOPO used for subcloning the dQC.

Recombinants were screened for presence of PCR inserts in the correct orientation by restriction digests using *AvaI*. *AvaI* cuts the expression vector containing the *Drosophila* QC (6805 bp) insert resulting in two fragments 2637 bp and 4168 bp in length. Incorrect orientation of the insert would have resulted in fragments 1671 bp and 5134 bp in length. Figure 15 displays the restriction digest. Colony 5 was selected for expression protocols and the insert was verified by sequencing. Sequencing results verified the correct construct was produced with no incorrect substitutions during PCR.

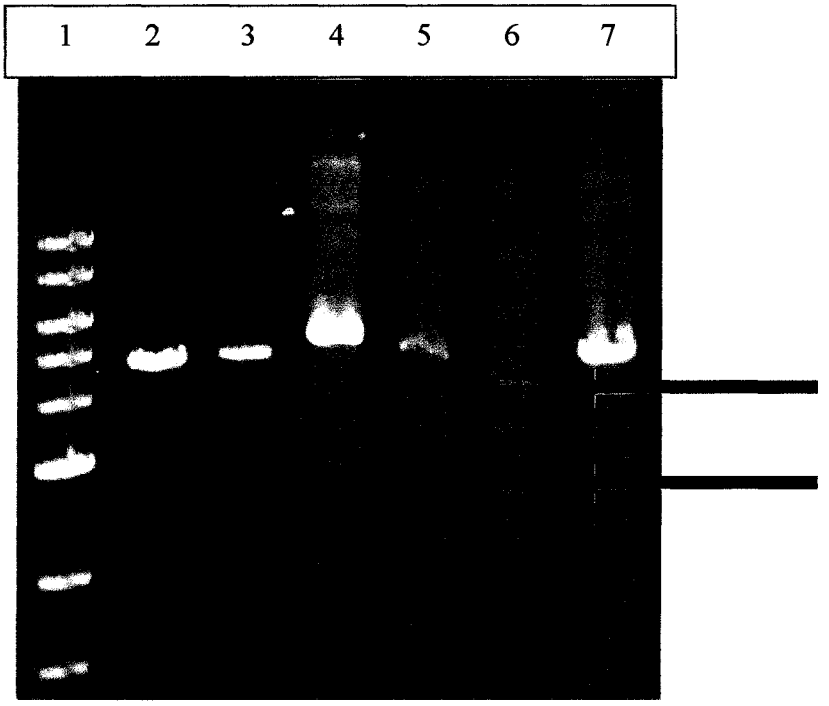

Figure 15: **Confirmation of dQC vector.** Lane 1 contains the 1Kb ladder. Lanes 2 through 7 contain colonies 1-6 digested with *AvaI*. Lane 6 contains colony 5 which has bands in the correct locations of 2637 bp and 4168 bp.

The pilot expression, shown in figure 16, was completed to examine the production of protein. The pET160/GW/D-TOPO with the dQC insert produces a fusion protein which is composed of the amino terminal poly-His tag and Lumio tag (6.7 kD) combined with the dQC (36.8 kD). Therefore, expected size of the dQC protein is 44 kD. Initial expression of dQC at various time points and temperatures in the presence of 0.1 mM IPTG resulted in production of an approximately 44 kD protein as evidenced by SDS-PAGE. It was determined the optimum expression temperature was 25°C and the optimal time for induction was 4 hours.

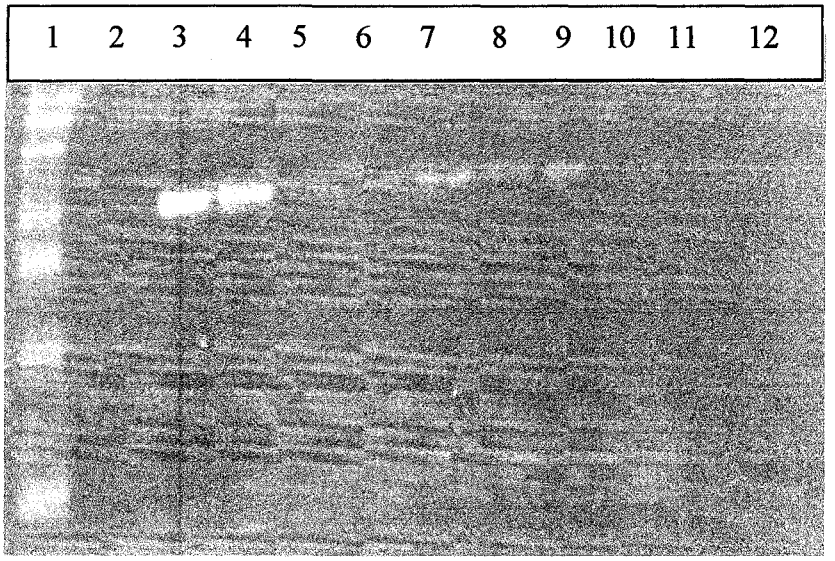

Figure 16: **Expression Profile of dQC_{pET}.** Lane 1 represents a protein standard. Lanes 2 – 5 represent dQC expression at 25°C for time points 0 hours, 4 hours, and 8 hours, and 4 hours (control). Lanes 6 – 9 represent dQC expression at 30°C for time points 0 hours, 4 hours, and 8 hours, and 4 hours (control). Lanes 10 – 12 represent dQC expression at 37°C for time points 0 hours, 4 hours, and 4 hours (control). Gel was visualized using the Lumio detection tag.

Initial attempts at Ni-NTA purification resulted in impure dQC enzyme. Therefore, optimization was completed using varying concentrations of salt and imidazole in wash buffers and elution buffers. Final purification using 10 mM imidazole and 50 mM imidazole sequential wash steps and 250 mM imidazole elution resulted in a pure protein of approximately 44 kD. SDS-PAGE gels of the dQC purification stained with coomassie blue and developed using the Lumio detection reagent are shown in figure 17.

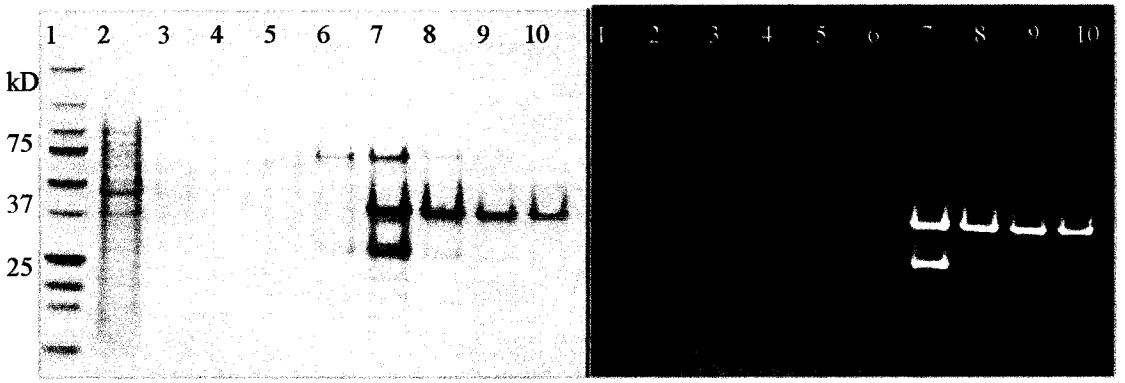

Figure 17: **Purification of expressed *Drosophila* QC**. 10% Tricine gel of Ni-NTA resin purification of expressed *Drosophila* QC. The figure to the left is stained with Simply Blue safestain (Invitrogen). The figure to the right is developed using the Lumio reagent (Invitrogen). Lane 1 contains a Precision Plus Protein standard (BioRad) with intense bands corresponding to 25kD, 55kD, and 75kD. Lanes 2-6 represent wash fractions and lanes 7 – 10 represent elution fractions exposed to 250 mM imidazole. For analysis, fractions 8 – 9 were pooled.

The *Drosophila* QC sequence was verified through specific sequence analyses using trypsin digest and MALDI-TOF. MALDI spectra resulted in a mass list corresponding to the predicted *Drosophila* QC sequence with a likelihood of greater than 70%. Further verification utilized MS-MS on various selected trypsin digest peaks. These results demonstrated the actual sequence of selected peaks which corresponded to the predicted dQC sequence. The smaller, 25 kD, band observed on purification gels was also verified as a degradation product by MALDI-TOF analysis corresponding to digestion at the trypsin site lysine 222.

Another dQC expression system was explored using the glutathione-S-transferase (GST) system previously used to express the human QC. The same dQC cDNA product used in production of the dQC-pET vector was subjected to a restriction digest and ligated into the GST vector. Following analyses for correct insertion and orientation the dQC vector was transformed into BL21 *E. coli* cells. The dQC protein was produced in the insoluble fraction. Therefore, the dQC could not be easily used for enzymatic analyses and was stored for later use.

Characterization of dQC

Purified dQC was checked for QC activity using the spectrophotometric and fluorometric assays. Initial results demonstrated QC activity using both Gln-NH_2 and Gln-tBE substrates in a time dependent manner. Enzyme activity was tested in the presence of known QC inhibitors imidazole, 1-methyl imidazole, and 1-10 phenanthroline. *Drosophila* QC was inhibited in the same manner as human QC suggesting the expressed peptide was a QC. Optimum assay pH was determined to be 7.5.

Kinetic analyses revealed virtually identical kinetic values for the expressed *Drosophila* QC when compared with published human QC values on all tested substrates. The Km values for spectrophotometric assay substrates Gln-NH_2 and Gln-tBE were 1.4 ± 0.4 mM and 6.6 ± 0.6 mM, respectively. The Km value for the fluorometric assay substrate Gln-βNA was 42 ± 5 uM. Table 6 provides a comparison of the values for dQC compared to the previously determined values for human QC. (*Booth 2003)

The kcat and kcat/Km values for the *Drosophila* QC are, however, much lower than the values for human QC demonstrating the expressed *Drosophila* QC has a lower turnover. Therefore, the dQC appears to be less efficient than the human QC. In order to determine if the enzyme activity was altered in the purification procedure, various changes were made to the protocol such as temperature, pH, ionic strength, etc. resulting in similar kinetic values. Therefore, it is possible that the lower enzyme activity is a natural characteristic but it is most likely due to the harsh conditions necessary for heterologous protein purification which can not be altered.

Table 6: **Kinetic parameters for the expressed *Drosophila* QC.**

Substrate	**Enzyme Type**	**Km (mM)**	**kcat (s^{-1})**	**kcat/Km ($mM^{-1}s^{-1}$)**
Gln-NH2				
	Drosophila QC	1.4 +/- 0.4	1.7 +/- 0.2	1.2 +/- 0.2
	*Human QC	1.4 +/- 0.2	13	9.3
Gln-tBE				
	Drosophila QC	6.6 +/- 0.6	2.6 +/- 0.2	0.4 +/- 0.06
	*Human QC	6.7 +/- 2	16.0	2.4
Gln-βNA				
	Drosophila QC	0.042 +/- 0.005	1.9 +/- 0.3	45 +/- 3
	*Human QC	0.060 +/- 0.006	18.8 +/- 0.7	313

Inhibition studies revealed the *Drosophila* QC was inhibited by imidazole, imidazole derivations such as 1-methyl imidazole, and metal chelators such as 1-10 phenanthroline. Determination of Ki values revealed essentially equal values when

compared to human QC. The Ki was evaluated for 1-methyl imidazole as 0.02 ± 0.01 mM, which is essentially equal to the Ki for human QC. This suggests the *Drosophila* QC and human QC have similar modes of inhibition with respect to the tested inhibitors. Figure 18 displays graphically the inhibition of dQC by imidazole, imidazole derivatives, and metal chelators.

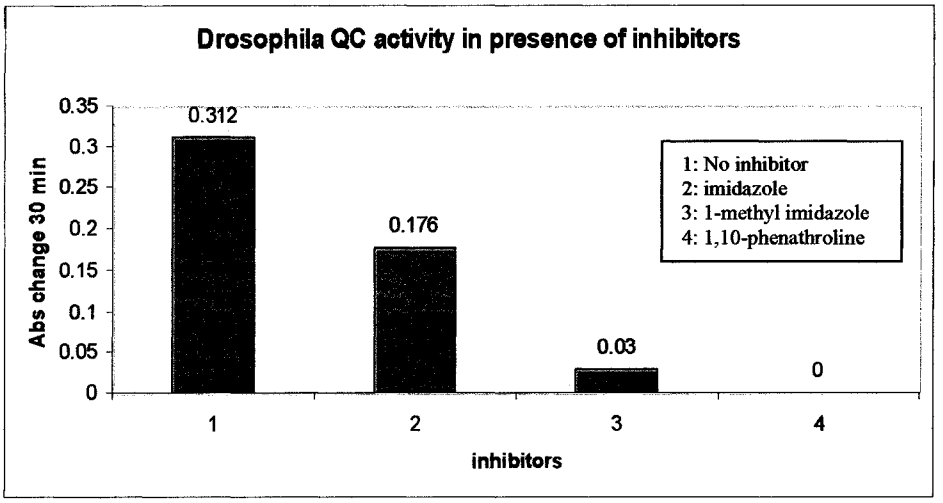

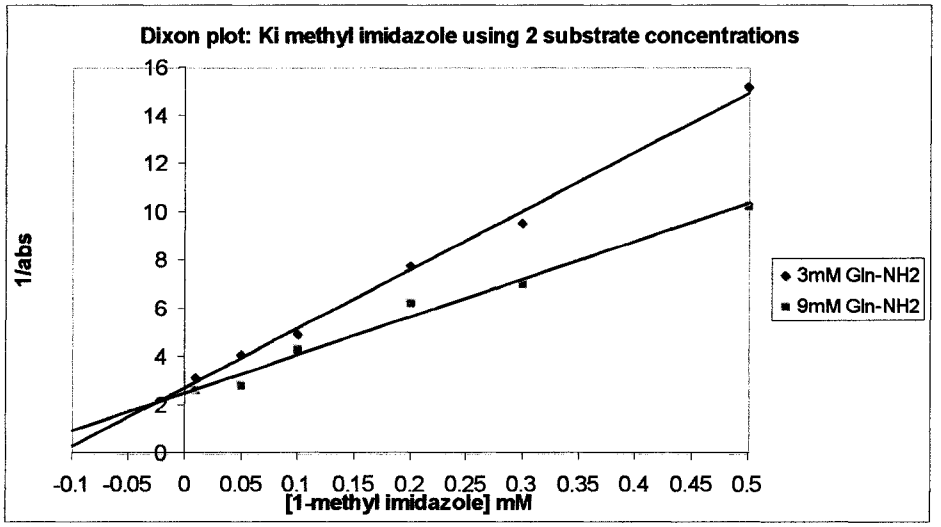

Figure 18: **Inhibition profile of dQC**. The column graph represents the inhibition profile of dQC. Column 1 represents uninhibited dQC in a 30 minute assay, column 2 represents inhibition by imidazole, column 3 represents inhibition by 1-methyl imidazole, and column 4 represents inhibition by 1,10-phenanthroline. This suggests dQC is inhibited in the same manner as hQC. The line graph to the left represents a Dixon plot of dQC inhibition by 1-methyl imidazole. The Ki was calculated at 0.02 mM +/- 0.01. Error is calculated from 3 runs of the same experiment. The Ki of 1- methyl imidazole with hQC is 0.03 mM.

Human QC has previously been purified using a reactive blue column demonstrating the ability of the human QC to bind the reactive blue. Attempts to demonstrate the binding of dQC to the reactive blue column revealed a similar binding pattern. As with hQC, the dQC was eluted from the column at a high pH of 8.5. This demonstrates a similar 3-D orientation of the dQC and the human QC.

Expression of *Drosophila* Glutaminyl Cyclase-Like (dQC-LK)

The *Drosophila* QC-LK coding region was amplified from the cDNA vector GH11174 resulting in a band of approximately 950 bp. The PCR product was directly subcloned into pET160/GW/D-TOPO (Invitrogen) for bacterial expression. Recombinants were screened for presence of PCR inserts in the correct orientation by restriction digests using *AvaI* and *NotI*. *AvaI* cut the expression vector containing the *Drosophila* QC-LK (6754 bp) insert resulting in three fragments 804 bp, 2499 bp, and 3451 bp in length. Incorrect orientation of the insert would have resulted in fragments 135 bp, 2499, and 4120 bp in length. All 4 colonies tested appeared to be in the correct orientation (figure 19). Colony 1 was selected for expression protocols and the insert was verified by sequencing. Sequencing results verified the correct construct was produced with no incorrect substitutions during PCR.

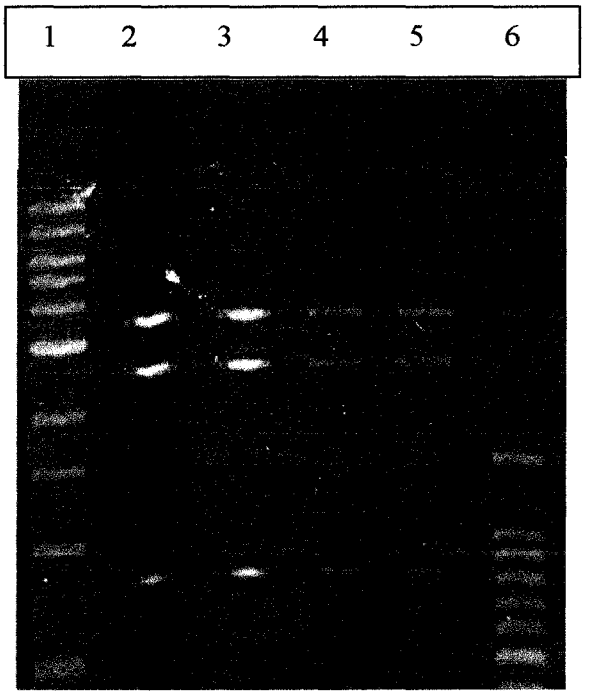

Figure 19: **Confirmation of dQC-LK vector.** Lane 1 contains the 1Kb ladder. Lanes 2 through 5 contain colonies 1-4 digested with *AvaI* and *NotI*. Lane 6 contains the 100 bp ladder. All lanes appear to be in the correct orientation.

The pilot expression was completed to examine the production of protein. The pET160/GW/D-TOPO produces a fusion protein which is composed of the amino terminal poly-His tag and Lumio tag (6.7 kD) combined with the dQC-LK (40 kD). Therefore, the expected size of dQC-LK protein is 47 kD. Initial expression of dQC-LK at 25°C for 3 hours in the presence of 0.1 mM IPTG resulted in protein expression primarily in the insoluble fraction. Small amounts of dQC-LK protein were observed at approximately 47 kD but due to the low concentration a different expression vector was used for expression studies, figure 20.

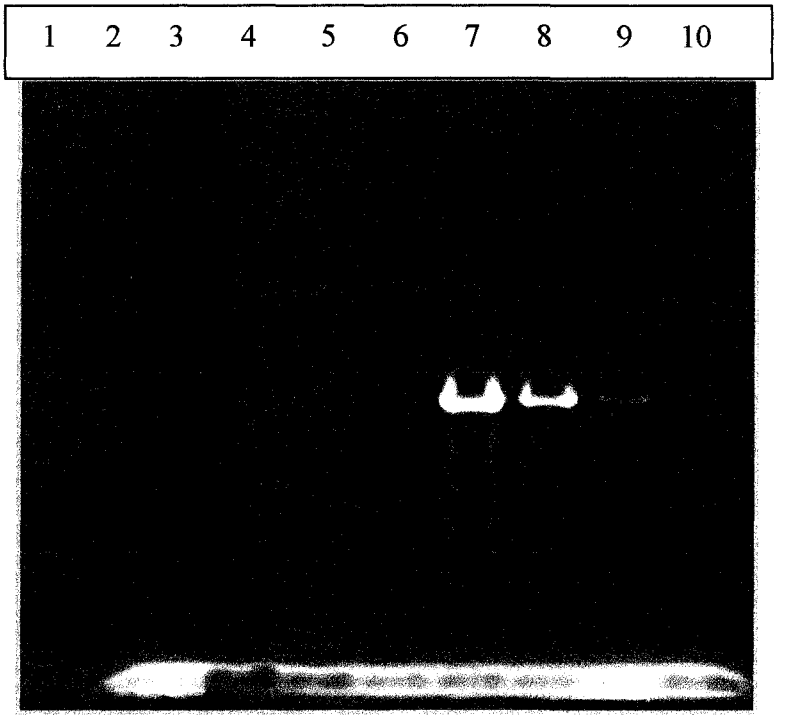

Figure 20: **Expression of dQC-LK$_{TOPO}$.** The figure represents a 10% Tricine gel of the soluble dQC-LK expression. The bands demonstrate the small amount of dQC-LK produced in the soluble fraction.

PCR amplification using specific primers resulted in a 1000 bp band sublcloned into the expression vector, pTXB1 (dQC-LK$_{IMPACT}$). Resulting colonies were analyzed by restriction digestion using *AvaI*. Correct clones would result in fragments of 164 bp, 2167 bp, and 5404 bp. Clones containing an insert in the incorrect orientation would result in fragments of 900 bp, 2167 bp, and 4641 bp. Colonies 1 and 6 appeared to contain the insert in the correct orientation (figure 21). Both were verified by sequencing.

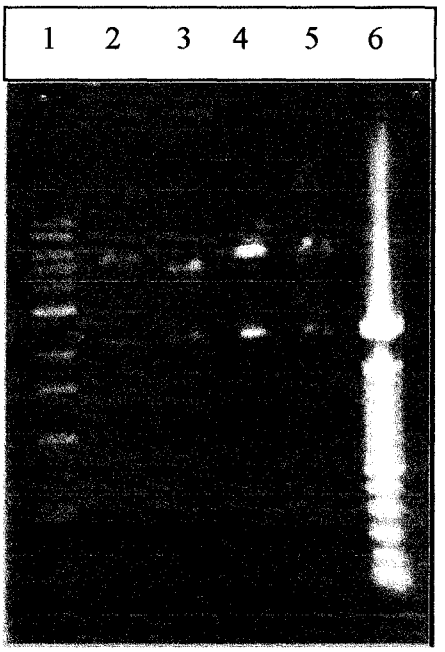

Figure 21: **Confirmation of dQC-LK$_{IMPACT}$ Vector.** Lane 1 contains a 1 Kb ladder, lanes 2 through 5 contain colonies 1, 5, 6, and 7, and lane 6 contains a 100 bp ladder. Colonies 1 and 6 appear to contain a 5 Kb fragment which suggests the colonies contain insert in the correct orientation.

Expression of the dQC-LK$_{IMPACT}$ vector in BL21pLys expression cells revealed a band of approximately 50 kD in the elution fractions. Elution bands were verified by MALDI following in-gel trypsin digest. As with the dQC, MS-MS was used to further verify the results. Figure 22 displays a SDS-PAGE gel of the dQC-LK purification stained with coomassie blue.

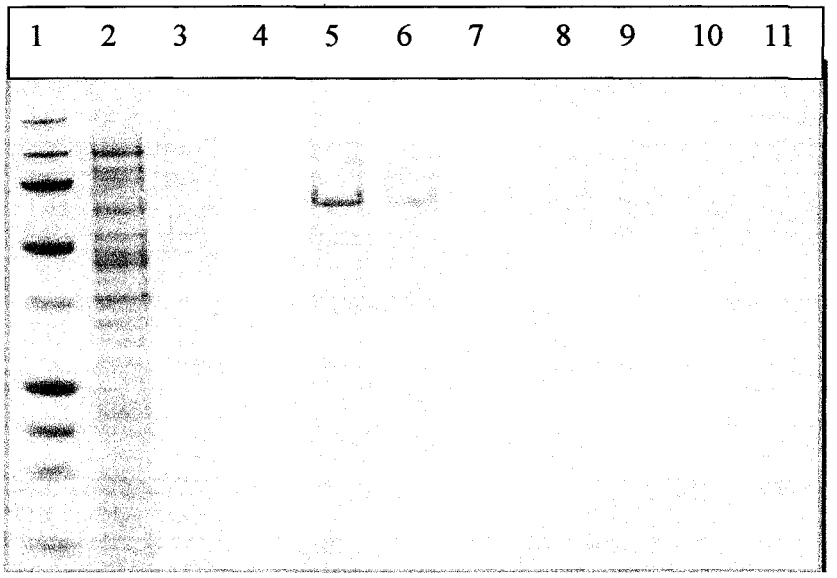

Figure 22: **Purification of dQC-LK$_{IMPACT}$.** Lane 1 contains a protein standard. Lanes 2-3 represent the wash fractions. Lanes 5-7 represent 1 mL elution fractions. The dQC-LK is located in all elution fractions.

The activity of the expressed dQC-LK was analyzed using the spectrophotometric assay previously described. The dQC-LK showed similar but slightly lower activity compared to the expressed dQC enzyme. Typical assays revealed 50 – 70 % of the activity observed in the dQC when the same amounts of protein were added to each enzyme assay. Figure 23 demonstrates the observed activity of purified hQC-GST, dQC$_{pET}$, and dQC-LK$_{IMPACT}$. Further analyses of the dQC-LK protein were completed by a competitor before kinetics experiments were finalized. Competing published data correlates to all results obtained.

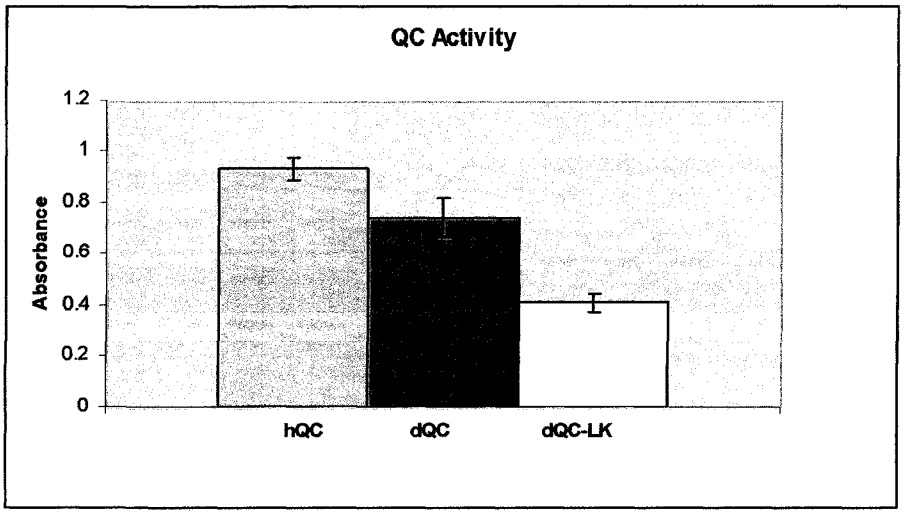

Figure 23: **QC activity of hQC, dQC, and dQC-LK.** This graph demonstrates the absorbance change over 60 minutes using the spectrophotometric assay under standard assay conditions. Errors are calculated from assays completed using three different preparations of dQC_{pET} and dQC-LK_{IMPACT} recombinant proteins. All assays were completed at least 3 times.

Analysis of dQC and dQC-LK aminopeptidase activity

Due to the overall structural similarity observed between human QC and bacterial aminopeptidase active site amino acids, the aminopeptidase ability of hQC, dQC, and dQC-LK was tested using the p-nitroaniline aminopeptidase assay described. Briefly, p-nitroaniline conjugated to various amino acids, typically leucine, was incubated with a leucine aminopeptidase as a positive control or the QCs. Reaction conditions were varied in pH and zinc concentrations. Glutamine conjugated p-nitroanilide is not commercially available.

Initial attempts to elicit aminopeptidase activity utilized the normal QC assay buffer of 50 mM MOPS at pH 7.5 and 1 mM leucine p-nitroanilide as substrate with a final zinc concentration of 0.1 mM. Initially, relatively small activity was observed in the QC tests. Results demonstrated the QCs' aminopeptidase activity was approximately 10% of the commercially available leucine aminopeptidase activity from porcine kidney. *Aeromonas proteolytic* aminopeptidase is not commercially available. Figure 24 demonstrates the results.

In all assays, controls containing substrate only and enzyme only were completed to verify that absorbance observed was due to aminopeptidase activity and not substrate breakdown. Analysis of controls for production of any absorbance was required due to the small absorbance increase observed in the QC samples. Typically, any absorbance observed in either the substrate only or enzyme only control was subtracted from the tested samples containing both substrate and enzyme.

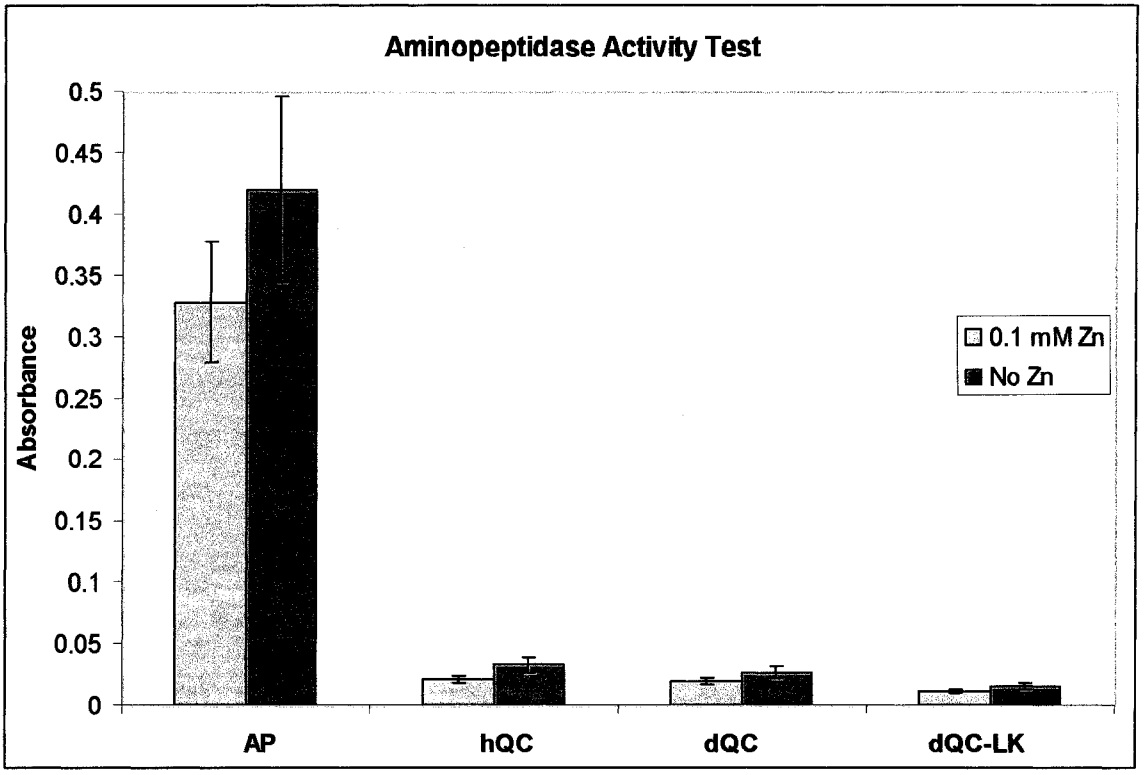

Figure 24: **Aminopeptidase Activity Test.** This graph demonstrates the aminopeptidase activity observed by aminopeptidase (AP), hQC, dQC, and dQC-LK. The assay was completed at pH 7.5 using leucine p-nitroanilide as substrate. Standard errors were calculated from 6 trials of experiments.

In an attempt to induce higher aminopeptidase activity, assay conditions were altered. First, time courses were completed with various incubation times and it was determined that four hour incubations were required to reach maximal aminopeptidase activity in the QC tests. Various zinc concentrations ranging from 0 to 0.1 mM demonstrated no effect on activity even in the positive controls. Therefore zinc was omitted from the assays in further experiments. Out next attempt tested a pH range of 6.0 to 8.0 using a 30 mM MOPS, 30 mM MES mixture due to the differences in

aminopeptidase and QC assay pH optima. The aminopeptidase is more active at a slighty basic pH than QC which is more active around pH 7.2 – 7.5. Surprisingly, results indicated the most aminopeptidase activity of the QC in the more acidic range at pH 6.5 while the aminopeptidase was most active at pH 7.5 and pH 8.0 as expected. Figure 25 demonstrates the results.

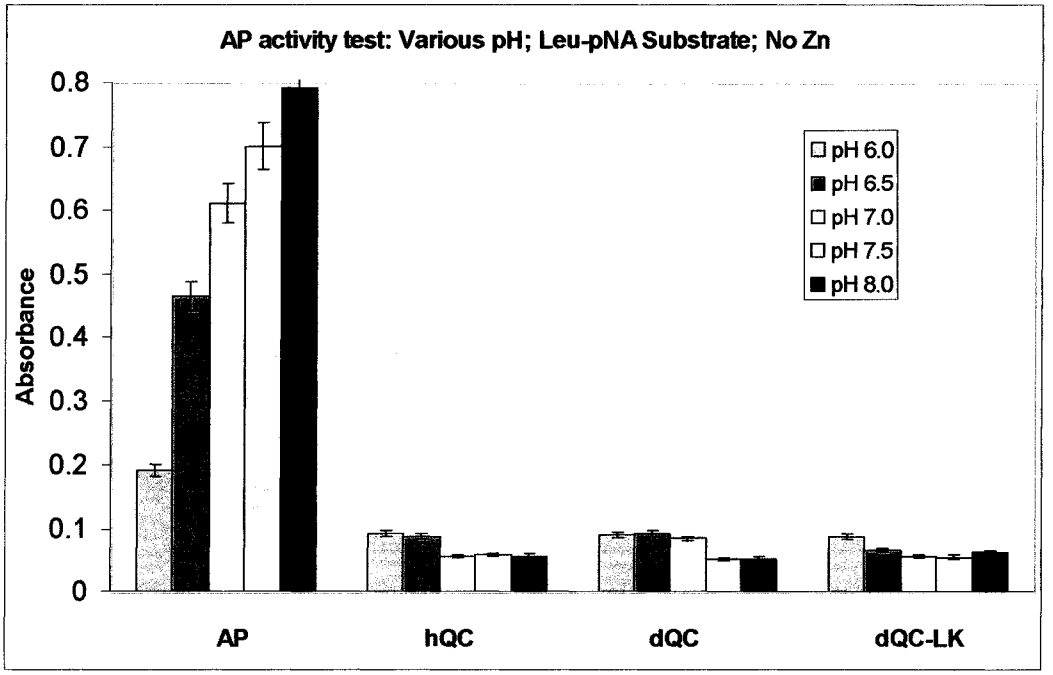

Figure 25: **Aminopeptidase Activity of QC at Various pHs.** This bar graph demonstrates the aminopeptidase activity observed by aminopeptidase (AP), hQC, dQC, and dQC-LK at pH 6.0, 6.5, 7.0, 7.5, and 8.0. Standard errors were calculated from 6 trials of experiments.

Similar experiments were completed using alanine p-nitroanilide and glycine p-nitroanilide. Both substrates revealed similar levels of aminopeptidase activity in QC with the leucine p-nitroanilide substrate. However, the leucine p-nitroanilide resulted in

the highest aminopeptidase activity and was used for all following assays. Finally, the amount of QC added to the assay was increased 100-fold which resulted in a very slight increase in aminopeptidase activity. Therefore, the results suggest only approximately 10 – 15 % aminopeptidase activity could be obtained from the hQC, dQC, or dQC-LK compared to the commercially available leucine aminopeptidase.

Due to the apparent low levels of aminopeptidase activity of the QCs on leucine p-nitroanilide, further testing was completed using various leucine peptides. The aminopeptidase activity results suggested the QCs were capable of binding the leucine. Therefore, commercially available leucine amide (leu-NH_2), leucine-glycine (leu-gly), leucine-alanine (leu-ala), and leucine-leucine (leu-leu) were tested as QC inhibitors.

Several leucine peptides demonstrated inhibition of hQC and dQC. At a concentration of 1 mM, addition of leucine peptide resulted in a loss of activity demonstrated in both the spectrophotometric and fluorometric assays. Figures 26 and 27 demonstrate typical results of hQC and dQC activity in the presence of all peptides. However, no activity loss was observed in the presence of leu-NH_2.

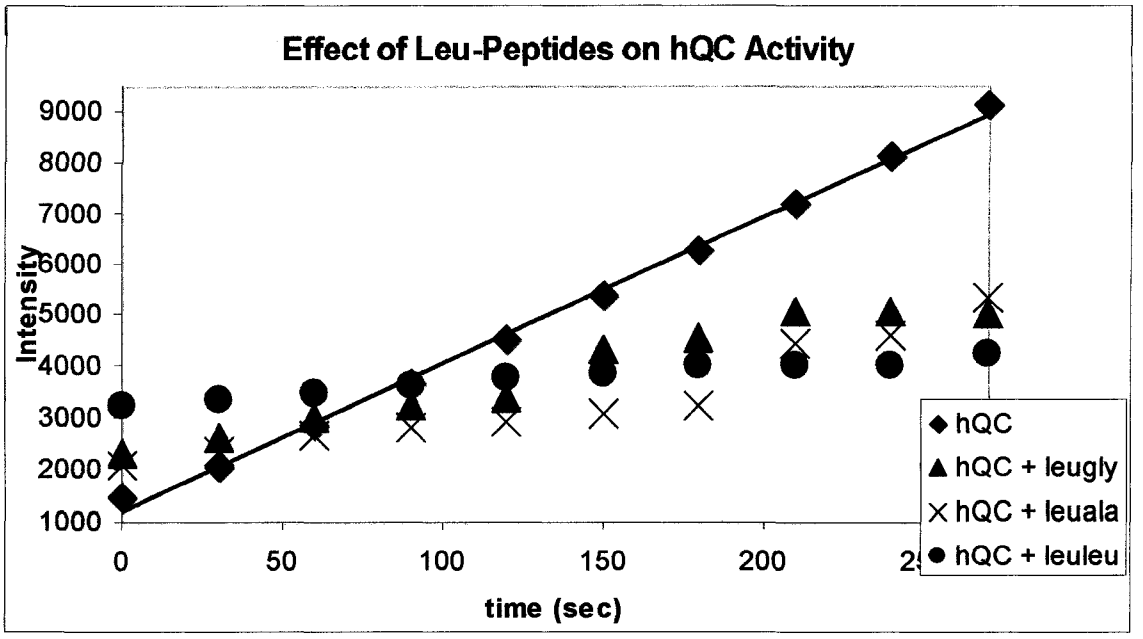

Figure 26: **Inhibition of hQC with Leu-peptides.** This graph demonstrates the inhibition of hQC by leu-gly, leu-ala, and leu-leu using the fluorometric assay.

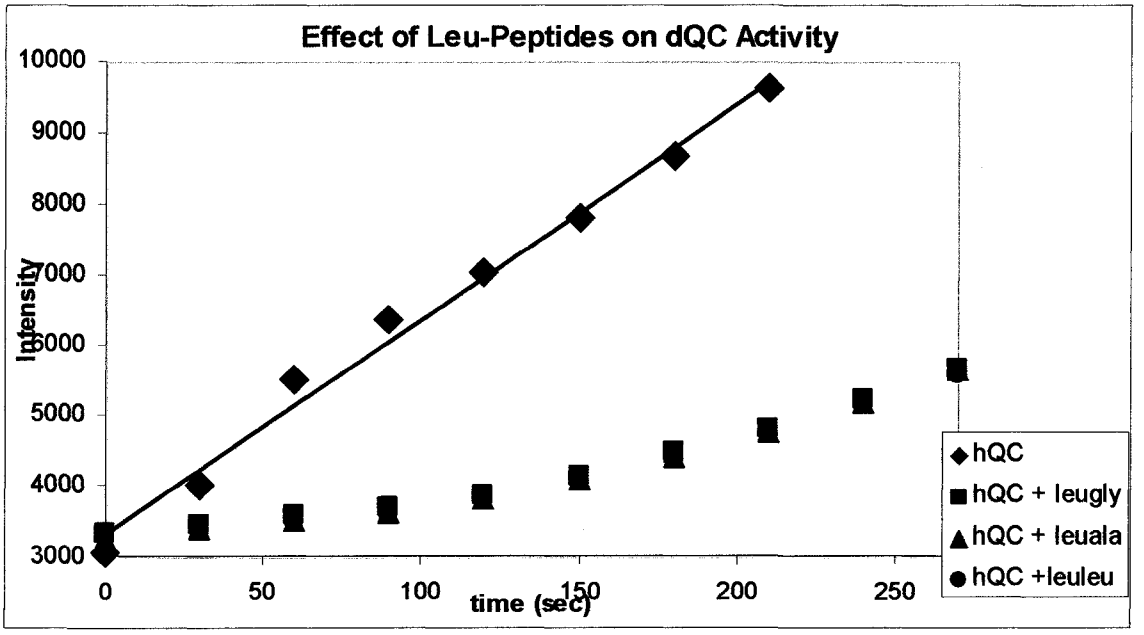

Figure 27: **Inhibition of dQC with Leu-peptides.** This graph demonstrates the inhibition of dQC by leu-gly, leu-ala, and leu-leu using the fluorometric assay.

To further evaluate the inhibition of QC by leucine peptides, using hQC as enzyme, inhibition data was plotted using both Dixon plots (figure 28) and Lineweaver-Burke plots (figure 29). Ki values were determined for leu-gly, leu-ala, and leu-leu from the Dixon plots. The results are demonstrated in figure 28. The Ki values for leu-gly, leu-ala, and leu-leu were calculated as 1.02 +/- 0.44 mM, 0.97 +/- 0.32 mM, and 0.47 +/- 0.33 mM, respectively. hQC was most strongly inhibited by leu-leu followed by leu-ala and leu-gly. Since leucine did not inhibit hQC, these results suggest a larger group bound to the leucine increases the inhibition. Both plots verify the leucine is a competitive inhibitor binding to the enzyme active site.

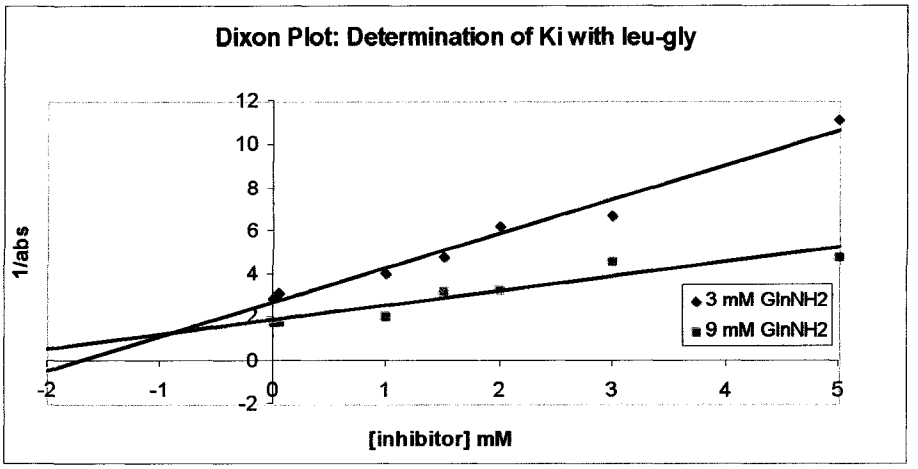

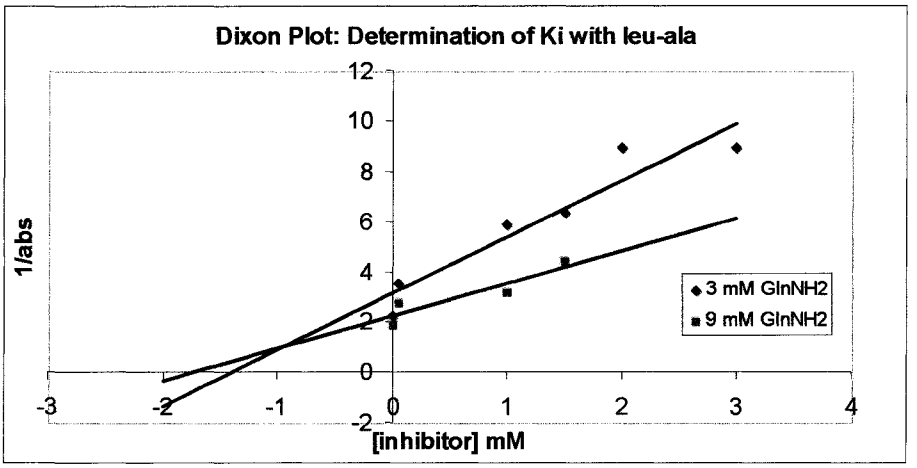

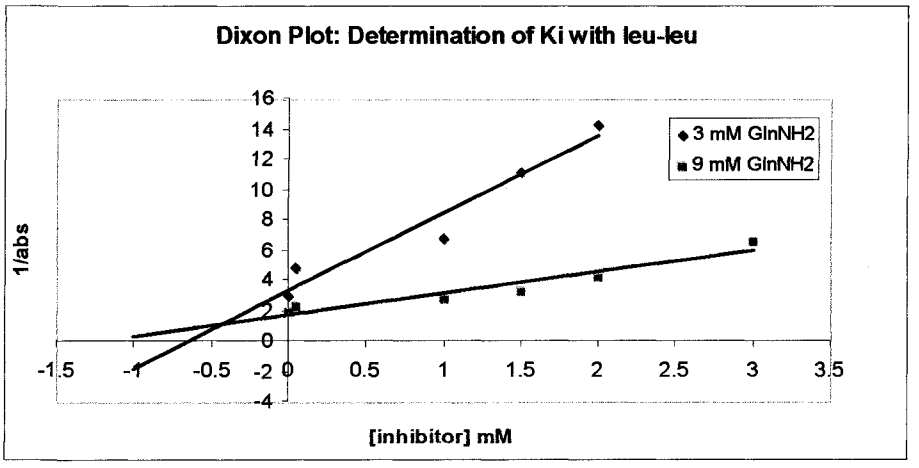

Figure 28: **Dixon plots of leucine peptide inhibition.** This figure demonstrates the Dixon plots for hQC in the presence of leu-gly, leu-ala, and leu-leu. All graphs were created as averages of a minimum of three experimental runs.

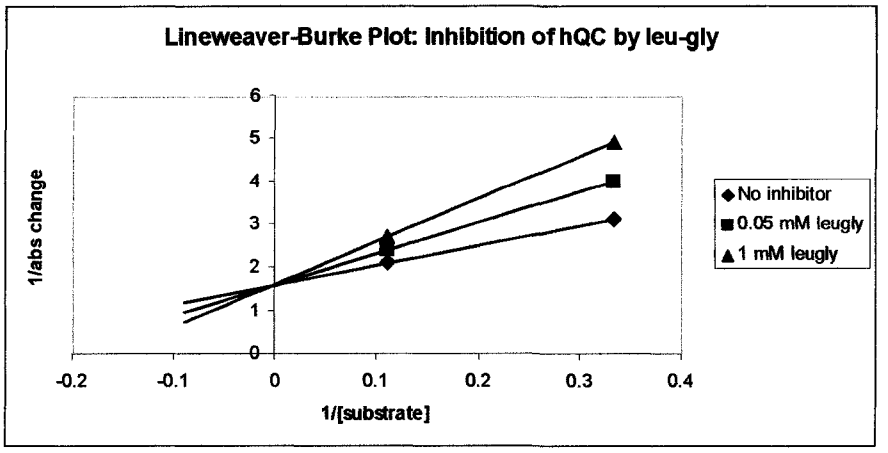

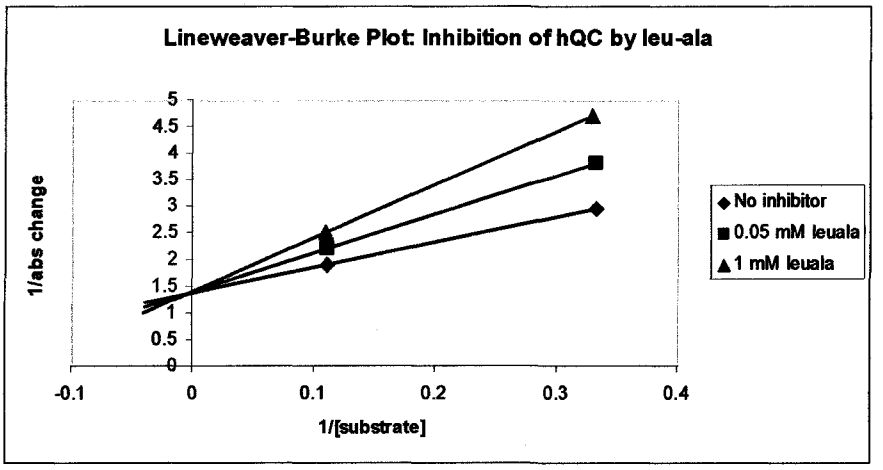

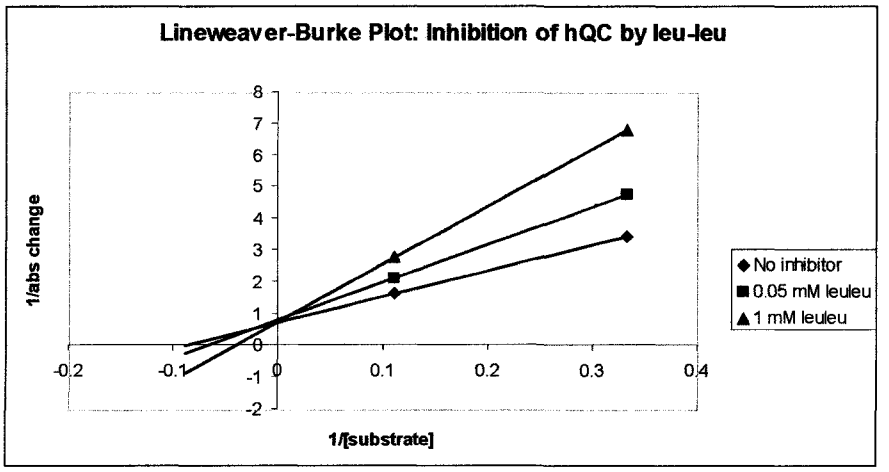

Figure 29: **Lineweaver-Burke plots of leucine peptide inhibition.** This figure demonstrates the Lineweaver-Burke plots for hQC in the presence of leu-gly, leu-ala, and leu-leu. All graphs were created as average of a minium of three experimental runs.

Verification of the QC binding to leucine was further evaluated by testing the effect of other di-peptides and leucine derivatives on the QC activity. Using similar studies it was determined the enzymatic rate was unaffected by addition of ala-ala. This suggests the enzyme is interacting specifically with the leucine. Competition experiments using the common flurometric assay substrate, GlnβNA in a typical reaction, with LeuβNA added revealed a decrease in enzyme activity with both substrates added to the assay reaction compared to a reaction containing just GlnβNA. This demonstrated the ability of QC to bind leucine.

Further testing revealed a possible irreversible inhibition by another leucine derivative, leucine chloromethyl ketone (leu CMK). Addition of 1 mM leuCMK to hQC or dQC resulted in a time dependent loss of activity. Literature has demonstrated the ability of Leu CMK to act as an affinity label in various enzymes containing an active site histidine residue. After 30 minutes of enzyme preincubation with 1 mM leu CMK, 25% of the hQC activity was lost and 45% of the dQC activity was lost. Results are shown in figure 30. Due to the activity loss increase observed over time, the leu CMK serves as a possible affinity label of QC. These results further demonstrate leucine binding of QC and also the presence of a histidine residue within the active site.

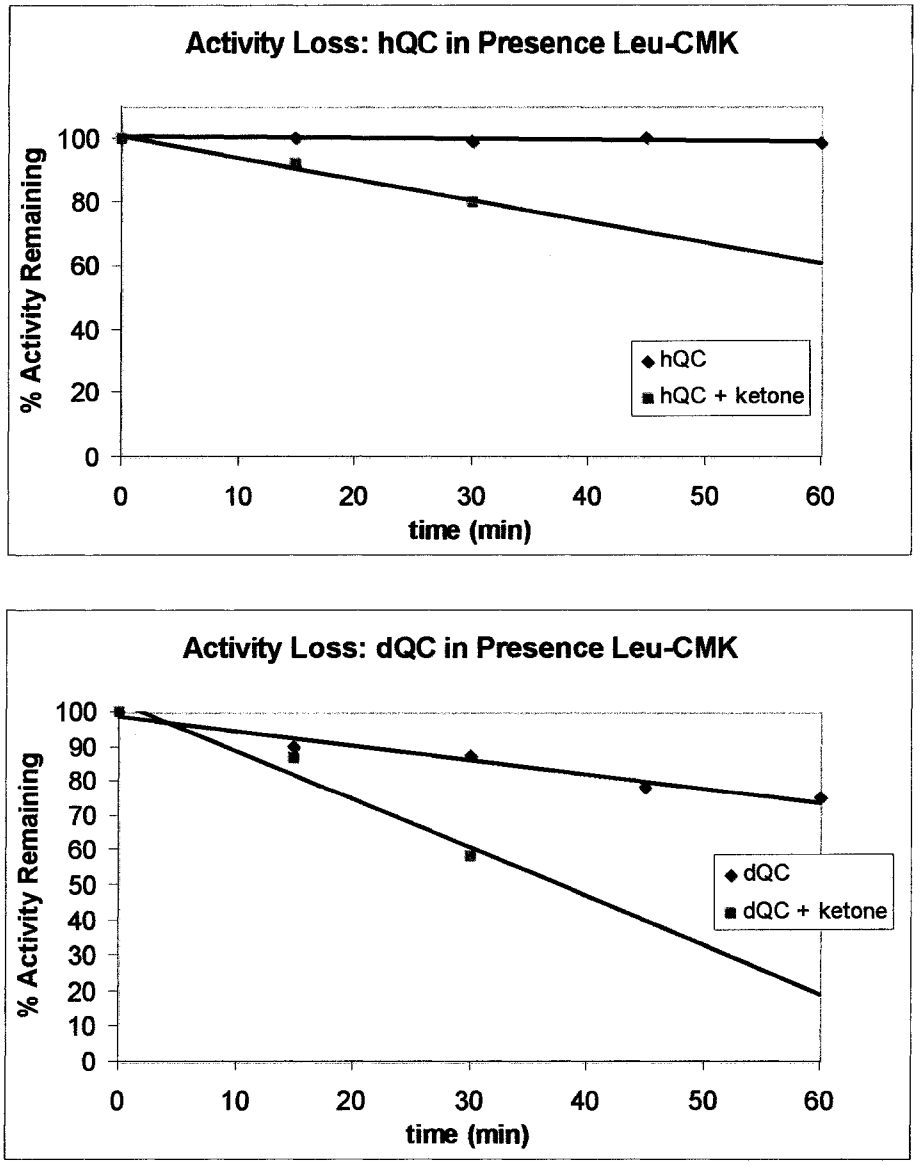

Figure 30: **Activity Loss in Presence Leucine Chloromethyl Ketone.** The top figure displays the activity loss of hQC in the presence of 1 mM leuCMK. The bottom graph displays the activity loss of dQC in the presence of 1 mM leuCMK.

Analyses of Native *Drosophila* Glutaminyl Cyclases

Initial experiments utilized the commercial polyclonal and monoclonal QC antibody and previously developed peptide QC antibody. Antibody specificity was

verified using expressed hQC, dQC, and dQC-LK. The polyclonal antibody specifically binds the hQC and dQC recombinant enzymes but not the dQC-LK. The peptide antibody specifically binds the hQC and dQC-LK recombinant enzymes. These results were verified by competition experiments. However, the monoclonal antibody did not bind either dQC or dQC-LK in the Western Blot analyses. Western blots demonstrating the specificity of the two antibodies for each recombinant protein is shown in figure 31. A single immunogenic band was observed in both *Drosophila* S2 cells and whole *Drosophila* fly lysates using the polyclonal and peptide antibody. This band was visualized by both the polyclonal and peptide antibody. It was approximately 75 kD in size suggesting some post-translational modification occurs.

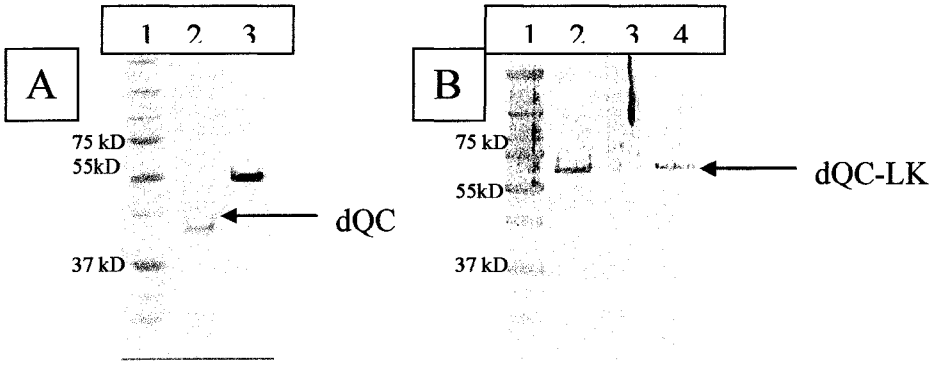

Figure 31: **Western Blot of Recombinant QC Enzymes.** Image A represents a western blot containing dQC in lane 2 and hQC in lane 3 developed with the commercial polyclonal antibody diluted 1/2000. Lane 4 contained the dQC-LK recombinant protein with no staining was observed. Image B represents a western blot containing hQC in lane 1, dQC in lane 2, and dQC-LK in lane 3 developed with the peptide antibody 5247 diluted 1/5000. Only the dQC-LK was detected with the peptide antibody.

Immunocytochemistry of *Drosophila* Embryos

Immunocytochemistry was used to localize both the dQC and dQC-LK proteins within the wild type (Oregon R) and dQC-LK mutant *Drosophila melanogaster* embryos. (For mutant production and genotype see methods) Following standard procedures, the following results were obtained as shown in figure 32. The peptide antibody did not produce any staining in the embryos. However, this is commonly observed in *Drosophila* embryo immunocytochemistry. The polyclonal antibody, which is specific to the dQC, revealed specificity for a protein in the hypopharynx region. The dQC-LK mutant also showed the same specificity. Due to possible cross-reactivity of the dQC isoforms, the immunocytochemistry results were not definitive. Definitive results would require production of a dQC mutant and dQC/dQC-LK specific antibodies.

Figure 32: **Polyclonal antibody staining of embryo.** This image demonstrates the staining of the hypopharynx region in the *Drosophila* embryo using the polyclonal antibody. This embryo is a stage 13 embryo oriented anterior to posterior.

In situ Hybridization of *Drosophila* Embryos

In situ hybridization of *Drosophila* embryos was used to localize both the dQC and dQC-LK RNA transcripts. Experiments utilized overnight embryo collections of

wild-type (Oregon R) *Drosophila melanogaster*. Following standard procedures, the following results were obtained. The dQC-LK RNA transcript was identified as early maternal transcript throughout the entire embryo in stage 5. In later developmental stages 12 – 15, the transcript was identified in the mesoderm, hypopharynx, gut, and in the developing ventral nerve cord. Verification of the identification of dQC-LK in the nerve cord was accomplished by a nerve cord dissection. All tracheal staining was considered non-specific due to the presence of tracheal staining in sense controls. Tracheal staining is typically observed due to RNA probe degradation. The dQC RNA transcript was identified in very low amounts as maternal transcripts in stage 5 embryos and possibly in epidermal tissues, including the hypopharynx, in later stages 12 - 15. Again, non-specific tracheal staining was observed in both experimental antisense and control sense embryos. The dQC-LK appears to be more diversely localized within the developing embryo and in a higher quantity. Figures 33 – 35 demonstrate the *in situ* localization studies.

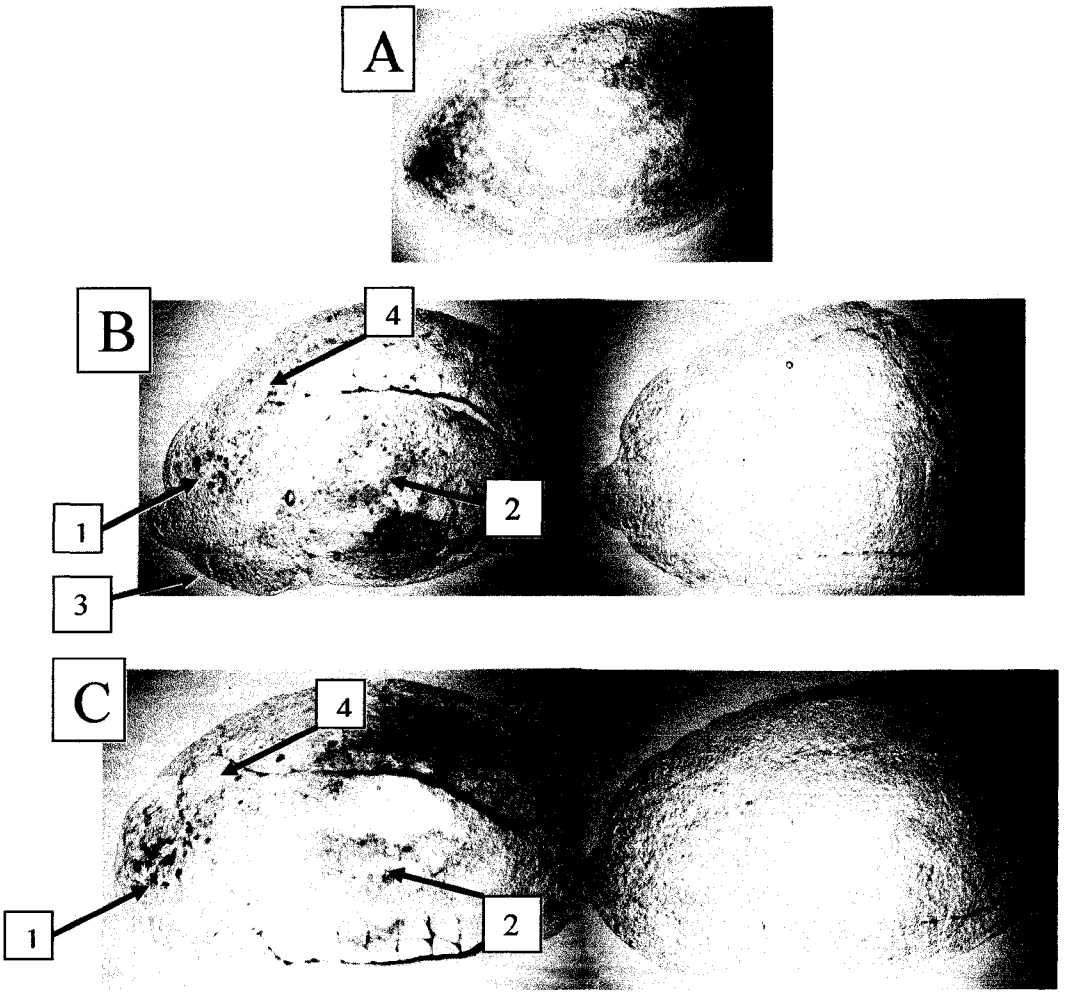

Figure 33: **RNA *in situ* using dQC-LK probe.** (A) This figure contains stage 5 embryos demonstrating the staining of maternal transcript. (B) This figure contains stage 13 embryos with experimental on the left and control on the right. Arrow 1 indicates the staining of the hypopharynx, arrow 2 indicates the gut, arrow 3 indicates the mesoderm, and arrow 4 indicates the ventral nerve cord. The trachea is found in both the control and experimental embryos. (C) This figure contains stage 15 embryos with experimental on the left and control on the right. Arrow 1 indicates the staining of the hypopharynx, arrow 2 indicates the gut, arrow 3 indicates the mesoderm, and arrow 4 indicates the ventral nerve cord. The trachea is found in both the control and experimental embryos. All embryos are oriented anterior-posterior with the ventral facing up.

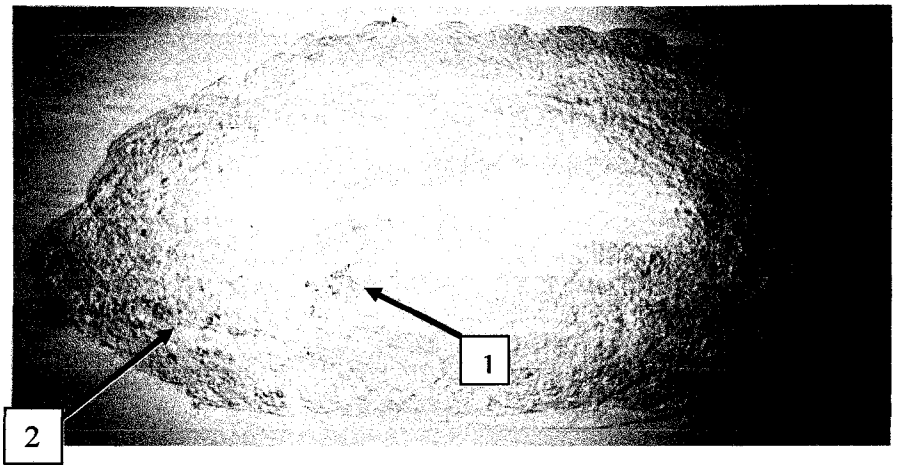

Figure 34: **RNA *in situ* using dQC probe.** Stage 14 embryo demonstrating the faint staining of the hypopharynx (1) and epidermis (2). The embryo is oriented anterior-posterior with the ventral facing up.

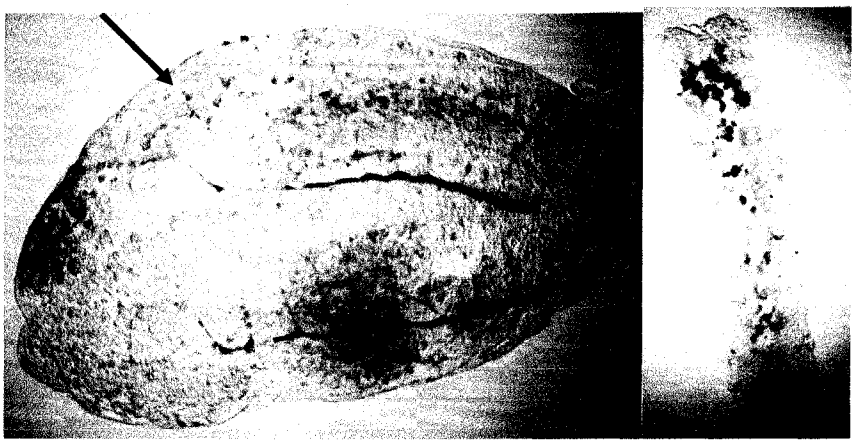

Figure 35: **RNA *in situ* using dQC-LK probe nerve cord dissection.** The image to the left demonstrates a stage 14 embryo with the location of the ventral nerve cord indicated. The image to the right demonstrates the staining in the dissected nerve cord. The staining indicates no defined neuronal expression pattern. The pattern suggests a vesicular pattern.

Analyses of Native Mammalian Glutaminyl Cyclase

Immunostaining of commercial blots containing various tissues from fetal through 7 day old mice revealed the expression of QC in all tissues. However, unexpectedly, the highest expression appeared in the skin and eye. Both commercial polyclonal antibody and peptide antibody yielded a similar staining pattern. The Western blots are shown in figure 36.

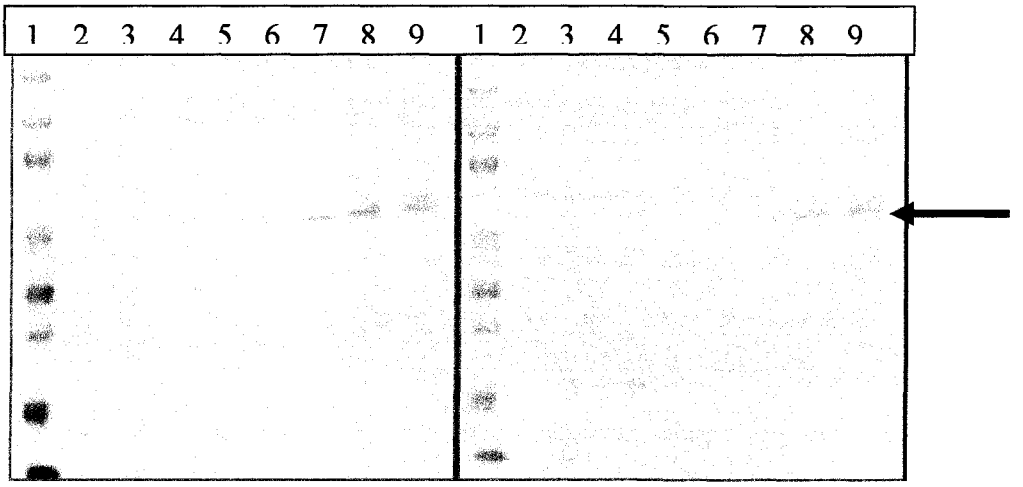

Figure 36: **Immunocytochemistry of mouse QC.** Commercial mouse blots containing a protein standard in lane 1, lane 2 contains 7 days old adrenal, lane 3 contains 0 days old brain, lane 4 contains 7 days old brain, lane 5 contains 7 days old cerebellum, lane 6 contains 7 days old thymus, lane 7 contains 7 days old skin, lane 8 contains 7 days old eye, and lane 9 contains whole fetus. The red arrow indicates the band corresponding to a size of approximately 37 kD, the predicted size of mouse QC.

CHAPTER IV

DISCUSSION

Expression of *Drosophila* AKH and Human GnRH Hormones

Expression of both the *Drosophila* AKH and human GnRH hormones in the *Drosophila* S2 cell line resulted in cell death upon induction of hormone expression. The production of peptide hormones at specific times in the cell is used as a signal to exert a specified function. Sudden induction of large amounts of the hormones during normal cellular activity could have traumatized the cells in culture resulting in cell death. It is also possible that expression of large amounts of heterologous protein in cell culture led to cell death due to the unnatural accumulation of protein. Therefore, the *Drosophila* cell line could not be used for the study of *in vivo* peptide hormone processing under the conditions employed.

Glutaminyl Cyclase activity of *Drosophila* QC and *Drosophila* QC-like proteins

Glutaminyl cyclase (QC) is a post-translational processing enzyme necessary for the conversion of N-terminal glutamine to pyroglutamic acid in various peptides. Published studies thus far have identified QC in various organisms from humans to yeast with highly conserved amino acid sequences and enzymatic function. However, these studies had not identified QC activity in insects. A bacterial expression system was used to express putative QCs from *Drosophila* for characterization. In the system both a *Drosophila* QC and QC-LK protein were identified, expressed, and purified from cDNA vectors with enzymatic activity. Biochemical characterization revealed both enzymes were comparable to the previously expressed and purified human QC. These results were

independently obtained by Parker (Parker 2007; Parker 2008) and Schilling et al. (Schilling 2007).

Table 7 demonstrates the characteristics of the dQC and dQC-LK proteins determined experimentally compared to the previously identified and characterized papaya QC and human QC. These results indicated the QCs were glutaminyl cyclases due to the similarities between all the QCs. Both *Drosophila* QCs were similar in size, pH activity optima, and Km values. The *Drosophila* QCs appear to be more similar to the mammalian QC due to the imidazole inhibition observed and the reactivity to mammalian QC antibodies.

Table 7: **Summary of QC Characteristics from purified *C. papaya* QC, human QC-GST construct, *Drosophila* QC and *Drosophila* QC-LK.**

	C. papaya QC	hQC-GST	*Drosophila* QC	*Drosophila* QC-LK
Molecular weight (kDa)	33	68	44	50
pH activity optimum	8.0	7.5	7.5	7.5
Km (mM)				
Gln-NH_2	1.95	1.5	1.4	N/A
Gln-tBE	N/A	N/A	6.6	N/A
Inhibited by imidazole	No	Yes	Yes	Yes
Antibody reactivity				
hQC polyclonal	No	Yes	Yes	No
peptide antibody	No	Yes	No	Yes

The values obtained experimentally for the *Drosophila* QC and QC-LK proteins correlate well to the published data for the same proteins by Schilling et. al. (Schilling 2008) Expressed proteins in both laboratories revealed virtually identical enzymatic properties. Data from both groups revealed the protein corresponding to the expressed dQC protein had the most catalytic activity and was most similar enzymatically to the human and other mammalian QCs. The kinetic data shown for the *Drosophila* QC and

QC-LK also correlates to the kinetic data published for the same proteins though the Km values obtained were about 25% higher in our laboratory. The group observed the same low catalytic efficiency observed for the expressed dQC and dQC-LK further validating the results obtained. Both laboratories revealed the *Drosophila* QCs were inhibited by imidazole derivatives with the same Ki values for commonly used QC inhibitors within the experimental error.

The *Drosophila* QC and QC-LK protein sequences were verified through specific sequence analyses using in-gel trypsin digest and MALDI-TOF. MALDI spectra resulted in a mass list corresponding to the predicted *Drosophila* QC sequence with a likelihood of greater than 70% for dQC and dQC-LK recombinant proteins. This proves the expressed proteins do correspond to the protein sequences predicted from the *Drosophila* cDNA vectors.

Computer analyses of the putative *Drosophila* QC sequence revealed various physical properties of the proteins. Table 8 provides a comparison of these predictions along with the published physical properties of human QC. The calculated molecular weight of *Drosophila* QC is 41 kD and 38 kD for *Drosophila* QC-LK. Both values are very similar to the molecular weight of 41 kD for the human QC sequence. The theoretical pI of 6.3 for *Drosophila* QC and 6.8 for *Drosophila* QC-LK is also very similar to 6.1, the pI of human QC.

Table 8: **Predicted properties of human QC, *Drosophila* QC, and *Drosophila* QC-LK proteins.**

Enzyme Property	Human QC	*Drosophila* QC	*Drosophila* QC-LK
Molecular weight	41 kD	41 kD	38 kD
pI	6.1	6.3	6.8
Glycosylation sites	N49; N296	N43	N157
Disulfide bonds	C139 – C164	C136 – C158	C113 – C137
Subcellular localization	Secretory pathway signal	Mitochondrial signal	Secretory pathway signal

Subcellular localization predictions suggest the two *Drosophila* QC isoforms may exhibit different subcellular localizations due to differences in the signal sequences. The *Drosophila* QC-LK protein signal sequence predicts a secretory pathway localization which is predicted as well as observed for the human QC. However, the DNA sequence of the *Drosophila* QC protein has two potential signal sequences which arise from alternative splicing events. One potential signal has a predictable mitochondrial subcellular localization a significant threshold score. The other potential signal has a predictable secretory subcellular localization; however, the threshold score was rather low.

3-D structural comparisons showed the predicted 3-D structures of *Drosophila* QC and *Drosophila* QC-LK were very similar to the published crystal structure of human QC (figures 37 and 39). This further confirms the inclusion of the expressed *Drosophila* QC and QC-LK into the family of known mammalian QC enzymes. The core of the proteins, including the secondary structure, superimposes well with only the loop regions showing differences. These results were confirmed by Schilling et. al. through the use of circular dichroism. Analysis of the active site residues revealed not only the conservation

of known binding and/or catalytic residues, but also the conservation of the location of important residues within the 3-D structure. The *Drosophila* QC and QC-LK predicted structures also appear to contain a pocket for zinc in a similar location as the human QC. Schilling et. al. revealed the *Drosophila* QC proteins do contain one zinc per catalytic unit as predicted with the structures. Figures 38 and 40 demonstrate this active site region with residues labeled.

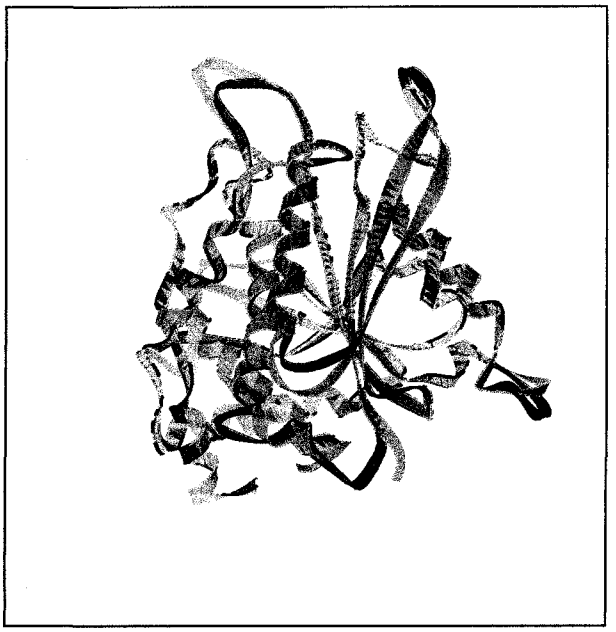

Figure 39: **Predicted 3-D Structure of dQC-LK.** Predicted 3-D structure of *Drosophila* QC-LK (purple) compared to the crystal structure of human QC (blue).

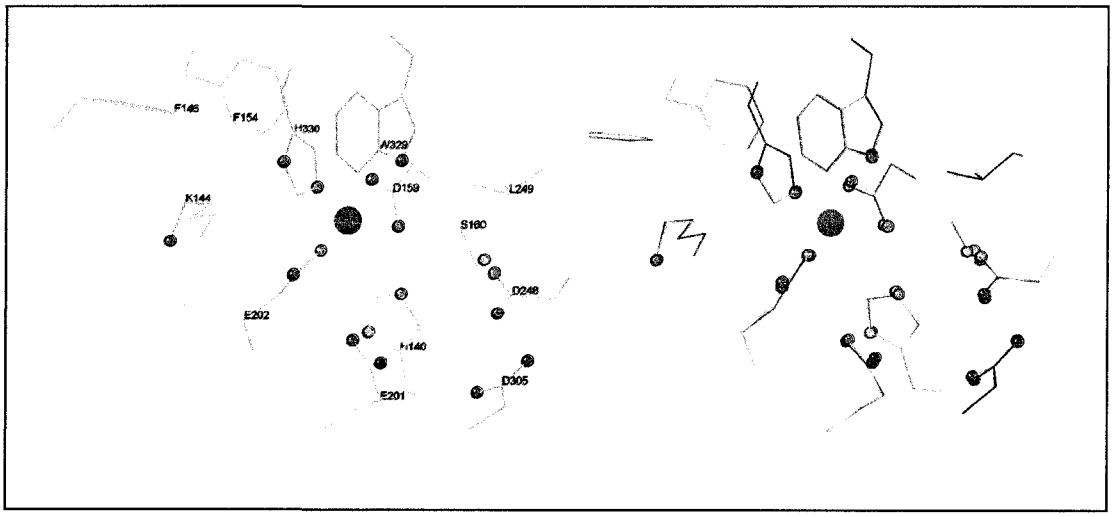

Figure 40: **dQC-LK Predicted Active Site Residues.** Active site comparison of predicted three-dimensional structure of Drosophila QC-LK (purple) compared to the crystal structure of human QC (blue). Left panel contains labels of important active site residues verified by the hQC crystal structure and mutagenesis studies. (Huang, Liu et al. 2005)

Prediction programs (iPSORT) demonstrated a probability of similar sites of N-linked glycosylation among the putative *Drosophila* QCs and human QC. Human QC is known to be glycosylated at asparagine 49 and asparagine 296. (Booth 2003) These amino acids do not appear to be conserved in sequence alignments. Prediction programs suggest possible N-glycosylation sites at N43 and N57 in the dQC sequence. Comparison of the dQC predicted tertiary structure to the hQC crystal structure reveals the N43 is in the same location relative to the N49 of hQC. Similarly, N42 and N157 are predicted as possible N-linked glycosylation sites in dQC-LK. However, only the N157 of dQC-LK is located in the same area of the protein to an N-linked glycosylation site of hQC in the tertiary structure comparisons. There is not a possible N-linked glycosylation site corresponding to the N296 site in the hQC for either *Drosophila* QC. The fact that both N43 of dQC and N157 of dQC-LK are located in the same area of the proteins as the N49 of hQC, along with the glycosylation prediction programs, suggests these are the best candidates for N-linked glycosylation. The location of the predicted glycosylation sites for dQC and dQC-LK are shown in figures 41 and 42 compared to the human crystal structure. Immunocytochemistry of whole *Drosophila* lystates revealed a single, high molecular weight band suggesting post-translational modification of the *in vivo Drosophila* QCs. This provides some experimental evidence to the presence of glycosylated asparagine residues.

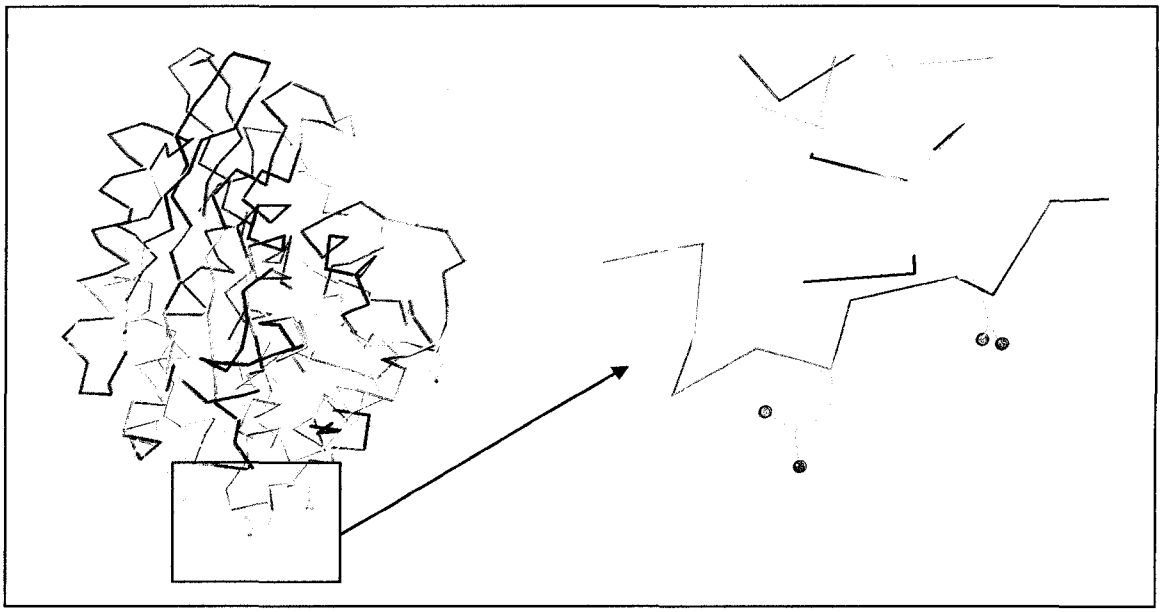

Figure 41: **Comparison of hQC and dQC glycosylation sites.** The figure to the left demonstrates the location of glycosylation sites of hQC, N49 and N296, along with the predicted glycosylation site, N43 of dQC. The human mainchain is shown in black and the *Drosophila* mainchain is shown in yellow. Human sidechains are shown in blue and *Drosophila* sidechains are shown in pink.

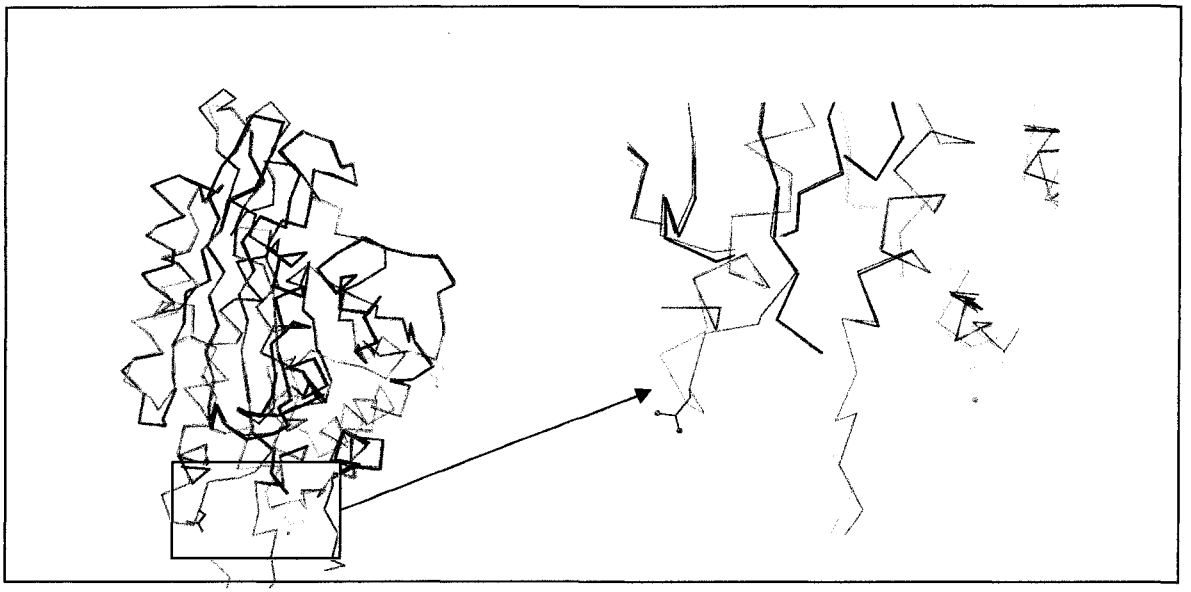

Figure 42: **Comparison of hQC and dQC-LK glycosylation sites.** The figure to the left demonstrates the location of glycosylation sites of hQC, N49 and N296, along with the predicted glycosylation site, N157 of dQC-LK. The human mainchain is shown in black and the *Drosophila*-like mainchain is shown in green. Human sidechains are shown in blue and *Drosophila*-like sidchains are shown in purple.

The human QC contains a disulfide bond between residues C139 and C164. (Schilling 2002) The predicted structure of the *Drosophila* QC and QC-LK does contain cysteine residues in the same location and very similar orientations suggesting the disulfide bond is conserved among speices. (figure 43) The cysteine residues conserved in *Drosophila* QC are C136 and C158. The predicted structure of the *Drosophila* QC-LK also contains two conserved cysteine residues, C113 and C137, suggesting the conservation of the disulfide bond. An overlay of the tertiary structure of hQC, dQC, and dQC-LK are shown in figure 42 with the conserved cysteine residues highlighted.

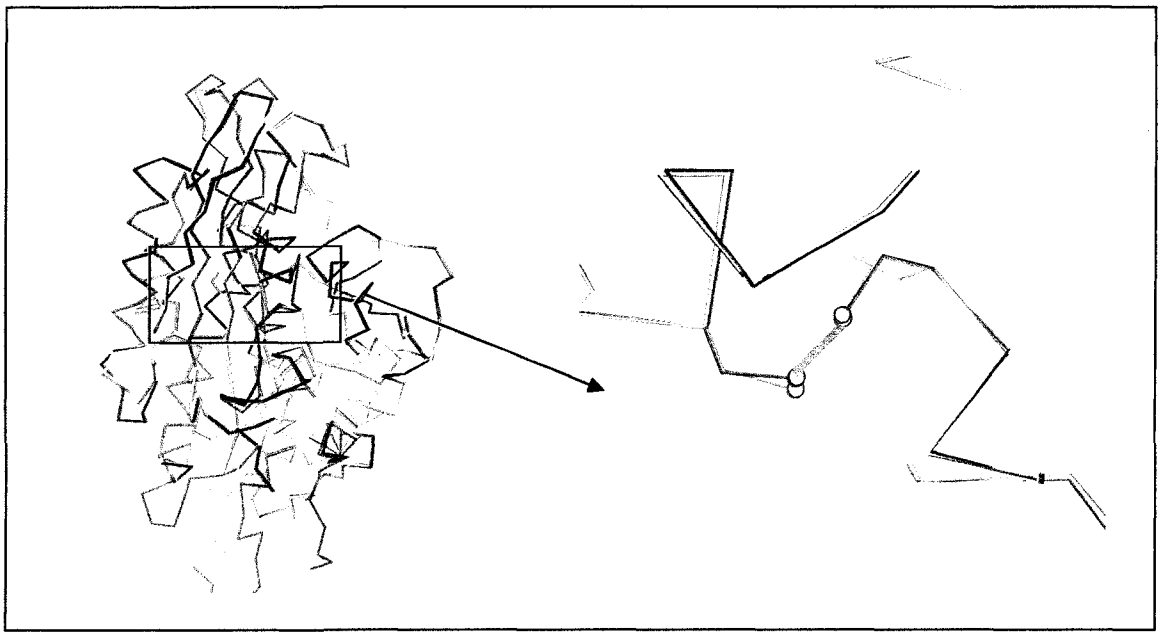

Figure 43: **Comparison of hQC and dQC isoforms disulfide bonds.** This image to the demonstrates the location of the hQC and predicted dQC and dQC-LK disulfide bonds within the tertiary structure of the protein. The human mainchain is shown in black, the *Drosophila* mainchain in yellow, and the *Drosophila*-like mainchain in green. Human sidechains are shown in blue, *Drosophila* in pink, and *Drosophila*-like in purple. The orientation of the disulfide bond is shown in orange.

The predicted conservation of the glycosylation sites and disulfide bonds further validates the predicted tertiary structures constructed for the *Drosophila* QCs. The identical location of the cysteine residues, as well as the similar locations of glycosylated asparagine residues, suggests the predicted structures reveal clues to the conservation of enzyme structure. The conservation of these sites helps reveal the evolutionary relationship among the *Drosophila* QCs and other mammalian QCs, which will be further discussed.

Location and expression levels of Glutaminyl cyclase in *Drosophila*

High throughput RNA *in situ* databanks indicated a high expression of the dQC-LK in early embryonic stages from maternal influence and in the embryonic hypopharynx during later embryonic stages. In constrast, microarray data indicated high levels of mRNA in the male and female sexual organs, the head, and the crop. However, no RNA *in situ* or microarray data was available in the database for the dQC gene. Therefore, in a better attempt to understand the overall function and purpose for two distinct *Drosophila* QCs, the location and expression levels of dQC and dQC-LK were investigated using RNA *in situ* methods and immunocytochemistry.

Both the dQC and dQC-LK RNA transcripts were identified in the early embryo via maternal transcripts as well as some epidermal and mesodermal tissues. However, a high expression level of the dQC-LK transcript was observed in the developing nerve cord suggesting the importance of the dQC-LK in early embryonic nerve cord and neuropeptide development. Location of the dQC-LK transcript appears in the midline of the nerve cord localized within segment polarity stripes. The unpatterned staining of the nerve cord suggests a vesicular pattern for the expression. Figure 44 compares the staining observed in the developing nerve cord with the dQC-LK RNA probe to a stain of a typical neuronal pattern. The lack of a repeating pattern in the dQC-LK staining demonstrates the dQC-LK is not located in an organized neuronal pattern, but instead likely near the secretory vesicles randomly located throughout the nerve cord. Typically localized pools of mRNA transcripts are generated far away from the cell body and especially, in the CNS, pooled in the synapses to produce localized protein on demand. It is possible the dQC-LK mRNA may not be in the vesicles, but located near vesicles

within a budding synapse. This would make the mRNA pattern appear vesicular. The non-patterned staining of the nervous tissues has been observed in RNA *in situ* studies with other *Drosophila* post-translational processing enzymes. RNA *in situ* and immunocytochemistry studies of the *Drosophila* PHM and PAL proteins, proteins which together form the bifunctional PAM homolog, demonstrated a non-patterned staining in the larval CNS. This was further demonstrated to mirror the pattern observed with immunocytochemistry of various neuropeptides and peptide hormones in *Drosophila.* (Kohlekar 1997) Therefore, the non-patterned staining observed in the *Drosophila* nerve cord with the dQC-LK RNA *in situ* could also mirror the non-patterned staining observed in peptides which require the post-translational modification. Also, the localization of the dQC-LK mRNA to the neuronal system into secretory vesiclular region is similar to the localization of the mammalian QC into secretory vesicles of the nervous tissues as observed in published mammalian QC localization studies. (Pohl 1991) (Bockers 1995)

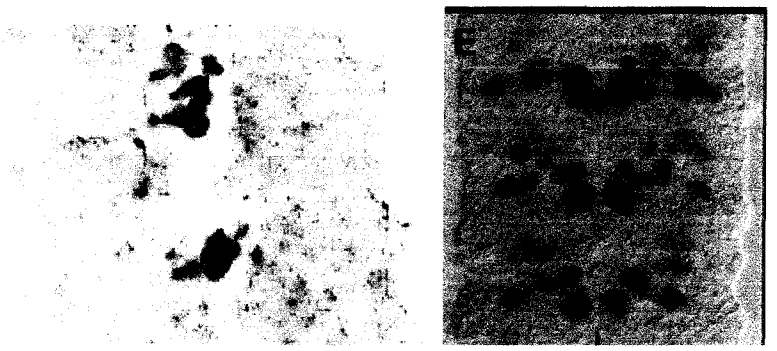

Figure 44: **Nerve cord staining.** The figure to the left demonstrates segments of a dissected nerve cord developed with the dQC-LK RNA probes. The image to the right demonstrates a typical staining of a neuronal expression pattern. (Leal, S., *unpublished data*)

Though the RNA *in situ* analyses did localize the dQC-LK to the hypopharynx as previously described in the database studies, various other tissues were also identified. This could be due to the probe type used. For analyses, total transcript length probes were utilized. This allows all transcripts produced, even in the event of alternative splicing, to be identified. No information was available to determination the length of probes used in the database studies.

Localization studies suggest the dQC-LK is expressed at a higher level than the dQC-LK throughout embryonic development. Equal amounts of probe were added during experimental procedures resulting in comparable data. The lack of staining in the dQC embryos demonstrates the dQC is not expressed at a high level and that the dQC-LK is the dominant isoform expressed in *Drosophila* during embryonic development.

Immunocytochemistry revealed only slight staining in the hypopharynx region. Low levels of staining could indicate either expression within only the early developing hypopharynx or low antibody specificity within the organism as compared to recombinant protein. Further investigation would require production of *Drosophila* QC specific antibodies. The results observed with the polyclonal antibody demonstrated a granular staining pattern. Similar results were obtained in the immunocytochemistry study of the *Drosophila* PAM homologs, dPAL1 and dPAL2. The dPAL1 homolog demonstrated a granular staining pattern as well. (Han 2004) This result could provide some clues into the subcellular distribution of the dQC protein suggesting the dQC protein is a intracellular protein and not secreted.

Published localization studies of other *Drosophila* secretory pathway processing enzymes revealed similar results. The *Drosophila* PAM homologs, dPAL1 and dPAL2,

were localized within the endoplasmic recticulum and within developing neurons. Similar to the localization of dQC-LK observed by RNA *in situ*, dPAL2 was distributed randomly throughout neuronal processing. This indicates the dQC-LK and dPAL2 are located within similar regions aiding the confirmation of the results obtained from *Drosophila in situ* hybridization studies. The similar locations suggest the dQC-LK and dPAL2 serve similar functions in the *Drosophila*. (Han 2004)

Biological Role of Glutaminyl Cyclase-like proteins

The identification of another QC in the *Drosophila* genome was followed by the identification of QC-LK proteins in many other species including humans. As in *Drosophila*, the human QC-LK is not the result of a gene duplication event. The genes are located on different chromosomes. Therefore, an attempt to explain the presence of QC-LK proteins would need to address its presence in various species.

Localization studies suggest the two different isoforms are located within different areas in *Drosophila*. Therefore, we believe the presence of two isoforms may be necessary for the proper pGlu formation in the whole fly for various peptides. Various neuropeptides require the activity of QC to produce the pGlu residue. The presence of dQC-LK in the developing nerve cord could serve this function. Peptides other than neuropeptides may use the dQC for proper pGlu formation.

Schilling et. al. suggested the presence of one *Drosophila* QC isoform, corresponding to the dQC in our studies, in the mitochondria due to signal sequence predictions, subcellular distribution of enzyme activity, and double-staining experiments. They demonstrated the dQC was co-localized with the mitochondria and activity was

present in the cell debris and heavy membrane fraction. The isoform corresponding to dQC-LK in our studies demonstrated activity in the cell culture media, suggesting the enzyme is secreted. Other evidence for the subcellular localization of the dQC protein include the granular immunocytochemical staining we observed.

There are mitochondria peptides which contain an N-terminal pyroglutamic acid residue. Other than the secretory pathway peptides containing an N-terminal pGlu residue such as adipokinetic hormone and coazonin, there are several peptides containing N-terminal sequences signaling transport into the *Drosophila* mitochondria that contain an N-terminal pGlu residue. Proteins such as acyl-CoA dehydrogenase and succinate dehydrogenase, contain an N-terminal signal sequence which allows the peptides to be transported into the mitochondria. (Schilling 2007) Once past the mitochondrial lumen, the signal sequence is cleaved and an N-terminal pGlu residue is observed. This could suggest a mitochondrial QC is required for proper protein maturation. dQC detected in low levels in the *Drosophila* embryos could function as the mitochondrial QC and possibly not be capable of any specified staining. However, it is likely that the pyroglutamate modification occurs outside the mitochondria prior to the protein's entrance.

We have also hypothesized that the two isoforms are required for activity in both the regulated secretive and constitutive secretive pathways. Various known neuropeptides have been localized to the regulated secretive pathway which require an N-terminal pGlu residue for proper maturation. However, other proteins known to use the constitutive pathway also require N-terminal pGlu suggesting the requirement for a glutaminyl cyclase in this pathway as well. For example, ranpiranse (onconase®), a

ribonuclease enzyme originally isolated from frog oocytes which has been proposed for cancer treatment, contains an N-terminal pGlu residue. Onconase matures through the constitutive pathway and requires an N-terminal pGlu residue for toxicity.

Immunocytochemistry revealed a single, higher molecular weight band in the *Drosophila* whole fly lysate suggesting possible post-translational modifications of the *Drosophila* QC proteins *in vivo*. Computer analysis led to the identification of differential phosphorylation sites in the dQC and dQC-LK proteins suggesting the two isoforms could also be under phosphorylation dependent regulation. Therefore, the two isoforms would be necessary for activity during different cellular conditions. Prediction programs suggested 20 tyrosine phosphorylation sites, 60 serine phosphorylation sites, and 5 threonine phosphorylation sites on dQC as opposed to 3 tyrosine phophorylation sites, 7 serine phosphorylation sites, and 3 threonine phosphorylation sites predicted on dQC-LK. Therefore, differential regulation could lead to the activation of a specific isoform during specific cellular events resulting in a need for two different QC isoforms.

Location and expression levels of glutaminyl cyclase in mammals

Analysis of the location and expression levels of QC in mammals utilized commercial mouse tissue blots. Previous localization information crudely localized mammalian QC to secretory granules in cow tissue. (Bockers 1995) A bovine tissue distribution study demonstrated QC was abundant in brain and pituitary. (Sykes 1999) However, no localization for mouse was previously evaluated. The mouse tissue blots indicated expression of QC in all tissues tested when both the commercial polyclonal and purified peptide antibody were used. Highest expression levels were identified in fetus,

eye, skin, and adrenal glands in descending order though levels were detected in all tissues examined. These preliminary results indicate the QC is an important enzyme in widely varying cellular locations.

The high level expression of mouse QC in the fetus suggests QC may be very important during the early development stages of the mouse. This finding would agree with the finding that a *Drosophila* QC isoform is highly expressed at high levels in areas such as the nervous system, during the early development.

Comparison of the results obtained from the tissue blot also correlate well to the Northern blot analysis of bovine QC presented by Pohl et al. Other than the high levels of QC identified in the brain and pituitary, QC was observed in various other tissue types including heart and skeletal muscle. (Pohl 1991) Further analyses and conclusions would require differentiation between the two QC isoforms also found in mice through production of mouse isoform specific antibodies.

Are Glutaminyl Cyclase and Aminopeptidase promiscuous enzymes?

Promiscuous enzymes catalyze two different, though often related, enzymatic reactions utilizing the same active site. Due to the tertiary structure and active site similarities of human QC and bacterial zinc aminopeptidase, along with the similarity of enzymatic reaction catalyzed, the possibility of QC and aminopeptidase acting as promiscuous enzymes was hypothesized. Our results demonstrated the ability of both human and *Drosophila* QC to cleave N-terminal amino acids from a typical leucine aminopeptidase substrate, hence, demonstrating aminopeptidase activity.

Due to the observed aminopeptidase activity of QC on the leucine substrates, it was hypothesized that QC must have the ability to bind leucine. Therefore, the use of leucine derivatives as inhibitors was explored. In the presence of tested leucine derivatives including leu-NH_2, leu-gly, leu-ala, leu-leu, leuβNA, and leucine chloromethyl ketone, a decrease in QC activity was observed. Decrease in activity in the presence of leu-peptide analyzed graphically suggests the substrates were binding in a competitive manner. Therefore, the leucine peptides were capable of binding the QC active site.

The *Aeromonas proteolytica* aminopeptidase (AAP) most efficiently cleaves leucine also demonstrating a high affinity for this amino acid. The aminopeptidase reaction mechanism first requires the amino acids C-terminal to the leucine residue to bind to the S1 pocket. The S1 pocket is a hydrophobic pocket formed by two cysteines, C223 and C227, along with M180, F244, and Y251. Next the carbonyl group binds the zinc 1, which is the zinc that corresponds to the zinc found in QC. Next the N-terminal amide group interacts with zinc 2. However, experimental data has demonstrated the aminopeptidase is over 80% active with the loss of zinc 2 suggesting the neighboring Asp 117 or Asp 179 can act as the amide binding groups. Formation of the intermediate initiates the Glu 151 to act as a nucleophile, or general base, resulting in the dissociation of the carbonyl group. The zinc 1, now bound Glu 151, attacks the carbonyl group forming the tetrahedral intermediate. Finally Glu 151 donates a proton and allows the amide group to form the leaving group. (Lowther 2002) The active site amino acids are shown in figure 45.

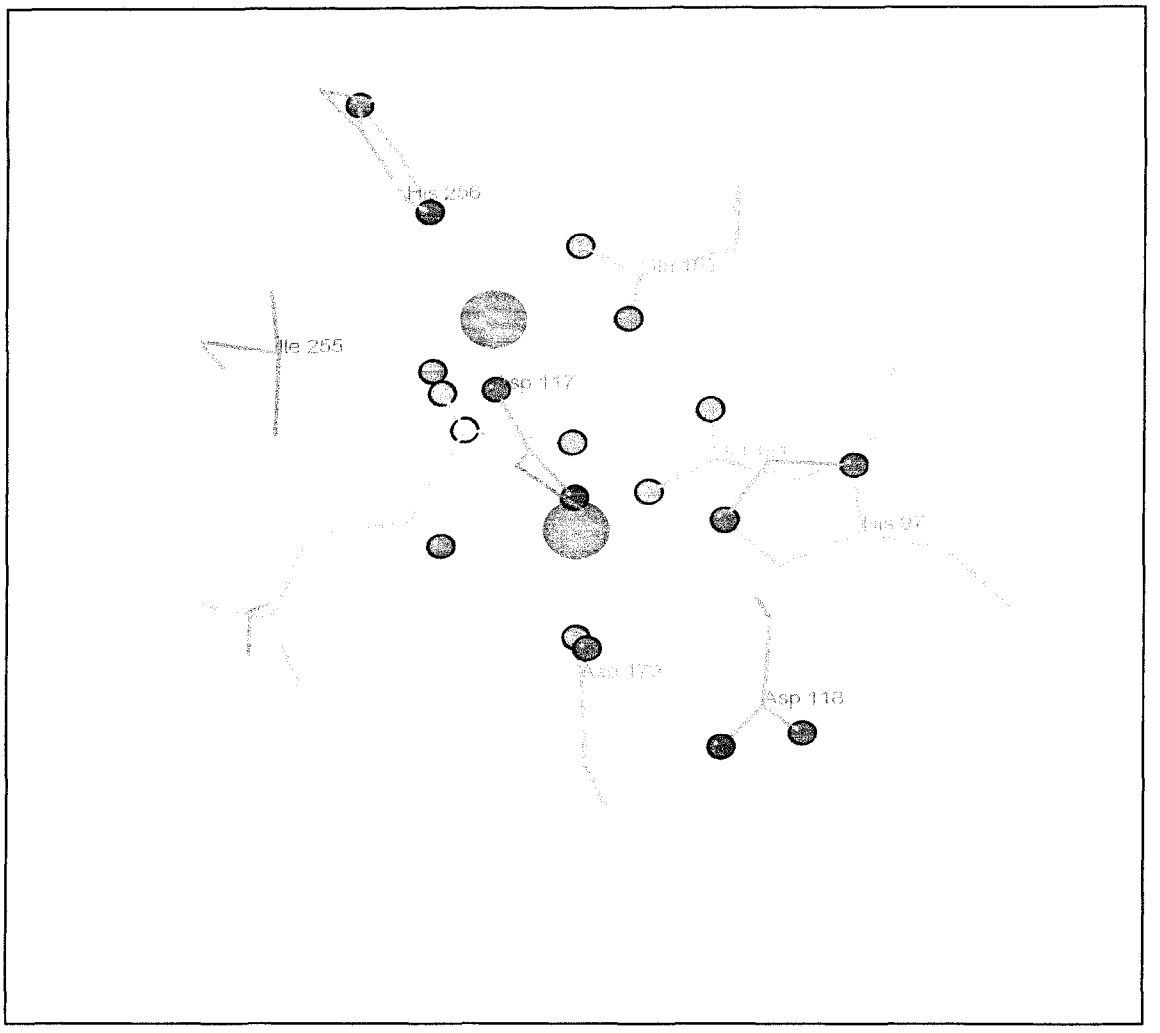

Figure 45: ***Aeromonas*** **aminopeptidase active site residues.** Structure of *Aeromonas* aminopeptidase active site bound to leucine phosphonic acid. Amino acids are shown in blue, inhibitor in pink, and zinc metals in gray.

Comparison of the AAP and hQC active sites provide some evidence for the ability of QC to specifically bind to a leucine peptide. The 3-D structure demonstrates the two active sites are virtually identical with conservation of all catalytic residues as demonstrated in figure 46. The absence of zinc 2 in the QC structure is mechanistically

compensated by the presence of a conserved aspartate residue, Asp 248, which corresponds to Asp 179 of the aminopeptidase capable of performing the zinc 2 catalytic function.

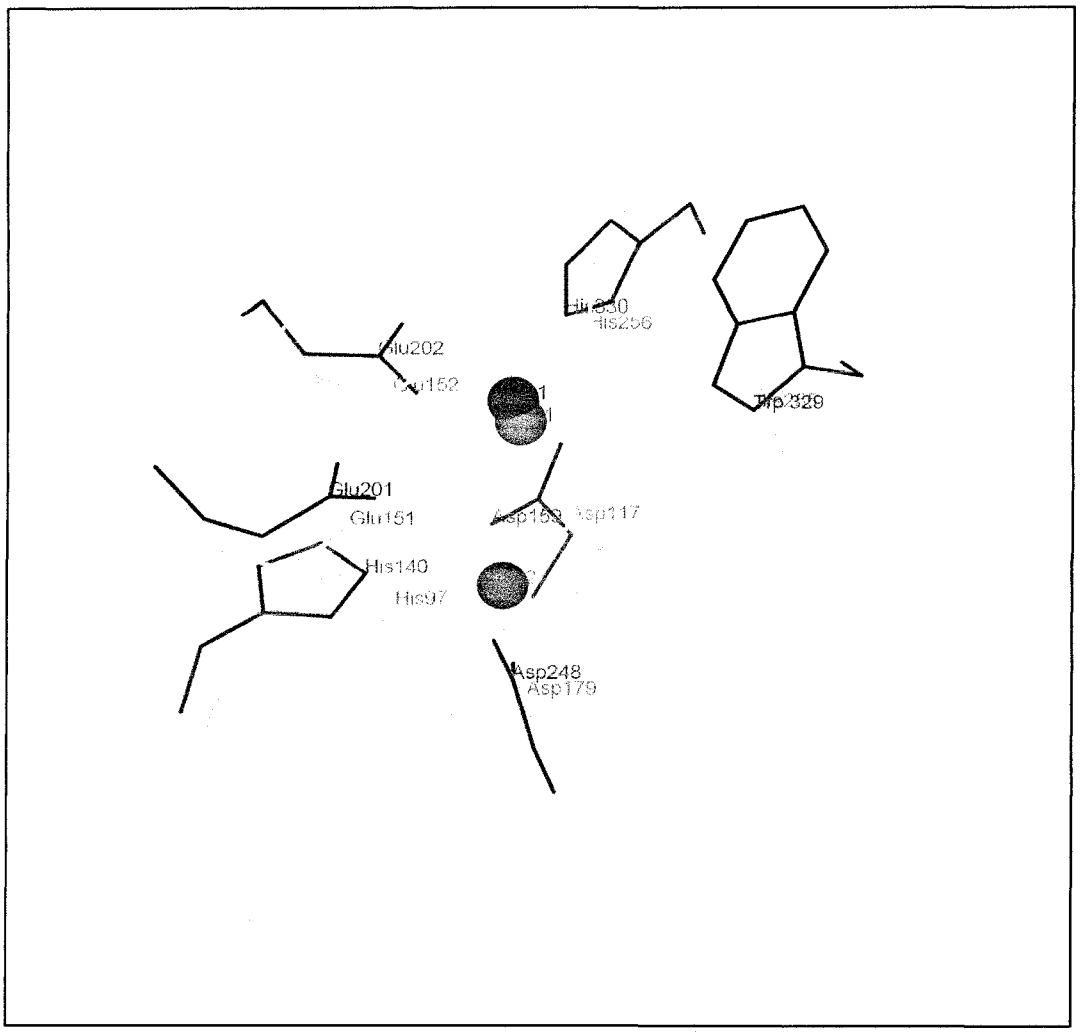

Figure 46: ***Aeromonas*** **aminopeptidase active site hQC overlay.** This figure demonstrates the conservation of 3-D structure of all aminopeptidase active site residues in the hQC crystal structure. AAP is shown in yellow with labels in green and hQC is shown in blue with labels in red.

The ability of the leucine chloromethyl ketone to act as an affinity label with the mammalian family QCs is due to the slight alteration of the enzyme active site. All chloromethyl ketones react with free active site histidine residues. In the AAP active site the His 97 reacts with the second zinc and is therefore unable to react with the ketone. This explains the reversible inhibition observed by leucine chloromethyl ketone with AAP. The loss of the second zinc in the human QC active site would allow the corresponding histidine, His 140, to freely react with the chloromethyl ketone. This explains the irreversible inhibition observed with human QC in the presence of leucine chloromethyl ketone.

The most observable variation in the two 3-D structures of the AAP and hQC lies in the S-pocket. As demonstrated by Huang et. al. in the development of the hQC crystal structures, the substitution of Phe 244 in hQC results in loss of the S-pocket, a hydrophobic pocket responsible for interacting with the C-terminal portion of the peptide cleaved by the aminopeptidase. Therefore, only the N-terminal residue has access to the hQC active site as opposed to the aminopeptidase which binds a larger portion of the peptide destined for cleavage. However, this change does not affect the normal enzymatic activity of either enzyme because the two enzymes bind their natural substrates in a different manner. The normal binding of hQC to a glutamine peptide and AAP to a leucine peptide is shown in figure 47. The hQC binds the glutamine in the active site with the C-termnial portion of the protein not interacting with any of the amino acids displayed in the region. However, the AAP binds the leucine in the active site with the C-terminal portion of the protein interacting with the amino acids displayed. These amino acids make up the S-pocket.

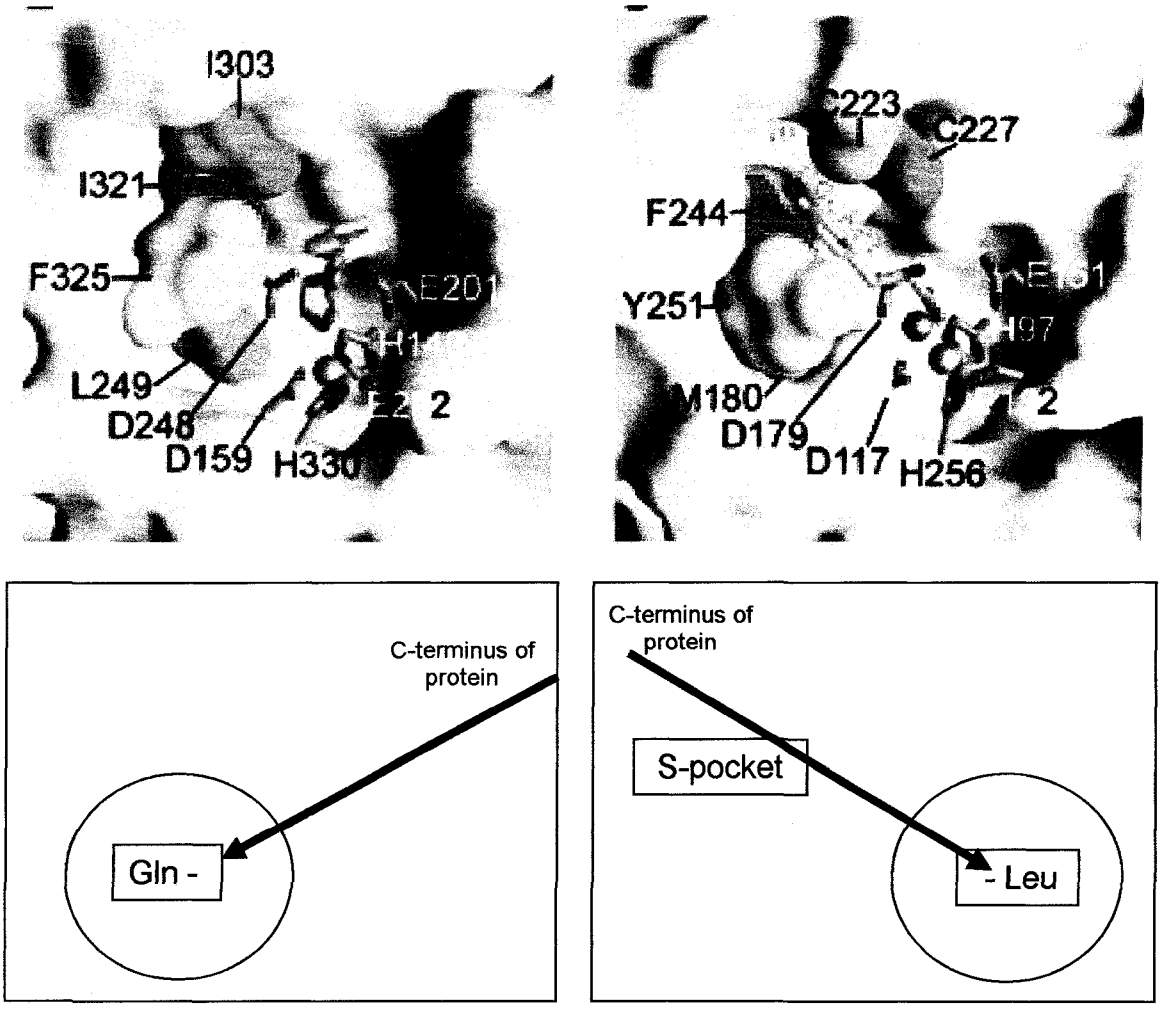

Figure 47: **Comparison of AAP and hQC Active Site Binding Orientations.** The top image displays the orientation of a peptide binding both the hQC (to the left) and AAP (to the right). (Huang 2005) The bottom image displays a schematic drawing. The arrow in the bottom images demonstrates the orientation of the peptide bound to the enzymes with the the N-terminal amino acid listed. This figure demonstrates the hQC binds only the N-terminal glutamine residue with the C-terminus extending outward.

The small leucine peptides ability to bind the QC as inhibitors is possible due to the small size of the leucine peptides. Only the leucine residue must bind the conserved

active site residues demonstrated in the active site overlay. Therefore, loss of the S-pocket does not affect the binding of inhibitors. In a similar manner the low levels of aminopeptidase activity in the QCs tested are also conceivably due to the type of aminopeptidase substrate used. The aminopeptidase substrates were single leucine amino acids coupled to a p-nitroanilide. Figure 48 demonstrates the binding of the leucine inhibitor to AAP. The leucine destined for cleavage does not interact with the S-pocket.

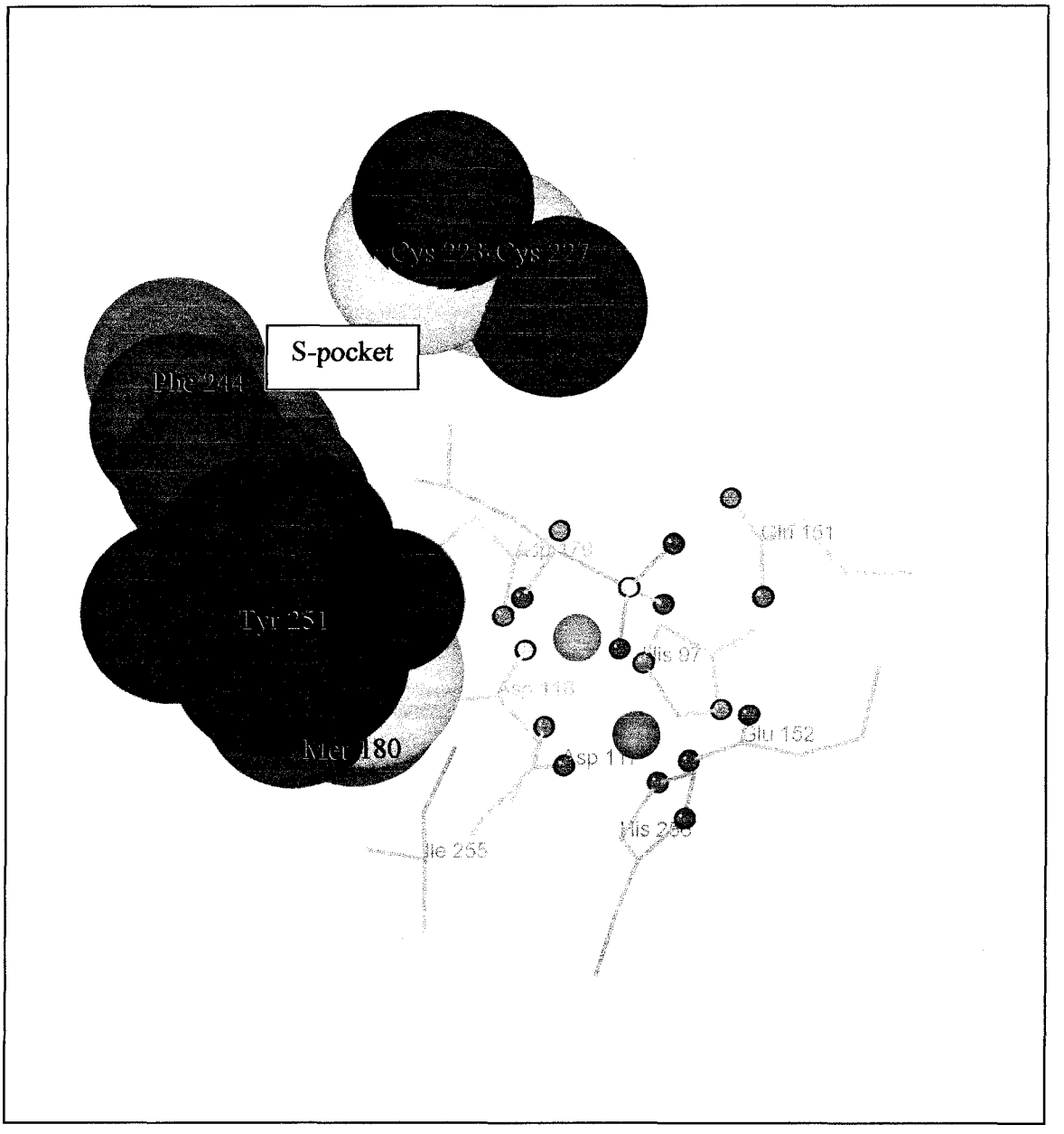

Figure 48: **Space filling model *Aeromonas* aminopeptidase S-pocket.** This image demonstrates the S-pocket formed in the AAP for binding of the C-terminal peptide chain in aminopeptidase reactions.

The lack of the S-pocket suggests the human QC would not be able to bind long peptides in the same manner as the AAP. This would provide some insight into the aminopeptidase ability of QC *in vivo*. Without the hydrophobic S-pocket to bind the C-terminal portion of the protein destined for N-terminal amino acid cleavage, QC would not be able to complete aminopeptidase reactions *in vivo*.

Evolution of Glutaminyl Cyclase

Evolution of the animal QC enzyme family appears to be linked to the evolution of the aminopeptidase enzyme family due to similarity in catalytic reaction and tertiary structure. The ability of QC to catalyze an aminopeptidase reaction and bind leucine substrates further demonstrates the relationship between the two enzyme families. These conclusions suggest a divergent evolution in which two closely related enzyme families have a common evolutionary origin but have diverged over time to develop specific functions within the organism.

To further analyze the relationships among the various QCs, development of phlyogenetic trees (figure 49) based on a comparison of the tertiary structures of plant, bacterial, and animal QCs, along with various aminopeptidases, were completed. As evident from the tree, the human QC is more closely related to the bacterial and some leucine aminopeptidases than to the plant QC. The close evolutionary relationship theorized further explains the aminopeptidase activity and leucine binding ability of the mammalian QCs. The plant and bacterial QCs appear to have the most distant phylogenetic relationship when compared to the bacterial aminopeptidases and other QCs.

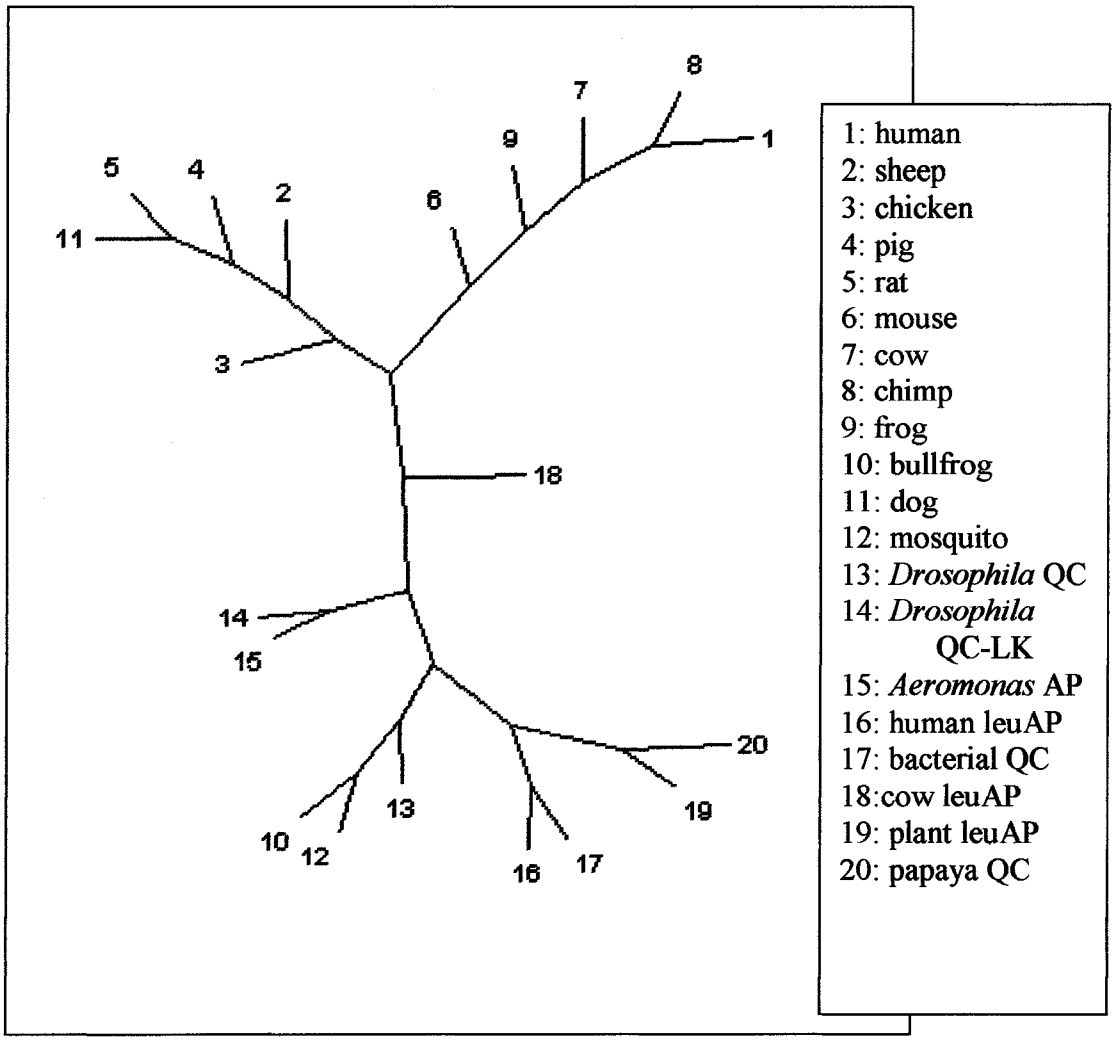

Figure 49: **Tertiary structure based neighbor-joining phylogentic tree.** This tree demonstrates the relationship of various QCs to the AP protein family due to tertiary structure similarity. Number 1 represents human QC. Numbers 2 – 14 represent various QCs from yeast to mammals. Numbers 15 – 19 represent various aminopeptidases. Number 20 represents papaya QC.

Final Conclusions

Experimental work, along with the phylogenetic tree analysis, has led to the conclusion that the animal QC family and bacterial aminopeptidases represent an instance of divergent evolution. The use of same catalytic residues, location of zinc in the active site, tertiary structure similarity, active site binding of leucine, and AP activity of QC all suggest the two enzymes evolved from a common ancestor. However, the animal QC family and plant QC family represent an instance of convergent evolution. Due to the very different tertiary structure, active site residues, and location of zinc in structure suggest the two evolved from a different ancestor to have the same function.

WORKS CITED

Amrani, A., Wintjens, R., Zerhouni, S., Azarkan, M., Nijs, M., Vincentelli, J., Looze, Y. (1997). "The conversion of N-terminal glutaminyl residues of plant protein into 5-oxoproline: A post-translational modification in quest of a physiological function." Recent Res Devel In Phytochemistry **1**: 25-37.

Arner, P. (2000). "Obesity - a genetic disease of adipose tissue?" British Journl of Nutrition **83**(S1): S9-S16.

Ashrafi, K., Chang, F., Watts, J., Fraser, A., Kamath, R., Ahringer, J., Ruvkun, G. (2003). "Genome-wide RNAi analysis of *Caenorhabditis elegans* fat regulatory genes." Nature **421**: 268-271.

Azarkan, M., B. Clantin, et al. (2005). "Crystallization and preliminary X-ray diffraction studies of the glutaminyl cyclase from Carica papaya latex." Acta Crystallograph Sect F Struct Biol Cryst Commun **61**(Pt 1): 59-61.

Bateman, R. C., Jr. (1989). "A spectrophotometric assay for glutaminyl-peptide cyclizing enzymes." J Neurosci Methods **30**(1): 23-8.

Bateman, R. C., Jr., J. S. Temple, et al. (2001). "Evidence for essential histidines in human pituitary glutaminyl cyclase." Biochemistry **40**(37): 11246-50.

Bear, M. F., Connors, B.W., Paradiso, M.A. (2001). Neuroscience: Exploring the Brain. Baltimore, Maryland, Lippincott Williams & Wilkins.

Beck, B. J. and J. B. Russell (1994). "Electrogenic glutamine uptake by Peptostreptococcus anaerobius and generation of a transmembrane potential." J Bacteriol **176**(5): 1303-8.

Beinfeld, M. C. (1998). "Prohormone and Proneuropeptide Processing." Endocrine **8**(1): 1-5.

Berman, Y., Mzhavia, N., Polonskaia, A., Devi, L.A. (2001). "Impaired Prohormone Convertases in Cpe fat/ Cpe fat Mice." J Biol Chem **276**(2): 1466-1473.

Bernasconi, P. (1994). "Molecular cloning of a Drosophila melanogaster gene coding for an homologue of human carboxypeptidase E." Arch Biochem Biophys **27**(3): 169-178.

Bockers, T. M., M. R. Kreutz, et al. (1995). "Glutaminyl-cyclase expression in the bovine/porcine hypothalamus and pituitary." J Neuroendocrinol **7**(6): 445-53.

Booth, R. E., S. C. Lovell, et al. (2004). "Human glutaminyl cyclase and bacterial zinc aminopeptidase share a common fold and active site." BMC Biol **2**: 2.

Booth, R. E., S. A. Misquitta, et al. (2003). "Human pituitary glutaminyl cyclase: expression in insect cells and dye affinity purification." Protein Expr Purif **32**(1): 141-6.

Busby Jr. WH, Q. G., Humm J, Youngblood WW, Kizer JS (1987). "An enzyme that converts glutaminyl-peptides into pyroglutamyl-peptides." J Biol Chem **262**: 8532-8536.

Busby, W. H., et. al. (1987). "An enzyme that converts glutaminyl-peptides into pyroglutamyl-peptides." J Biol Chem **262**: 8532-8636.

Canaff, L., Bennett, H.P.J., Hendy, G.N. (1999). "Peptide hormone precursor processing: getting sorted?" Molecular and Cellular Endocrinology **156**: 1-6.

Chamorro, M., Schwartz, D., Vonica, A., Bricanlou, A., Cho, K., Varmus, H. (2005). "FGF-20 and DKK1 are transcriptional targets of β-catenin and FGF-20 is implicated in cancer and development." The EMBO Journal **24**: 73-84.

Checler, F., Vincent, B. (2002). "Alzheimer's and prion diseases: distinct pathologies, common proteolytic denominators." TRENDS in Neurosciences **25**(12): 616-620.

Chen, G. J. and J. B. Russell (1989). "Transport of glutamine by Streptococcus bovis and conversion of glutamine to pyroglutamic acid and ammonia." J Bacteriol **171**(6): 2981-5.

Chintapalli, V. R., Wang, J. and Dow, J. A. T. (2007). "Using FlyAtlas to identify better Drosophila models of human disease." Nature Genetics **39**: 715-720.

Coillie, E., Proost, P., Aelst, I., Struyf, S., Polfliet, M., Meeseter, I., Harvey, D., Damme, J., Opdenakker, G. (1998). "Functional Comparison of Two Human Monocyte Chemotactic Protein-2 Isoforms, Role of the Amino-Terminal Pyroglutamic Acid and Processing by CD26/Depeptidyl Peptidase IV." Biochemistry **37**: 12672-12680.

Consalvo, A. P., S. D. Young, et al. (1988). "A rapid fluorometric assay for N-terminal glutaminyl cyclase activity using high-performance liquid chromatography." Anal Biochem **175**(1): 131-8.

Curto, E. V., Lambert, G., Davis, R., Wilborn, T., Dooley, T. (2002). "Biomarkers of Human Skin Cells Identified Using DermArray DNA Arrays and New Bioinformatics Methods." Biochemical and Biophysical Research Communications **291**: 1052-1064.

Cynis, H., S. Schilling, et al. (2006). "Inhibition of glutaminyl cyclase alters pyroglutamate formation in mammalian cells." Biochim Biophys Acta **1764**(10): 1618-25.

Damodaran M, A.-N. P. (1938). "Enzymatic proteolysis. I. Ammonia formation from proteins." Biochem J **32**: 1877-1889.

Ezura, Y., M. Kajita, et al. (2004). "Association of multiple nucleotide variations in the pituitary glutaminyl cyclase gene (QPCT) with low radial BMD in adult women." J Bone Miner Res **19**(8): 1296-301.

Fischer, W. H. and J. Spiess (1987). "Identification of a mammalian glutaminyl cyclase converting glutaminyl into pyroglutamyl peptides." Proc Natl Acad Sci U S A **84**(11): 3628-32.

Forloni, G., Lucca, E., Angeretti, N., Torre, P.D., Salmona, M. (1997). "Amidation of B-Amyloid Peptide Strongly Reduced the Amyloidogenic Activity Without Alteration of the Neurotoxicity." J Neurochem **69**(5): 2048-2054.

Gabreels, B. A. T. F., Swaab, D.F., De Kleijn, D.P.V., Dean, A., Seidah, N.G., Van, J.W., De Loo, V., Van de Ven, W.J.M., Martens, G.J.M., Van Leeuwen, F.W. (1998). "The Vasopressin Precursor is not Processed in the Hypothalamus of Wolfram Syndrome Patients with Diabetes Insipidus: Evidence for the Involvement of PC2 and 7B2." Journal of Clinical Endocrinology and Metabolism **83**(11): 4026 - 4033.

Gololobov, M., I. Song, et al. (1994). "Steady-state kinetics of glutamine cyclotransferase." Arch Biochem Biophys **309**(2): 300-7.

Gololobov, M. Y., Wang, W., Bateman, R.C. (1996). "Substrate and inhibitor specificity of glutamine cylcotransferase (QC)." Biol Chem Hoppe Seyler **377**: 395-398.

Guillaume, R. M., J-R., Chidami, S., Veenstra, J.A., Philippe, R. (2005). "AKH-producing neuroendocrine cell ablation decreases trehalose and induces behavioral changes in Drosophila." Am J Physiol Regulatory Integrative Comp Physiol **288**: 531-538.

Han M, P. D., Vanderzalm PJ, Mains RE, Eipper BA, Taghert PH (2004). "Drosophila uses two distinct neuropeptide amidating enzymes, dPAL1 and dPAL2." J Neurochem **90**(1): 129-141.

Hao, X., Sun, B., Hu, L., Lahdesmaki, H., Dunmire, V., Feng, Y., Zhang, S., Wang, H., Wu, C., Wang, H., Fuller, G., Symmans, W., Shmulevich, I., Zhang, W. (2004). "Differential Gene nd Protein Expression in Primary Breast Malignancies and Their Lymph Node Metastases as Revealed by Combined cDNA Microarray and Tissue Microarray Analysis." Cancer **100**(6): 1110-1122.

Huang, K. F., Y. L. Liu, et al. (2005). "Crystal structures of human glutaminyl cyclase, an enzyme responsible for protein N-terminal pyroglutamate formation." Proc Natl Acad Sci U S A **102**(37): 13117-22.

Huang, K. F., Y. L. Liu, et al. (2005). "Cloning, expression, characterization, and crystallization of a glutaminyl cyclase from human bone marrow: a single zinc metalloenzyme." Protein Expr Purif **43**(1): 65-72.

Hwang, J. R., D. E. Siekhaus, et al. (2000). "Interaction of Drosophila melanogaster prohormone convertase 2 and 7B2. Insect cell-specific processing and secretion." J Biol Chem **275**(23): 17886-93.

Jarzab, B., Wiench, M., Fujarewicz, K., Simek, K, Jarzab, M., Oczko-Wojciechowska, M., Wloch, J., Czarniecka, A., Chmielik, E., Lange, D., Pawlaczek, A., Szpak, S., Gubala, E., Swierniak, A. (2005). "Gene Expression Profile of Papillary Thyroid Cancer: Sources of Variability and Diagnostic Implications." Cancer Res **65**(4): 1587-1597.

Kimura, N., Pilishowska, M., Okamoto, H., Kimura, I., Aunis, D. (2000). "Immunohistochemical Expression of Chromogranins A and B, Prohormone Convertases 2 and 3, and Amidating Enzyme in Carcinoid Tumors and Pancreatic Endocrine Tumors." Mod Pathol **13**(2): 140-146.

Koger, J. B., J. Humm, et al. (1989). "Assay of glutaminylpeptide cyclase." Methods Enzymol **168**: 358-65.

Kolhekar, A. S., M. S. Roberts, et al. (1997). "Neuropeptide amidation in Drosophila: separate genes encode the two enzymes catalyzing amidation." J Neurosci **17**(4): 1363-76.

Lee, H., Lin, E., Liu, L., Smith, J. (2003). "Gene expression profiling of tumor xenografts: *In vivo* analysis of organ-specific metastasis." Int J Cancer **107**: 528-534.

Lindberg, I. (1996). Polypeptide hormones: biosynthesis, processing, and secretion. The Encyclopedia of Molecular Biology. R. A. Myers. Weinheim, Germany, VCH Press.

Lowther, W. T., Matthews, B.W. (2002). "Metalloaminopeptidases: Common Functional Themes in Disparate Structural Surroundings." Chem Rev(102): 4581-4607.

Messer, M. (1963). "Enzymatic cyclization of L-glutamine and L-glutaminyl peptides." Nature **197**: 1299.

Messer M, O. M. (1965). "Isolation and properties of glutamine cyclotransferase of dried papaya latex." C R Trav Lab Carlsberg **35**: 1-24.

Oberg, K. A., J. M. Ruysschaert, et al. (1998). "Papaya glutamine cyclase, a plant enzyme highly resistant to proteolysis, adopts an all-beta conformation." Eur J Biochem **258**(1): 214-22.

Parker, A. T., Bateman, R.C. (2007). Expression, Purification, and Characterization of a *Drosophila* Glutaminyl Cyclase. Experimental Biology 2007, Washington, D.C.

Parker, A. T., Bateman, R.C. (2008). Expression, Purification, and Characterization of a *Drosophila* QC-like Protein. Experimental Biology 2008, San Diego, CA.

Pawlak, J. and R. Manjunatha Kini (2006). "Snake venom glutaminyl cyclase." Toxicon **48**(3): 278-86.

Pohl, T., M. Zimmer, et al. (1991). "Primary structure and functional expression of a glutaminyl cyclase." Proc Natl Acad Sci U S A **88**(22): 10059-63.

Rayburn, L. Y., H. C. Gooding, et al. (2003). "amontillado, the Drosophila homolog of the prohormone processing protease PC2, is required during embryogenesis and early larval development." Genetics **163**(1): 227-37.

Rovere, C., Viale, A., Nahon, J., Kitabgi, P. (1996). "Impaired Processing of Brain Proneurotensin and Promelanin-Concentrating Hormone in Obese *fat/fat* Mice." Endocrinology **137**(7): 2954-2958.

Russo, C., Violani, E., Salis, S., Venezia, V., Dolcini, V., Damonte, G., Benatti, U., D'Arrigo, C., Patrone, E., Carlo, P., Schettini, G. (2002). "Pyroglutamate-

modified amyloid β-peptides - AβN3(pE) - strongly affect cultured neuron and astrocyte survival." J Neurochem **82**: 1480-1489.

Saido, T. C., Iwatsubo, T., Mann, D., Shimada, H., Ihara, Y., Kawashima, S. (1995). "Dominant and Differential Deposition of Distinct β-Amyloid Peptide Species, AβN3(pE), in Senile Plaques." Neuron **14**: 457-466.

Schilling, S., H. Cynis, et al. (2005). "Isolation, catalytic properties, and competitive inhibitors of the zinc-dependent murine glutaminyl cyclase." Biochemistry **44**(40): 13415-24.

Schilling, S., T. Hoffmann, et al. (2004). "Glutaminyl cyclases unfold glutamyl cyclase activity under mild acid conditions." FEBS Lett **563**(1-3): 191-6.

Schilling, S., T. Hoffmann, et al. (2002). "Heterologous expression and characterization of human glutaminyl cyclase: evidence for a disulfide bond with importance for catalytic activity." Biochemistry **41**(35): 10849-57.

Schilling, S., T. Hoffmann, et al. (2002). "Continuous spectrometric assays for glutaminyl cyclase activity." Anal Biochem **303**(1): 49-56.

Schilling, S., C. Lindner, et al. (2007). "Isolation and characterization of glutaminyl cyclases from Drosophila: evidence for enzyme forms with different subcellular localization." Biochemistry **46**(38): 10921-30.

Schilling, S., Manhart, S., Hoffmann, T., Ludwig, H., Wasternack, C., Demuth, H. (2003). "Substrate Specificity of Glutaminyl Cyclases from Plants and Animals." Biol Chem **384**: 1583-1592.

Schilling, S., A. J. Niestroj, et al. (2003). "Identification of human glutaminyl cyclase as a metalloenzyme. Potent inhibition by imidazole derivatives and heterocyclic chelators." J Biol Chem **278**(50): 49773-9.

Schneider, I. (1972). "Cell lines derived from late embryonic stages of *Drosophila melanogaster*." Embryol Exp Morphol **27**: 353-365.

Setirle, S. H., Green, M.M.,Burtis, K.C. (1995). "The silver gene of Drosophila melanogaster encodes multiple carboxypeptidases similar to mammalian prohormone-processing enzymes." Proc Natl Acad Sci U S A **92**: 9470-9474.

Siekhaus, D. E., Fuller, R.S. (1999). "A Role for amontillado, the Drosophila Homolog of the Neuropeptide Precursor Processing Protease PC2, in Triggering Hatching Behavior." Journal of Neuroscience **19**(16): 6942-6954.

Song, I., C. Z. Chuang, et al. (1994). "Molecular cloning, sequence analysis and expression of human pituitary glutaminyl cyclase." J Mol Endocrinol **13**(1): 77-86.

Staubli, F., T. J. Jorgensen, et al. (2002). "Molecular identification of the insect adipokinetic hormone receptors." Proc Natl Acad Sci U S A **99**(6): 3446-51.

Steveson, T. C., Ciccotosto, G.D., Ma, X., Mueller, G.P., Mains, R.E., Eipper, B.A. (2003). "Menkes Protein Contributes to the Function of Peptidylglycine a-Amidating Monooxygenase." Endocrinology **144**(1): 188-200.

Sykes, P. A., S. J. Watson, et al. (1999). "Evidence for tissue-specific forms of glutaminyl cyclase." FEBS Lett **455**(1-2): 159-61.

Temple, J. S., Song, I., Burns, K.H., Bateman, R.C. (1998). "Absence of Essential Thiol in Human Glutaminyl Cyclase: Implications for Mechanism." Korean J Biol Sci **2**: 243-248.

Van der Horst, D. J., Marrewijk, W.J.A., Diederen, J.H.B. (2001). "Adipokinetic Hormones of Insect: Release, Signal Transduction, and Responses." International Review of Cytology **211**: 179-240.

Wand, G. S., Ney, R.L., Baylin, S., Eipper, B., Mains, R.E. (1985). "Characterization of a Peptide Alpha-Amidation Activity in Human Plasma and Tissues." Metabolism **34**(11): 1044-1052.

Wang, J., Xu, J., Finnerty, J., Furuta, M., Steiner, D.F., Verchere, C.B. (2001). "The Prohormone Convertase Enzyme 2 (PC2) is Essential for Processing Pro-Islet Amyloid Polpeptide at the NH_2 Terminal Cleavage Site." Diabetes **50**: 534-539.

Wintjens, R., H. Belrhali, et al. (2006). "Crystal structure of papaya glutaminyl cyclase, an archetype for plant and bacterial glutaminyl cyclases." J Mol Biol **357**(2): 457-70.

Zerhouni, S. A., A., Nijs, M, Smolders, M., Azarkan, M, Vincentelli, J., Looze, Y. (1998). "Purification and characterization of papaya glutamine cyclotransferase, a plant enzyme highly resistant to chemical, acid, and thermal denaturation." Biophysica Acta **1387**: 275-290.

Zhou, A., Webb, G., Zhu, X., Steiner, D.F. (1999). "Proteolytic Processing in the Secretory Pathway." J Biol Chem **274**(30): 20745-20748.